WL-TR-96-4009

DIGITAL CONTROL DESIGN & DEMONSTRATION FOR PULSED LASER DEPOSITION OF SUPERCONDUCTING FIRMS

S.P. MURRAY

TMCI
P.O. BOX 340345
BEAVERCREEK OH 45434

DECEMBER 1995

FINAL REPORT FOR 09/30/93-09/30/95

APPROVED FOR PUBLIC RELEASE; DISTRIBUTION IS UNLIMITED.

MATERIALS DIRECTORATE
WRIGHT LABORATORY
AIR FORCE MATERIEL COMMAND
WRIGHT PATTERSON AFB OH 45433-7734

NOTICE

When Government drawings, specifications, or other data are used for any purpose other than in connection with a definitely Government-related procurement, the United States Government incurs no responsibility or any obligation whatsoever. The fact that the Government may have formulated or in any way supplied the said drawings, specifications, or other data, is not to be regarded by implication, or otherwise in any manner construed, as licensing the holder, or any other person or corporation; or as conveying any rights or permission to manufacture, use, or sell any patented invention that may in any way be related thereto.

This report is releasable to the National Technical Information Service (NTIS). At NTIS, it will be available to the general public, including foreign nations.

This technical report has been reviewed and is approved for publication.

STEVEN R. LECLAIR, Chief
Materials Process Design
Integration & Operations Division
Materials Directorate

STEVEN R. LECLAIR, Chief
Materials Process Design
Integration & Operations Division
Materials Directorate

JOHN R. WILLIAMSON
Integration & Operations Division
Materials Directorate

If your address has changed, if you wish to be removed from our mailing list, or if the addressee is no longer employed by your organization please notify WL/MLIM, Wright Patterson AFB, OH 45433 to help maintain a current mailing list.

Copies of this report should not be returned unless return is required by security considerations, contractual obligations, or notice on a specific document.

REPORT DOCUMENTATION PAGE

Form Approved
OMB No. 0704-0188

1. AGENCY USE ONLY *(Leave blank)*	2. REPORT DATE	3. REPORT TYPE AND DATES COVERED
	DEC 1995	FINAL 09/30/93--09/30/95

4. TITLE AND SUBTITLE DIGITAL CONTROL DESIGN & DEMONSTRATION FOR PULSED LASER DEPOSITION OF SUPERCONDUCTING FIRMS

5. FUNDING NUMBERS
C F33615-94-D-5801
PE 62102
PR 2418
TA 90
WU 01

6. AUTHOR(S) S.P. MURRAY

7. PERFORMING ORGANIZATION NAME(S) AND ADDRESS(ES)
TMCI
P.O. BOX 340345
BEAVERCREEK OH 45434

8. PERFORMING ORGANIZATION REPORT NUMBER

9. SPONSORING/MONITORING AGENCY NAME(S) AND ADDRESS(ES)
MATERIALS DIRECTORATE
WRIGHT LABORATORY
AIR FORCE MATERIEL COMMAND
WRIGHT PATTERSON AFB OH 45433-7734

10. SPONSORING/MONITORING AGENCY REPORT NUMBER
WL-TR-96-4009

11. SUPPLEMENTARY NOTES

12a. DISTRIBUTION/AVAILABILITY STATEMENT
APPROVED FOR PUBLIC RELEASE; DISTRIBUTION IS UNLIMITED.

12b. DISTRIBUTION CODE

13. ABSTRACT *(Maximum 200 words)*

The design and implementation of a new Pulsed Laser Deposition system for growing High Temperature Superconducting film at Wright Labs is described and demonstrated. The capabilities of the new system go far beyond the typical laboratory deposition setup. The important system features include real-time data acqusition and storage, deposition process automation, and digital control of three key environmental variables, specfically the laser energy, substrate temperature, and chamber oxygen pressure. It is hoped that process repeatibility can be achieved through control of these environmental variables. Additional insitu measurements on plume characteristics should help increase the understanding of the PLD process in general. The effectiveness of the new system is demonstrated by the successful growth of superconducting films.

14. SUBJECT TERMS
Pulsed Laser Deposition, High Temperature Superconducting Films, Process Automation, Digital Control

15. NUMBER OF PAGES 140

16. PRICE CODE

17. SECURITY CLASSIFICATION OF REPORT	18. SECURITY CLASSIFICATION OF THIS PAGE	19. SECURITY CLASSIFICATION OF ABSTRACT	20. LIMITATION OF ABSTRACT
UNCLASSIFIED	UNCLASSIFIED	UNCLASSIFIED	SAR

PREFACE

I would like to thank a number of people who helped to make this thesis topic possible. First, a huge thanks to both my advisor Dr. Patrick Garrett and my mentor Dr. Samuel Laube. Without their direction and encouragement, this project would have never gotten off the ground. Also, thanks to Dr. Rand Biggers and Mr. David Dempsey whose numerous suggestions on the new system's capabilities helped to push me in the right direction when it came time to design the software/instrumentation interface. Finally, I would to thank the entire group of people that make up the Process Design Branch of the Wright Patterson Air Force Base Materials Directorate, especially Dr. Steven LeClair and Capt. Elizabeth Stark, for funding both the initial task and subsequent equipment purchases.

TABLE OF CONTENTS

LIST OF FIGURES

LIST OF TABLES

CHAPTER 1 - INTRODUCTION AND STATEMENT OF PROBLEM

1.1 Superconductors and PLD Background

Superconductors are a class of materials that, in sufficiently cold temperatures, exhibit the unique property of having no resistance to the flow of electricity. The fact that these materials have essentially zero resistance means that no power will be dissipated in them due to current flow. This simple observation has, quite obviously, important implications.

The benefits of zero resistance are not without cost, however, as all known superconducting materials need to be cooled to extremely low temperatures. The first materials known to enter the superconducting state were and still are of little practical use because the temperature required for the state change from normal conductor to superconductor (the transition temperature, or Tc) is around 4 K. Refrigeration systems that can reach these temperatures usually incorporate liquid helium. The high gains of zero resistance are offset by the large cost of the liquid helium. Recently, however, other superconductors have been found with Tcs well above 70 K. This greatly reduces the cost of the refrigeration because liquid nitrogen (about 6 cents a liter) can be substituted in place of liquid helium. Superconductors with a Tc above the liquid nitrogen temperature are typically referred to as high temperature superconductors (HTSCs).

One such HTSC is the ceramic compound yttrium barium copper oxide, with a theoretical transistion temperature of 92 K. The chemical symbol for this element is Y Ba_2 Cu_3 O_7, and it is usually referred to as YBCO in the literature. The unit cell structure of YBCO is shown in Figure 1.1. The dimensions for the

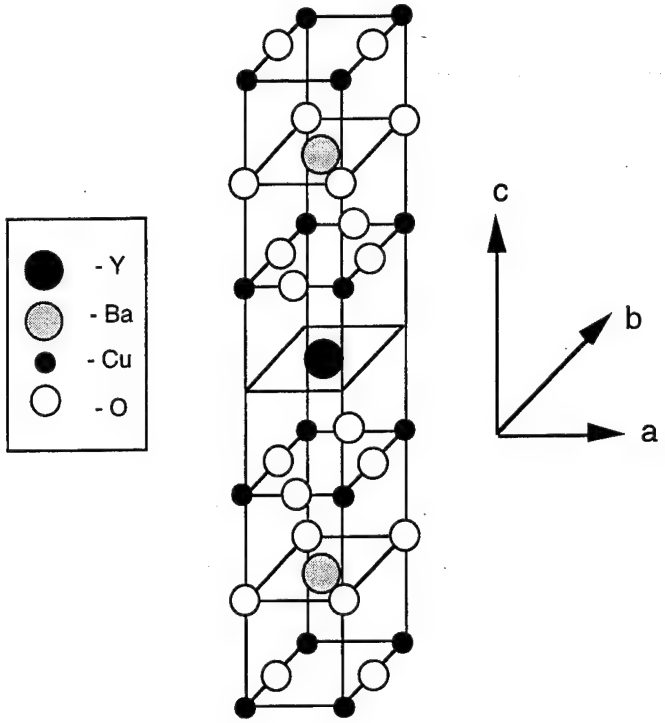

Figure 1.1 - *Unit Cell of YBCO* (Adapted from [1])

a, b, and c directions are as follows:[2]

a = .382 nm

b = .389 nm

c = 1.168 nm

The discovery of HTSCs means that using superconductors in various applications may be cheaper than using other 'normal' conductors such as copper. More importantly, however, are applications in which normal conductors could never approach the performance of superconductors no matter what the cost. One proven example of this deals with microwave resonators. Superconductors have the property of reflecting electromagnetic waves perfectly. When cavity walls are

[1]Thomas P. Sheahen, *Introduction to High-Temperature Superconductivity*, (New York: Plenum Press, 1994), 5.
[2]A. Bourdillon and N. X. Tan Bourdillon, *High Temperature Superconductors: Processing and Science*, (California: Academic Press, 1994), 44.

coated with a thin-film superconductor, the Q-factor of the resonant cavity is increased tremendously.[3,4] While this example deals with a passive device application, scientists at NASA Lewis in Cleveland,Ohio have already developed superconducting FET transistors.[5] The low channel resistance of these devices gives them an extremely high ON to OFF channel resistance ratio (typically 10^7) and the ability to switch at extremely fast rates.

To build exotic devices such as these, reliable fabrication techniques are needed. One such technique is Pulsed Laser Deposition (PLD), which allows the deposition and growth of thin films with a minimum experimental setup.[6] At the bare minimum, all that is required is a laser, optics and a vacuum chamber. A block diagram of a basic PLD system is shown in Figure 1.2.

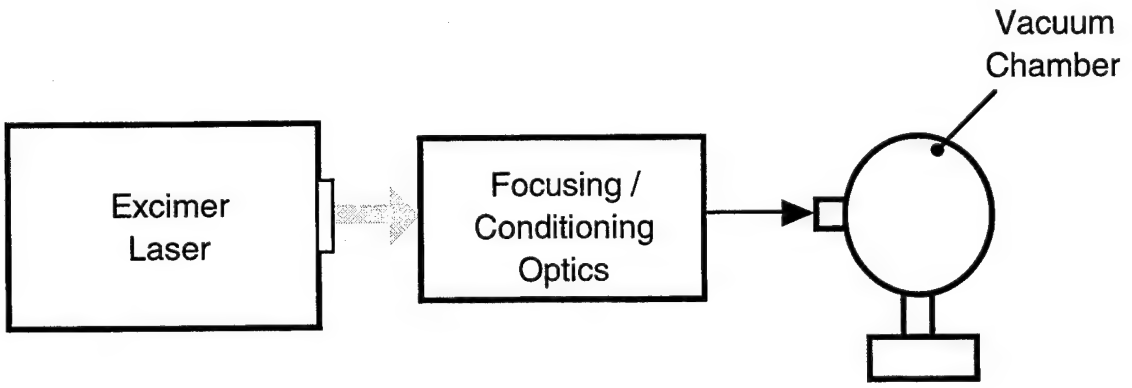

Figure 1.2 - *Block Diagram of Basic PLD System*

The typical laser used is of the excimer type, which emit energy in the ultraviolet region of the spectrum. The output of an excimer is not a continuous beam but is instead a series of extremely short pulses. The lasing medium in

---

[3]Thomas P. Sheahen, *Introduction to High-Temperature Superconductivity*, (New York: Plenum Press, 1994), 11.
[4]Douglas B. Chrisey and Arun Inam, "Pulsed Laser Deposition of High Tc Superconducting Thin Films for Electronic Device Applications", *MRS Bulletin*, February 1992, 37-43.
[5]Kul Bhasin and Robert R. Romanofsky, "Superconducting Field-Effect Transistors", *NASA Tech Briefs*, Vol. 19, No. 7, July 1995, 38.
[6]T. Venkatesan, X.D. Wu, R. Muenchausen, and A. Pique, "Pulsed Laser Deposition: Future Directions", *MRS Bulletin*, February 1992, 54.

excimers is a gas mixture. The gas is usually energized by a charged capacitor discharge into the laser cavity. The charging voltage is typically adjustable (kV range), allowing the operator to adjust the energy output per pulse. The laser pulse width depends directly on the capacitor discharge rate which is in turn related to the gas mixture in the cavity. The major portion of the gas mixture is a buffer gas, usually helium or neon. The buffer gas mediates the energy transfer, but does not contribute to the actual laser emission. The two other gases, a rare gas and a reactive gas, combine to form the excimer molecules. An excimer molecule is an atomic pairing of two constituent atoms that exists only in an excited state. A typical excimer pairing is krypton (rare gas) combining with flourine (reactive gas).[7]

Excimers are capable of delivering tremendous amounts of energy in short pulses. To determine the power delivered by the laser, the output energy (measured in Joules) is divided by the pulse width. With an energy of 1 J per pulse and a 25 ns pulse width, the output power would be approximately 40 MW during the firing time. While this is certainly a huge amount of power, the pulse width is much smaller than the repetition period, which is usually adjustable. At a repetition rate (rep-rate) of 100 Hz, the duty cycle of the pulse output is .00025%. This gives a reasonable figure of 100 W of *continuous* power. This amount of power is typical for commercial excimer lasers.

At the output of the laser are the focusing/conditioning optics. In comparison with other lasers, excimers have fairly divergent beams with large footprints. The beam is almost always focused down to reduce the size of the footprint. It is important to keep the initial focusing lens as close to the laser window as possible. This helps to reduce any energy loss due to beam divergence. If this is not possible, it may be necessary to aperture the beam directly in front of

[7]Jeff Hecht, *The Laser Guidebook*, (New York: McGraw-Hill, 1992), 59-89, 211-234.

the focusing lens. This will center the beam on the lens by blocking the peripheral divergent energy. This is necessary since properly ground lenses have the highest tolerance near the center. Towards the edges, the focused image can become slightly distorted. This can lead to problems with a focused beam due to interference patterns created by the distorted (out of phase) outer-edge energy. The only drawback to using an aperture is that the energy is reduced at the lens. This may be a problem in small lasers.

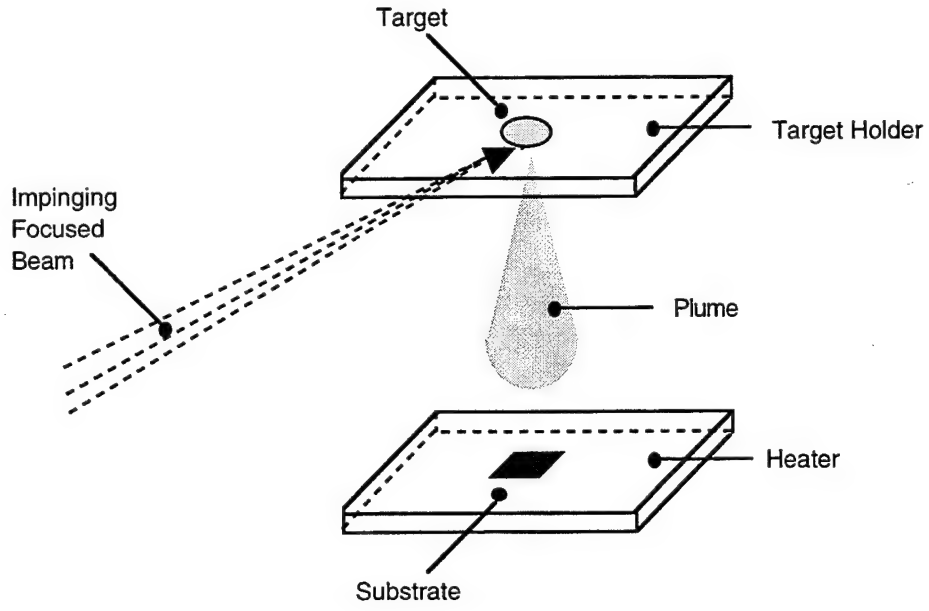

Figure 1.3 - *Laser-Target-Substrate Interaction*

Past the optics is the vacuum chamber, where the deposition takes place. A diagram of the laser, target, and substrate interaction is shown in Figure 1.3. As can be seen, the *target* and the *substrate* face each other. The target is composed of the material that will be deposited and the substrate is the surface onto which this material is deposited. Essentially, the focused beam enters the vacuum chamber and impinges of the target surface. The large amount of energy at the target surface causes material to be evaporated from the surface very rapidly.

This rapid expansion forms a characteristic *plume* of material. The plume constituents themselves (the target material constituents) are extremely excited. It is hoped that the arriving material's constituents will orient themselves in the preferred crystalline state.[8] Whether or not this happens depends on a number of deposition factors.

1.2 Statement of the Problem

Again, if superconducting devices are ever to make the transition from the laboratory to industry, it is necessary to find a way to manufacture them reliably. Research at several institutions has shown that reliable production of superconducting films of adequate quality is difficult. A thorough description of the processes involved in manufacturing thin film superconductors through PLD is not available at this time. These processess must be well understood and controllable for consistent film growth. Controlling the growth of thin films necessitates controlling the system operating parameters, an important fact overlooked in many deposition systems. Examples of the operating paramters are the laser energy and the substrate temperature. If these parameters are not monitored and controlled, it is unlikely that repeatable results can be achieved.

An example of superconductor PLD research is being performed at the Materials Directorate of Wright Patterson Air Force Base under the direction of Dr. Rand Biggers. He and others are attempting to produce high quality superconducting films from YBCO. While some good films have been produced, the *repeatability* of the manufacturing process is questionable. It is quite possible

---

[8]Roger Kelly and Antonio Miotello, "Mechanisms of Pulsed Laser Sputtering", Pulsed Laser Deposition of Thin Films, (New York: John Wiley & Sons, Inc., 1994), 55-85.

that the process repeatability problems are being caused by instabilities in the system operating parameters as discussed above. If, for example, the line voltage driving the heater stage varied over time, the temperature of the substrate would vary as well. If, however, the substrate temperature was measured and recorded, these variations could be tracked. Additionally, it might be possible to stabilize these parameter variations through feedback control.

With these problems in mind, a new PLD system for HTSCs was developed. The new system goes far beyond the basic requirements for a PLD system as shown in Figure 1.2. The solution approach was to develop a system that would serve two purposes, real-time data aquisition and digital control. Implementing the new system required three steps. First, the various system components needed to be selected. This included selecting both a new chamber assembly and the various instruments to monitor or control the deposition procedure (referred to as 'system assembly'). Second, the deposition procedure needed to be automated. This includes both automatically collecting data and allowing the operator to change system parameter settings from one central location. Data collection is especially important so that system changes can be tracked. As a final goal, some amount of feedback control was desired. This is necessary for any hope of deposition repeatability.

CHAPTER 2 - METHOD OF APPROACH

To achieve the three goals of a new chamber assembly, real-time data acquisition/system automation, and system feedback control, a completely new PLD system was designed. The following sections will describe each step in the complete process.

2.1 System Assembly

The first step in implementing the system was to purchase and build a new chamber assembly. This included purchasing a new chamber, heater stage, target holder, and vacuum pump station. The chamber, heater stage, and target holder were all purchased from Neocera. The pump station was purchased from Leybold.

Figure 2.1 shows diagrams of both the heater stage and target holder. As can be seen, the target holder has the capability of holding up to six targets. This is important for multi-layer depositions, where the material in each layer is different. The diagram also shows that the each of the target holders themselves rotate. This is important to minimize target damage. Continuously ablating a target in the same spot causes a hole to be formed. If the hole is deep enough, the plume will narrow considerably. Additionally, the amount of material that comes off will decrease rapidly.[9,10]

---

[9]T. Venkatesan, X.D. Wu, R. Muenchausen, and A. Pique, "Pulsed Laser Deposition: Future Directions", *MRS Bulletin*, February 1992, 55.

[10]A. Bourdillon and N. X. Tan Bourdillon, *High Temperature Superconductors: Processing and Science*, (California: Academic Press, 1994), 141.

The heater stage is a standard 600 W heater with an integrated thermocouple connection. It is capable of heating the substrates above 800° C. As can be seen, a substrate shutter is integrated in the design. Prior to a deposition, the target is usually cleaned to remove surface imperfections (due to handling, polishing, etc.). Research has shown that the outer layers of a target may not be stochiometrically correct due to handling, etc. An effective way to clean the target is to ablate the surface at low power levels. However, it is necessary to cover the substrate during cleaning to avoid possible contamination of the substrate surface. The cover simply slides in front of the substrate during cleaning.

The pump station is actually a combination of two pumps, a rotary vane pump, and a turbo-molecular pump. The rotary vane pump is used to quickly evacuate the system, while the turbo pump takes over when the pressure drops below 200 mT.

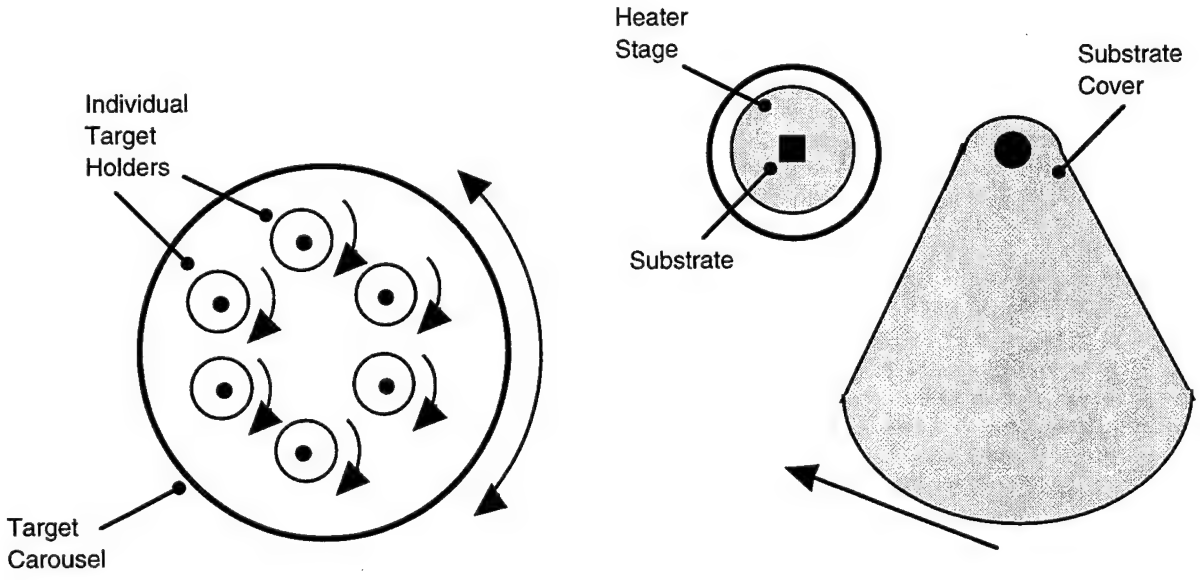

Figure 2.1 - *Target Holder and Substrate Heater*

In addition to the chamber assembly, it was necessary to select the instruments that would be used in the new system. This includes things such as the

laser used, the number and type of vacuum gauges used, etc. A complete list of the instruments/equipment used in the new system is given in Appendix B.

2.2 Data Acquisition and Deposition Process Automation

The deposition system is built around a Macintosh IIfx computer and three National Instruments' I/O cards. A block diagram of the system is shown in Figure 2.2. As can be seen from the diagram, there are four types of communication interfaces used in the system. The type of interface used depends entirely upon the capabilities of the instrument. Appendix B discusses these interfaces in detail.

National Instruments' LabVIEW was used to write the software that directs each of the instruments. The automation software was written with the intent of giving the operator as much or more instrument control than the previous manual system while at the same time making routine tasks easy. For instance, instruments and equipment can be set up automatically through the use of instrument data files. If, however, tests or calibration sequences need to be performed on certain pieces of equipment (e.g. laser, mirror controller), extensive instrument calibration and setup screens are available at the touch of a button. These setup screens, called 'front panels', have the capability to generate new setup data files which can be recalled and used at a future date. Additionally, process setpoints can be changed at any time during a deposition. This includes laser settings, temperature settings and pressure settings. All of the software is discussed in Appendices A and B. The software flowchart is given in Appendix C.

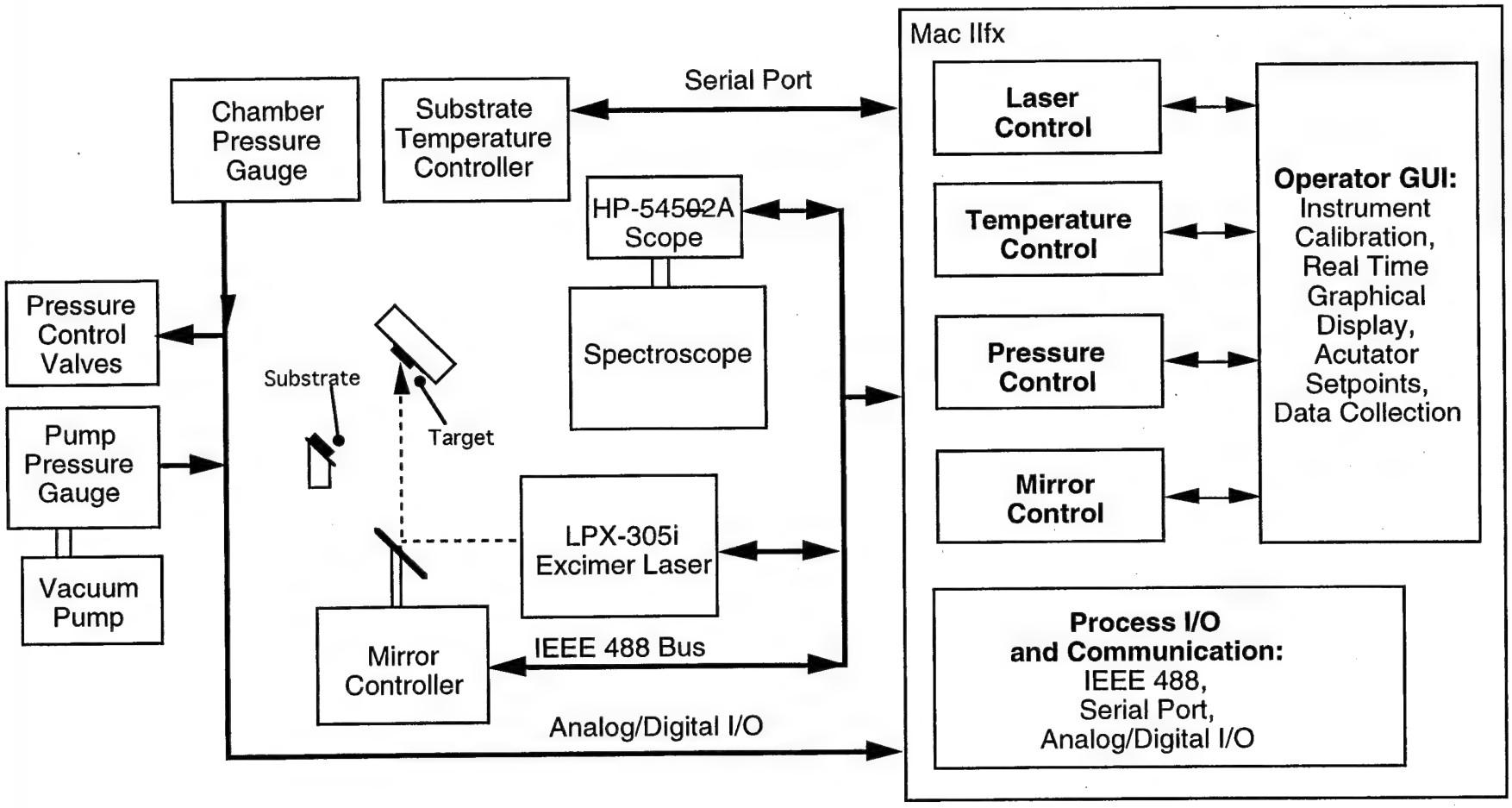

Figure 2.2 - *PLD System Architecture*

2.3 System Environmental Control Desciption

As a first step in determining the direction the control effort would take, the literature was examined to determine what deposition parameters affect the quality of PLD produced films, specifically YBCO films. A process influence diagram was then constructed as a result of this search. It is shown in Figure 2.3. As this figure shows, the important properties of the film are its morphology and stoichiometry. The stoichiometry of the film is a measurement of the specific chemical structure in the grains of the film while the morphology refers to the overall uniformity of the film (e.g. rough vs. smooth).

In order to adequately control the process, a hierarchical control structure based on the work of Garrett et al[11,12] was proposed. Figure 2.4 shows the proposed hierarchical control structure for PLD of YBCO. This control structure is divided into three distinct levels, each serving a different purpose. The three levels are the environmental level, the insitu level, and the qualitative level.

The process environmental level is where all actuations occur. The variables under control at this level tend to be limited to first-principle type quantities, such as temperature, pressure, level, and flow. From Figure 2.4, the proposed enviornmental control variables for the PLD system are the substrate temperature, the chamber O_2 process, the beam position on the target, and the laser energy per pulse. Note that the two other environmental variables at this level are the laser repetition rate and the deposition length. While these variables are presumably important for determining film characteristics, they require no special control (i.e. they are simply set to some value).

---

[11]Patrick H. Garrett, "Insitu Subprocess Control: Advanced Automata for Process Industries", To be submitted to *IEEE Transactions on Systems, Man, and Cybernetics*.

[12]Douglas C. Moore, "Subprocess Control Design Methods For Advanced Materials Processing", Master's Thesis, Electrical and Computer Engineering, University of Cincinnati, 1994.

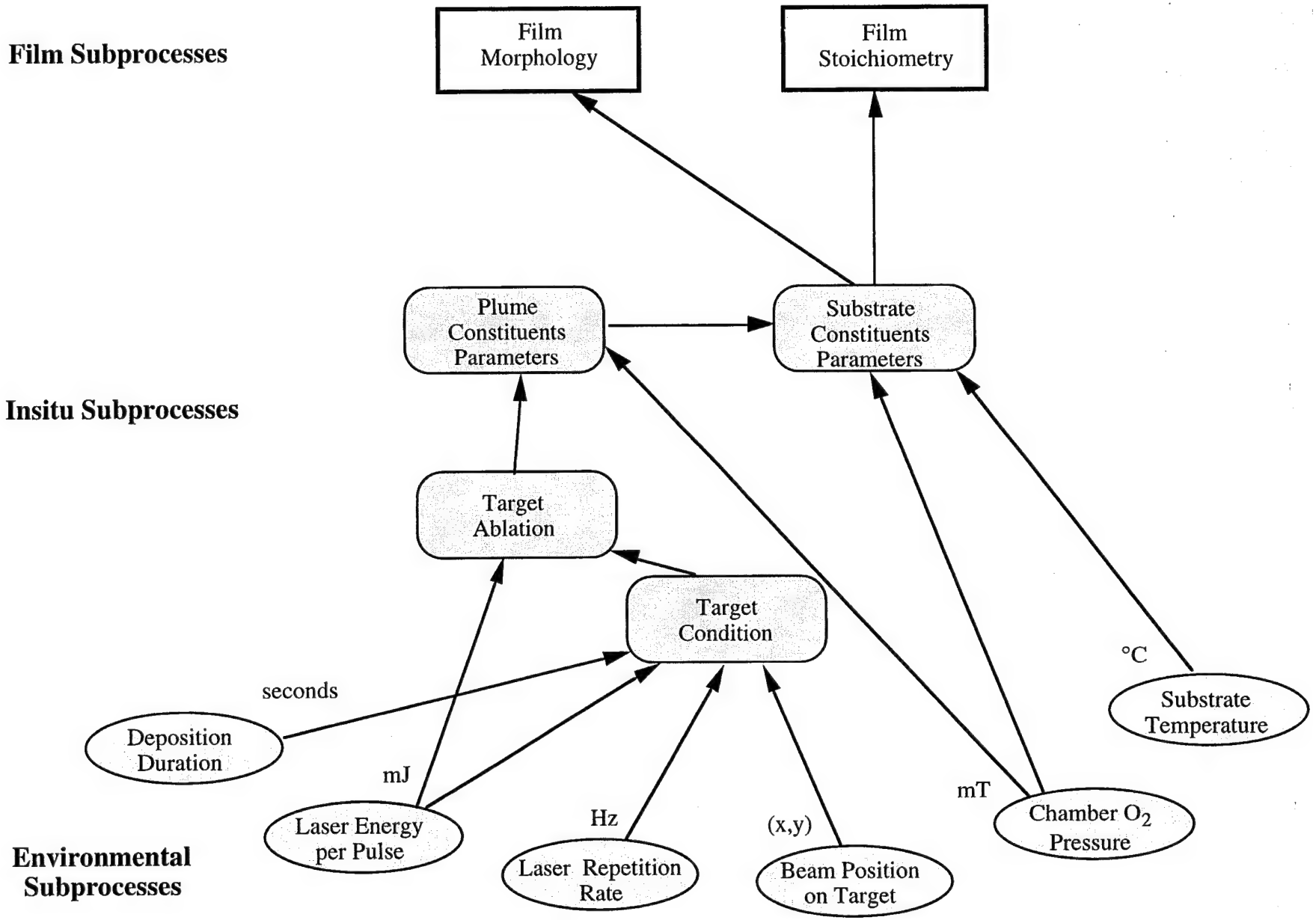

Figure 2.3 - *PLD Influence Diagram*

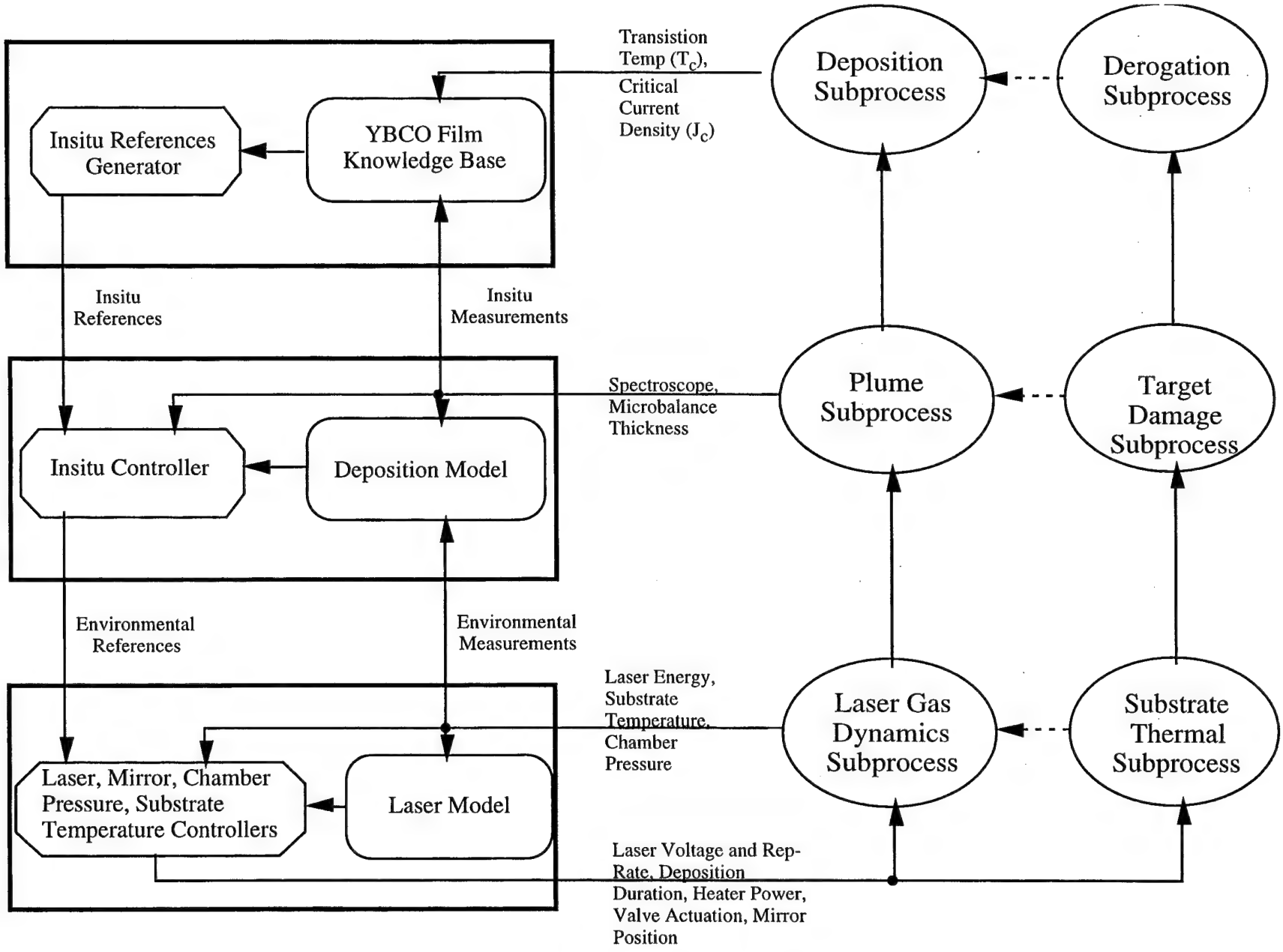

Figure 2.4 - *Proposed PLD Control Hierarchy*

The next level of control in the hierarchical control structure is the insitu level. Process variables at this level are not directly actuatable, but are instead the result of the actuation of one or more enviormental variable setpoints. If the process is static, insitu measurements will be useless. However, changing system conditions that are either uncontrollable (directly) or unaccounted for (system models are inaccurate) can be compensated out provided insitu measurements can detect them. Examples of these types of measurements in PLD systems are variables such as the the type and amount of a given plume constituent. Note that this type of a control variable is considered to be insitu since there is no setpoint 'control knob' for this variable. It is not *directly* controllable. It is instead a function of various environmental variables, such as the chamber oxygen pressure (see Figure 2.3).

The last and highest level in the hierarchical control structure is the qualitative level. This level is used to compensate for unmodeled process dynamics. The decision making portion of this level is usually implemented as an expert system. Regardless, the data the qualitative controller is based on is an input to output mapping generated from the combination of offline measurements of the end product's properties and insitu sensor measurements.

Rather than attempting to implement each of the three levels of control in addition to implementing all of the required software/hardware, the environmental level was concentrated on. From this level, four enviornmental variables were stabilized. As discussed before, these include the laser energy, the substrate temperature, the chamber pressure, and the mirror position on the target. Additionally, insitu plume changes were measured using a 2-channel fluorescence spectroscope. This was done to determine whether or not an insitu controller was needed. The following sections will discuss both the environmental control structure and the insitu level sensor techniques.

2.3.1 Laser Control Structure

The need for some type of laser control structure is based on two important requirements. The first requirement is that the operator (or computer control software) be able to specify a specific energy requirement at a given rep-rate. The problem is that the actual settable laser parameters are the cavity voltage and the rep-rate. The combination of these two parameters determine the actual output energy. The ability to specify a given energy as opposed to a laser voltage setting is important if the deposition software will be used on different lasers, since each laser has a specific voltage/rep-rate to energy relationship. Laser voltages are essentially meaningless even if they are used to describe a specific laser. This is because the laser output energy varies considerably from day to day, primarily due to the gas mixture's age. Growth conditions are always given as a measured laser energy at a given rep-rate; they are never described by a given voltage setting.

The second requirement deals with the fact that the laser dynamics themselves may change during a deposition. This implies some type of feedback control. For instance, the energy output of the laser is directly related to the length of time it is run. Specifically, the energy output increases as the laser heats up. Also, the gas-fill age may become important in deciding output energy. As the gas ages, the energy output decreases. During long depositions, it may be necessary to increase operating voltages slightly to compensate for this.

To meet these requirements, a two component control structure was implemented. A block diagram of the control structure is shown in Figure 2.5. The two control components are the lookup table and the PID controller/FIR filter combination. The lookup table maps a given voltage/rep-rate combination to a specific energy output (first requirement) while the PID controller tracks dynamic

changes in the laser (second requirement). Each of these pieces will be discussed in detail.

2.3.1.1 Lookup Prediction Table

The requirement that the deposition controller (operator or control software) be able to specify an energy requirement at a given rep-rate is accomplished via the lookup table. Prior to the control structure implementation, laser energies were estimated before the actual deposition. These estimates were based on external energy measurements. Typically, the operator would set the laser at a certain voltage and rep-rate and adjust the voltage setting up or down based on the observed response. The laser rep-rate was usually set to two Hz because the external power meter is not accurate above this frequency. During the actual deposition, however, the rep-rate is usually set much higher than this. It was shown through extensive experiments that the energy delivered per pulse varies significantly based on the rep-rate setting. Two three dimensional plots of the laser

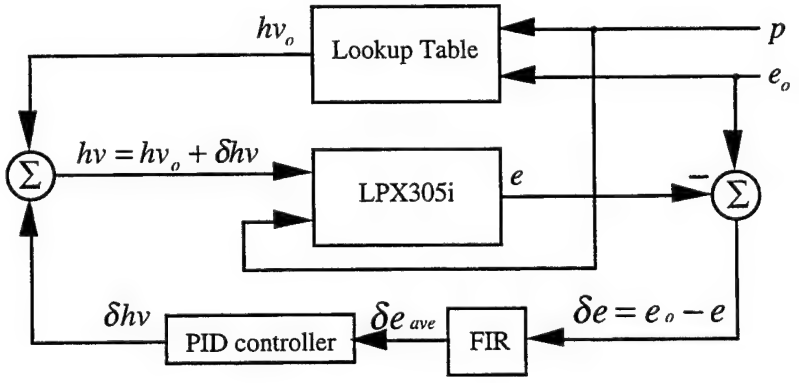

Figure 2.5 - *Laser Control Structure*

characteristics (energy as a function of laser voltage and rep-rate) are shown in Figure 2.6 (a) and (b).

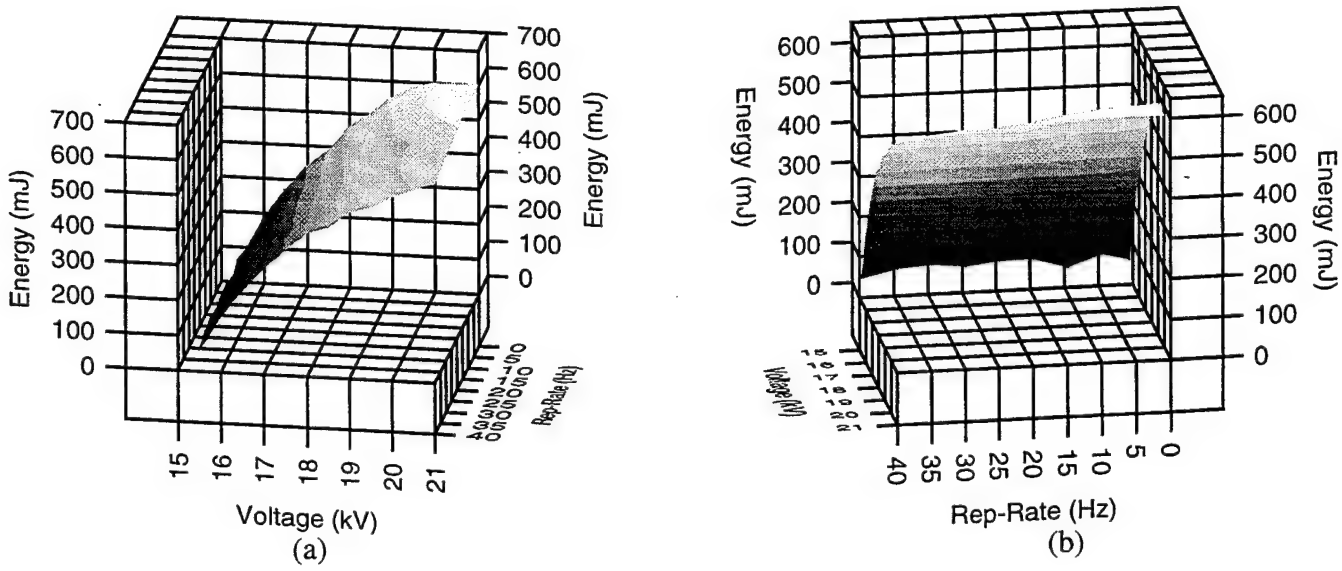

Figure 2.6 (a) and (b) - *Laser Energy Response*

These two plots were generated from the same experimental data set. They are rotated in each case so that the relationships between energy and cavity voltage or rep-rate are more clear. As expected, Figure 2.6 (a) shows that the energy delivered per pulse is highly dependent on the laser voltage, i.e. the greater the cavity voltage, the greater than energy. Perhaps unexpectedly, Figure 2.6 (b) shows that the energy *decreases* as the rep-rate *increases*.

This 3-D surface is what the lookup table is based on. It essentially serves as a prediction tool. From the block diagram in Figure 2.5, e_0 represents the desired energy, *rr* is the rep-rate setpoint, and hv_0 is the table's output laser set voltage. To illustrate its use in the control structure, a small portion of a sample table is shown in Table 2.1. Note that the first row and column are not actually part of the table; they are shown to aid in understanding how the table works.

	Voltages (kV):			
Rep-Rates (Hz):	15.5	16	16.5	17 . . .
1	40	80	171	226 . . .
5	35	72	122	214 . . .
10	35	66	143	203 . . .
15	30	60	137	200 . . .
.	.	.	.	. .
.	.	.	.	. .
.	.	.	.	. .

Table 2.1 - *Portion of Lookup Table*

Each number in the table corresponds to a measured energy in mJ for a given voltage and rep-rate. For example, at a rep-rate of 5 Hz with a cavity voltage of 16.5 kV, the energy output was found to be 214 mJ. The rep-rate extends to 40 Hz in 5 Hz increments (increasing number of rows) and the voltage extends to 21.0 kV in .5 kV increments (increasing number of columns). In this way the table size is kept small, containing only 108 entries. If each possible voltage/rep-rate combination was represented, it would contain 2200 elements. Since opening and closing the table each time a new voltage setpoint is needed is time-consuming, it is necessary to keep the table in memory. This requires that the table be relatively small to avoid taking up a large amount of system memory. Besides this, generating an initial table with each data point would take at least a week.

Since the table is incomplete in the sense that every voltage/rep-rate combination is not represented, it is necessary to use some type of interpolation scheme for in between points. The interpolation procedure can best be described as two linear 2-D interpolations over the 3-D surface function.

To illustrate the interpolation procedure, we will consider an example based on the partial table of Table 2.1. Given a desired energy at a required rep-rate, the two steps required to interpolate a laser voltage are as follows:

Step 1) Interpolate two possible set voltages voltages based on two distinct rep-rates and the desired energy.

Step 2) Interpolate one output voltage based on two distinct rep-rates and the two voltages from Step 1.

Suppose the operator (or controller) wants an energy of 100 mJ at 13 Hz.

Step 1: - Interpolate two voltages based on two distinct rep-rates and the desired energy.

First, we determine what interval the required rep-rate falls into based on Table 2.1. Quite obviously, the rep-rate interval is from 10 Hz to 15 Hz. These are the two distinct rep-rates, and they are called R_{min} and R_{max}. Since the procedure for finding a desired voltage (one of the two interpolation voltages) at either R_{max} or R_{min} is the same, we will consider only the R_{min} case. The voltage interpolated at R_{min} will be called $hv_{des\ @\ Rmin}$. For the 10 Hz row, it is seen that the desired energy (e_{des}) falls between the 16 and 16.5 kV columns. These will be called $hv_{min\ @\ Rmin}$ and $hv_{max\ @\ Rmin}$. From here, we can simply linearly interpolate between 66 mJ and 143 mJ to find $hv_{des\ @\ Rmin}$. From Figure 2.7, it is seen that we are in the R_{min} plane. Note that the interpolation itself is based on the two voltage values $hv_{min\ @\ Rmin}$ and $hv_{max\ @\ Rmin}$. Since we are in the Rmin plane, it is not considered to be part of the interpolation. Working through the basic linear interpolation,

General linear interpolation equation:

$$y = mx + b$$

$$hv_{\text{des}} = \left(\frac{hv_{\max} - hv_{\min}}{e_{\max} - e_{\min}} \right) \bullet e_{\text{des}} + hv_{\text{int}}$$

solving for hv_{int} with $e_{des} = e_{min}$ and $hv_{des} = hv_{min}$,

$$hv_{int} = hv_{des} - \left(\frac{hv_{max} - hv_{min}}{e_{max} - e_{min}} \right) \bullet e_{des}$$

$$= 16.0\,\text{kV} - \left(\frac{16.5\,\text{kV} - 16.0\,\text{kV}}{143\,\text{mJ} - 66\,\text{mJ}} \right) \bullet 66\,\text{mJ}$$

now solving for hv_{des},

$$hv_{des} = \left(\frac{16.5\,\text{kV} - 16.0\,\text{kV}}{143\,\text{mJ} - 66\,\text{mJ}} \right) \bullet 100\,\text{mJ} + 15.57\,\text{kV}$$

$$hv_{des} = 16.22\,\text{kV}$$

Now that we have an hv_{des} for R_{min}, we can find an hv_{des} for R_{max}. In this case, $hv_{des\ @\ Rmax}$ is 16.25 kV.

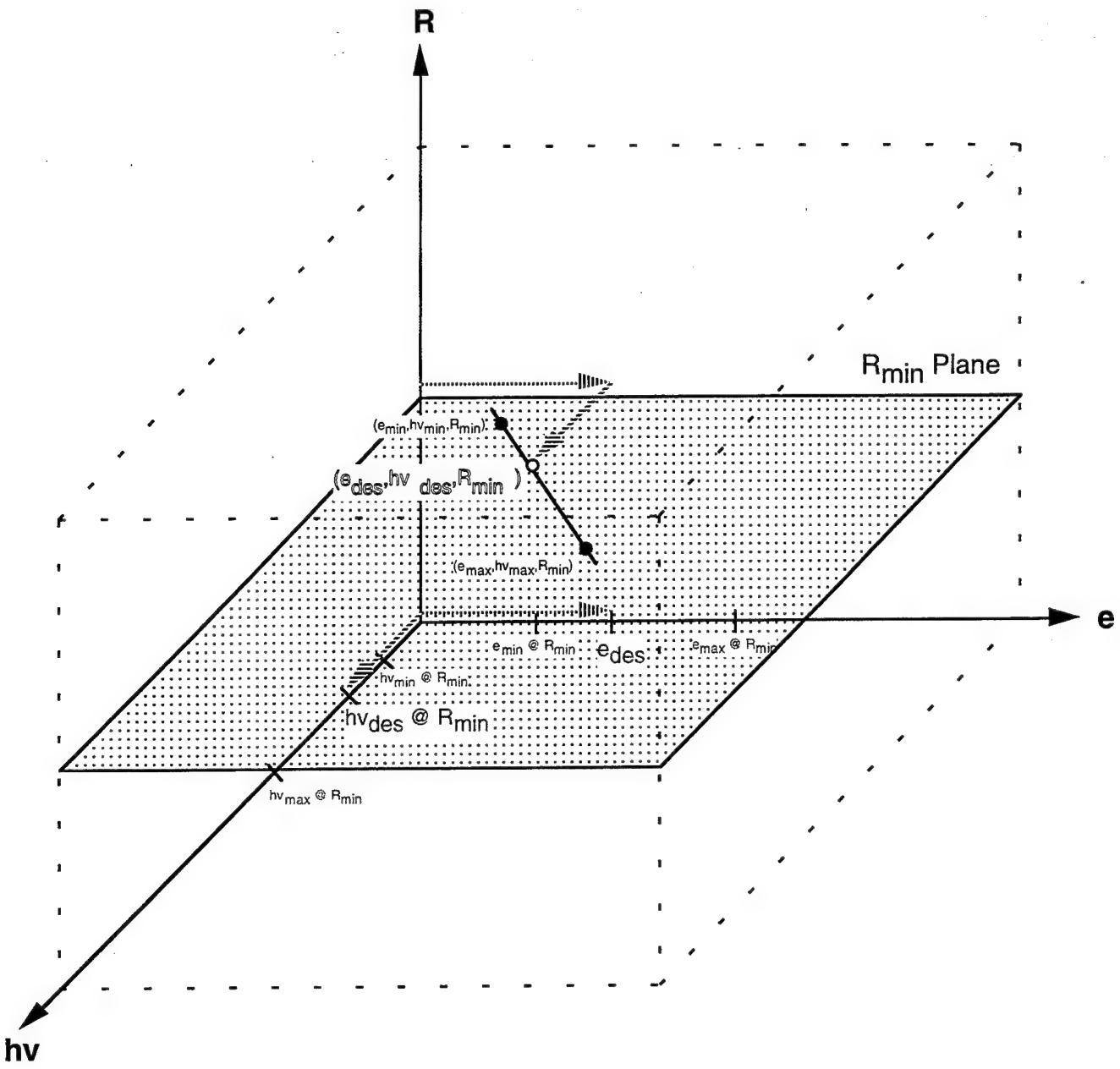

Figure 2.7 - *Linear Interpolation in R_{min} Plane*

Step 2. - Interpolate one output voltage based on two distinct rep-rates and the two voltages from Step 1.

We now have $hv_{des\ @\ Rmax}$ and $hv_{des\ @\ Rmin}$. Note that these two voltages are both at the desired energy of 100 mJ. Therefore, we can then linearly

interpolate the actual set voltage through the desired rep-rate and a linear equation representing the relationship between $hv_{des\ @\ Rmax}$ and $hv_{des\ @\ Rmin}$. Figure 2.8 shows the graphical representation. Again, since we are in the desired energy plane (e_{des} plane), this term is eliminated. This completes the 3-D interpolation by successive 2-D interpolations.

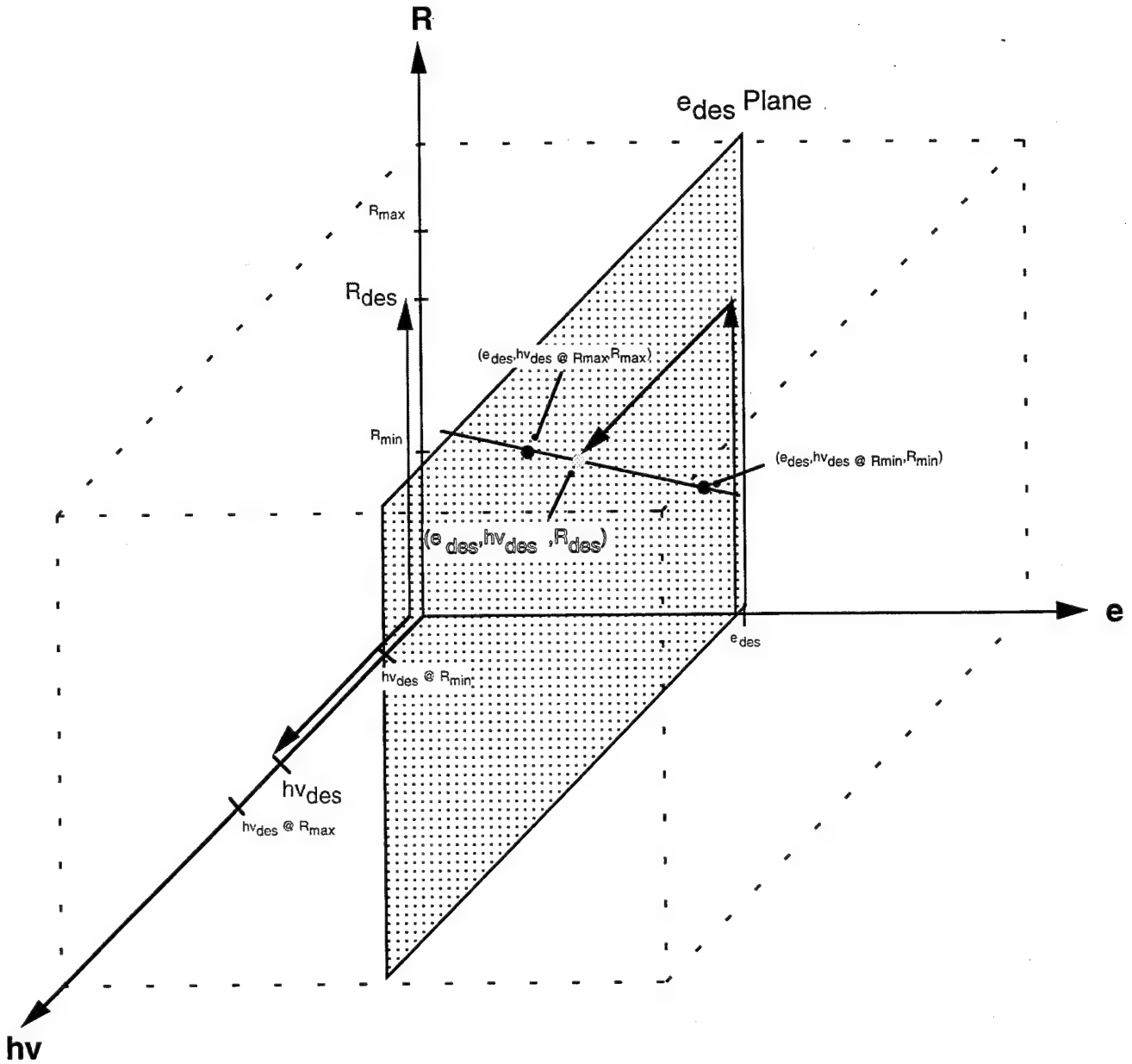

Figure 2.8 - *Linear Interpolation in e_{des} Plane*

Essentially, the lookup table serves as a model for the laser energy response based on cavity voltage and rep-rate. However, it is still necessary to generate an initial table from which future energy predictions can be made. This was done by developing a software routine to characterize the laser. The software randomly assigns one of the possible 108 voltage/rep-rate combinations to the laser and then collects internal energy monitor data for two minutes. This data is then averaged by dividing the total energy by the number of energy samples taken during the test. Note that each of the 108 possible combinations is tested one time. The laser modeling software randomizes the voltage/rep-rate assignments so that any test based biasing would be minimized. An example of possible test bias is to keep the rep-rate constant while ramping the voltage up one increment (.5 kV) consecutively. Excimer lasers exhibit the characteristic that received energy increases as the laser cavity heats up. This heating rate is strongly related to the energy discharged into the cavity at each pulse, which is in turn strongly related to the cavity voltage. The table will obviously reflect this bias if the test was completed in this fashion.

This approach would be fine if control variations such as this were to be expected. If, however, the PLD process is dynamic, this approach might not be adequate. As system conditions change, it is necessary that the table be as accurate as possible in any direction (i.e. any possible change in the energy requirement should give an accurate voltage/rep-rate setting, regardless of the new energy's position in the table).

The major problem with the lookup table approach is that the laser characteristics can change on a daily basis. For example, gas-fill age can significantly degrade the received energy. Along with gas-fill age, gas purity can significantly affect the received energy (this becomes an issue when gas bottles are

changed). The obvious answer to keeping the lookup prediction table up-to-date is to just re-run the laser characterization software. However, at two minutes per test and 108 possible test combinations, the length of time required to complete the whole test is prohibitive, at least on a daily basis. Therefore, a simple updating procedure was developed. Essentially, the laser is run at four distinct voltage/rep-rate combinations for thirty second intervals. The table is then updated based on these measurements prior to each deposition.

The procedure consists of the three steps as listed below. A description of each step is also given below this list.

Step 1) Run the laser at a constant 15 Hz rep-rate with voltages of 15.5 kV, 17.0 kV, 19.0 kV, and 21.0 kV. Collect internal energy readings for 30 seconds at each voltage.

Step 2) Find the difference between the predicted energy value (from the table) and the actual energy output (average over 30 seconds) for each test point and fit a cubic spline function to these four differences.

Step 3) With the above function, determine the error values for the remaining eight voltages. Algebraically add the set of twelve error values to each row in the table.

Step 1: In this step, the laser is automatically run for thirty second intervals at each voltage as listed above. These voltages span the entire range of possible setpoints in the sense that the two endpoints are covered along with two in-between points. The reason that the rep-rate is left fixed is because experiments have shown that the output energy is much more dependent on laser voltage than rep-rate. This relationship is shown in Figures 2.9 (a) and (b).

Figures 2.9 (a) and (b) show the energy response with the voltage fixed at 17.0 kV (rep-rate varying) and the rep-rate fixed at 15 Hz (voltage varying) respectively. Note that the energy change due to voltage changes are much more profound than that of rep-rate changes. The next graph also shows that rep-rate is somewhat important as well. Note that Figure 2.10 is simply Figure 2.6 (a) projected into two dimensions. The shaded regions represent the effect of the rep-rate on the energy received. The top and bottom edges of the projected curve represent 1 Hz and 40 Hz respectively. Note that higher voltages show a greater energy reduction due to increasing rep-rates. By testing only one rep-rate, the software assumes that the general curve shape at each rep-rate is similar.

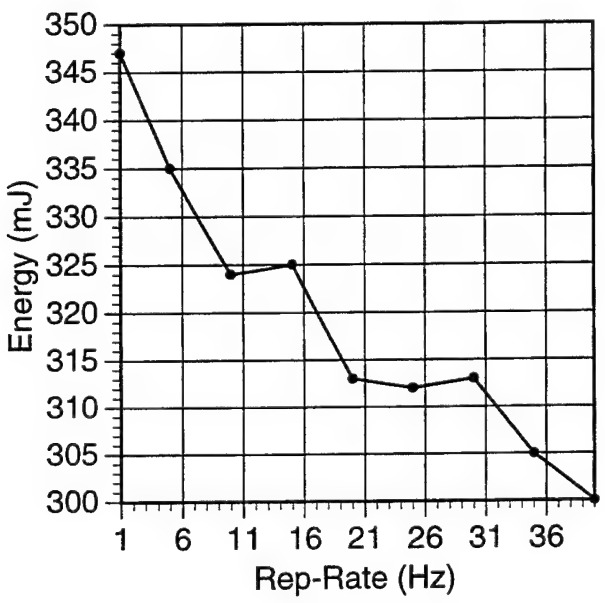

(a) Fixed Voltage

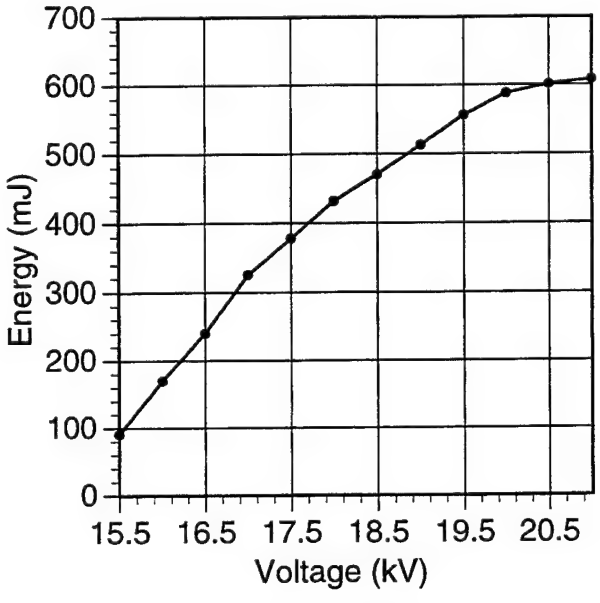

(b) Fixed Rep-Rate

Figure 2.9 (a) and (b) - *Laser Energy With a Fixed Voltage or Rep-Rate*

Step 2: Now that data has been collected at four data points, the next step is to spline fit a function to the *difference* of the previous table energy values and the new energy values. This was done by fitting a cubic spline between each

set of error points. Any of a number of curve fitting techniques could have been used in the curve fitting software. However, a simple linear fit over the whole set of error points would have given a fairly poor fit. This is obvious when looking at the laser characteristics curve. Regardless, cubic spline functions were used because the data has smooth regions which spline functions handle well. In addition, they also have the useful property of passing through every supplied data point.[13]

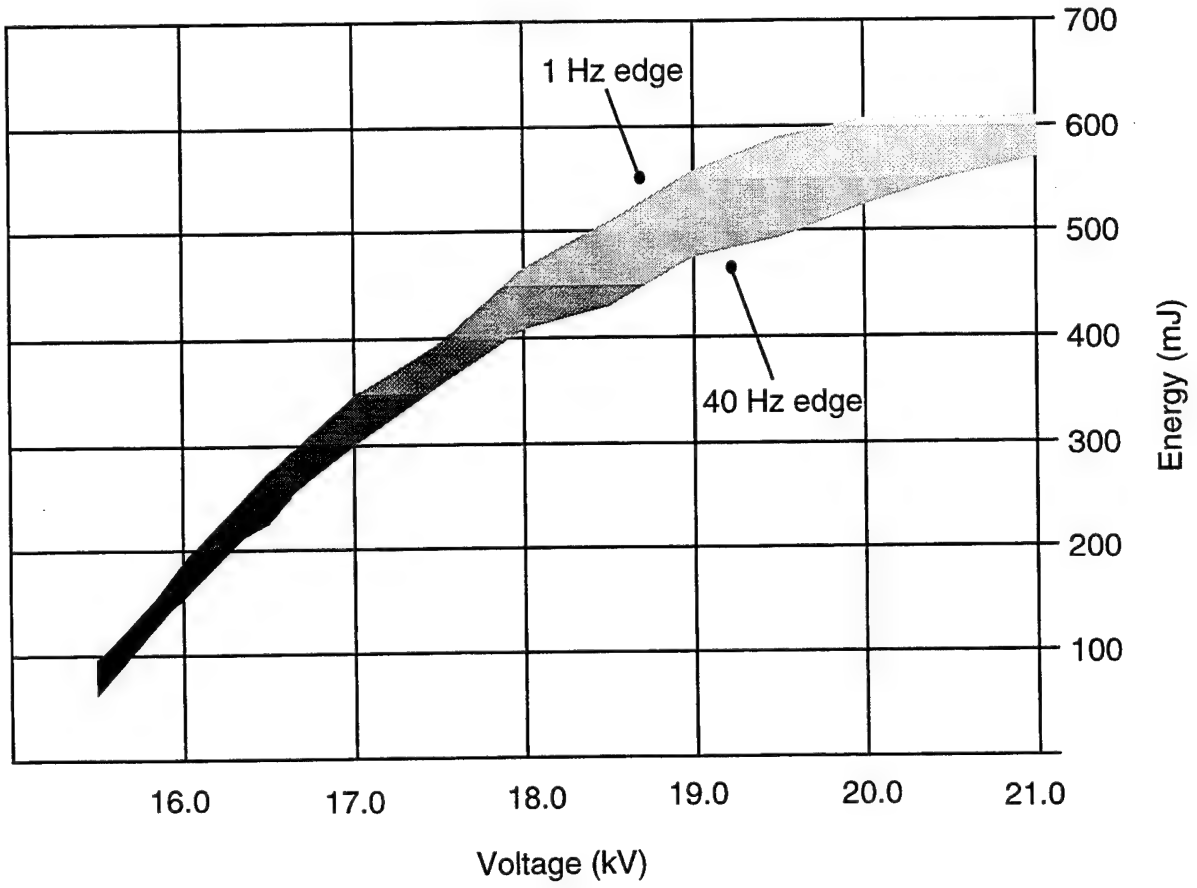

Figure 2.10 *-3-D -> 2-D Projection of Laser Energy*

Step 3: The final step is to algebraically add the spline function error value to

[13]Curtis F. Gerald and Patrick O. Wheatley, *Applied Numerical Analysis*, (Massachusetts: Addison-Wesley Publishing Company, 1994), 233-244.

each energy value in the table along the rep-rate rows. Although data was only collected for a rep-rate of 15 Hz, the function derived from this is applied to every rep-rate row. This was done so that the table update procedure is fairly fast (two minutes). If each rep-rate were tested, the update procedure would be increased to about an hour, by which time the laser characteristics would have probably changed.

2.3.1.2 PID Controller/FIR Filter

The PID Controller/FIR Filter combination is the second part of the overall laser control. Since the FIR filter drives the PID controller, it will be discussed first. Figure 2.11 shows a block diagram of the FIR filter itself.

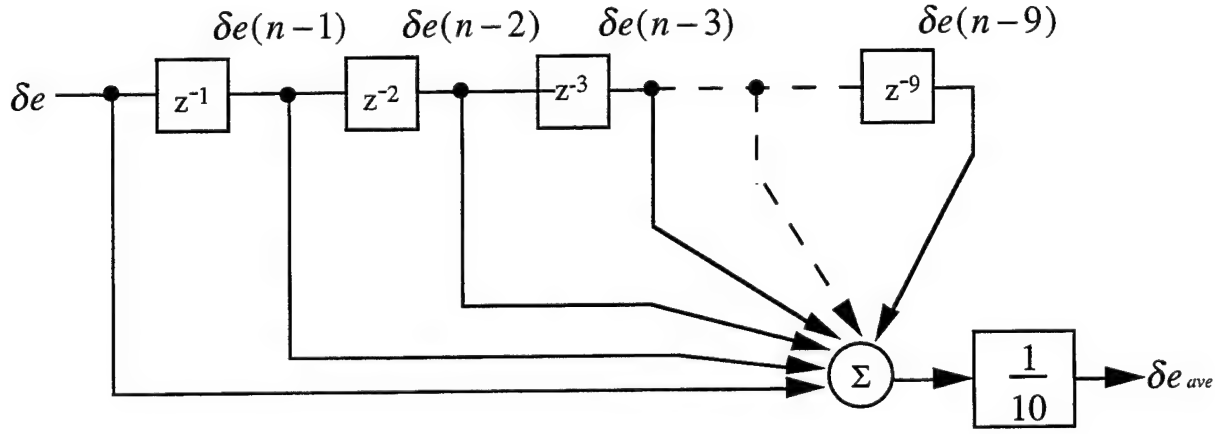

Figure 2.11 - *Laser FIR Filter*

The diagram shows that the controller is a simple non-recursive filter described by the difference equation

$$\delta e_{ave}(n) = \frac{1}{10} \bullet \sum_{k=0}^{k=9} \delta e(n-k)$$

where $\delta(n)$ is the current energy error, $\delta e(n - k)$ are the past k error terms, and $\delta e_{ave}(n)$ is the average of the past k error terms output voltage correction.[14] The purpose of this simple moving average filter is to filter the error signal. This is necessary beacause the error signal is very noisy. The noise is simply a function of the laser's characteristics, as all excimer lasers exhibit a significant amount of pulse-to-pulse variation. Figure 2.12 shows how drastic this variation can be. The FIR filter helps to keep the PID controller stable.

A block diagram of the PID controller is shown in Figure 2.13, where K_P, K_D, and K_I are the proportional, derivative, and integrating gain respectively.[15] Again, the PID Controller's main purpose is to track any dynamic laser changes. It also helps to correct for errors in the lookup table predictions. A major source of error comes from the fact that the table itself is incomplete. To keep the table size small, only 108 of the possible 2200 voltage/rep-rate combinations are represented. Therefore, a major source of the prediction error deals with the linear interpolation scheme used for in between (not represented) table entries. Prediction values may also be inaccurate due to the table update procedure since it only spline fits four data points and assumes that the general curve shape at each rep-rate is fairly consistent.

---

[14]Robert D. Strum and Donald E. Kirk, *First Principles of Discrete System and Digital Signal Processing*, (Massachusetts: Addison-Wesley Publishing Company, 1989), 529-608.

[15]Benjamin C. Kuo, *Automatic Control Systems*, (New Jersey: Prentice-Hall Inc., 1982), 539.

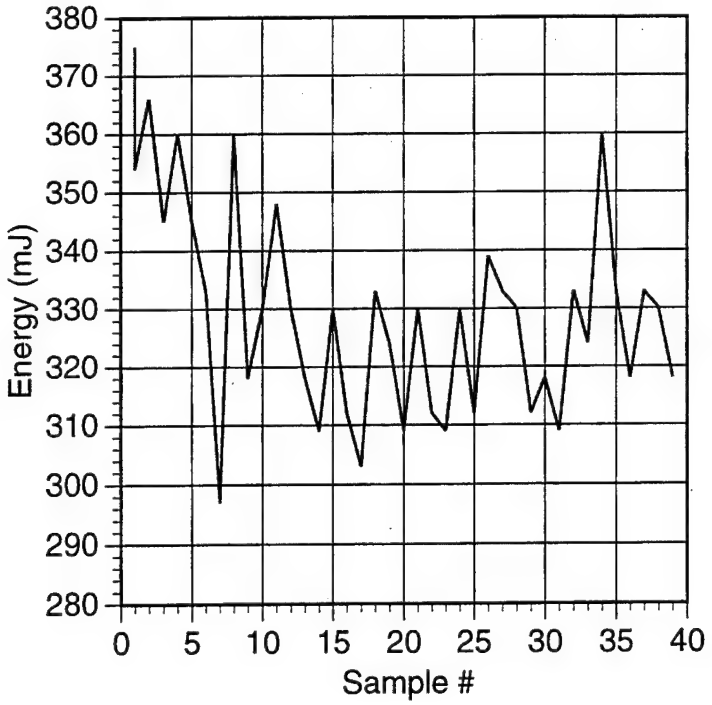

Figure 2.12 - *Shot-to-Shot Laser Energy Variation*

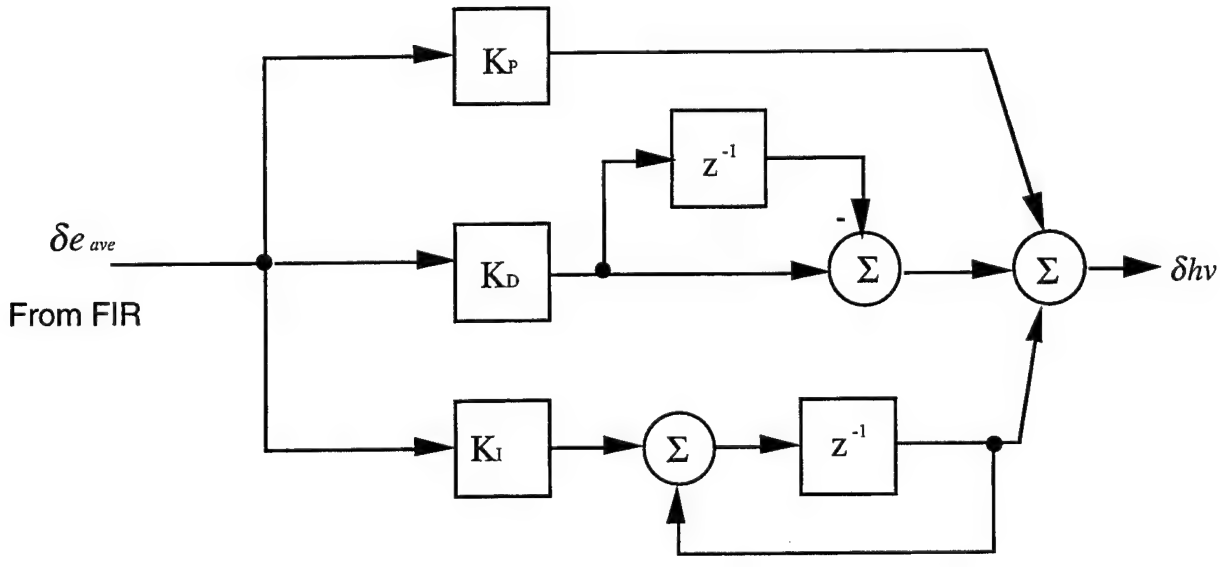

Figure 2.13 - *Laser PID Controller*

It might seem that a simple P controller could be used, since in theory the input signal is free from noise. To decrease the steady state error, the gain would simply be increased. This tends to increase the overshoot significantly. If a simple proportional controller is used, the controller is somewhat unstable at high gain settings. In terms of average energy and energy standard deviation, the performance of the 'compensated' system is in fact worse than the uncompensated system. The integrator serves the purpose of driving the steady-state error to zero. In this way, a small proportional gain can be used but the steady state error will still approach zero. In the case of large table errors, the proportional output will dominate, attempting to quickly compensate for the error. For small errors, the proportional output will have no effect, but the integrator will still attempt to zero the error, since all of the little errors will add up. In the case of actuator saturation (i.e. the laser voltage hits the maximum or minimum allowable setting), the software turns off the integrating action. This serves as a protection mechanism against integrator windup. To make the system even more stable, the derivative term was added. Without the FIR filter (running average), the derivative term would instead make the controller highly unstable. This is because the derivative term would be taking the derivative of a very noisy signal. By using a weighted average, the input signal is much more stable.

The values for the proportional, derivative, and integrating gains were chosen based on trial-and-error tests. These tests attempted to maximize the correction speed of the controller while still keeping the system stable. Since it may be necessary to re-tune the controller, these gain values are operator accessible.

2.3.2 Substrate Temperature Control Structure

The substrate temperature is regulated automatically through the use of feedback control. The heater provides additional energy for the arriving species to assume the correct crystal positions. Essentially, heating the substrate adds to the mobility of the arriving constituents. It is therefore likely that controlling the substrate temperature is necessary for repeatable results.[16,17] Figure 2.14 shows the system hierarchy, where everything inside the dashed box is part of the feedback control structure. Note that the Macintosh performs two functions, supplying a temperature setpoint, and reading the heater temperature. The control loop itself consists of an LFE PID Controller, a EUROTHERM SCR Driver (phase-angle fired), and the heater stage itself with an integrated thermocouple (type K - chromel/alumel). The hardware and software required to implement the loop are discussed in detail in Appendix A.2.

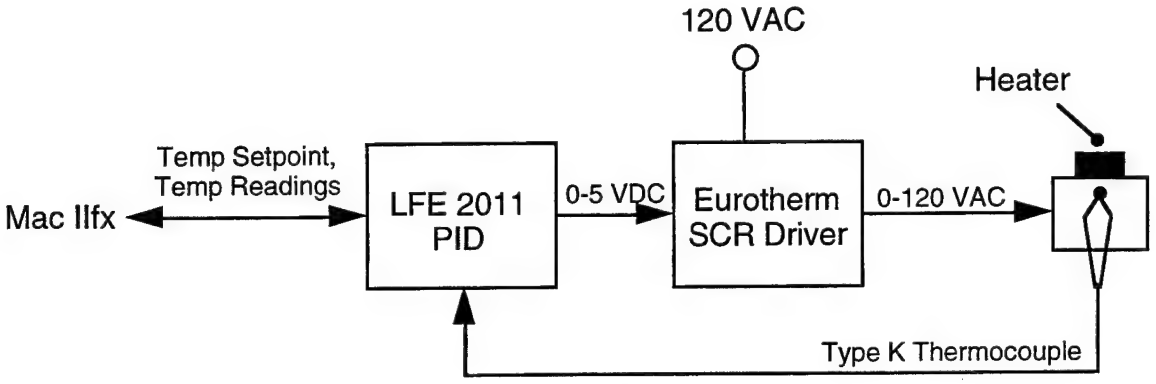

Figure 2.14 - *Substrate Temperature Control Structure*

[16]Graham K. Hubler, "Pulsed Laser Deposition", *MRS Bulletin*, February 1992, 26.
[17]T. Venkatesan, X.D. Wu, R. Muenchausen, and A. Pique, "Pulsed Laser Deposition: Future Directions", *MRS Bulletin*, February 1992, 56

2.3.3 Chamber Pressure Control Structure

Numerous studies have shown that a background oxygen pressure is necessary to grow quality superconducting films. This background gas is absorbed into the substrate during growth.[18] Oxygen pressure regulation is accomplished via an ON/OFF type control structure using pneumatically actuated vacuum-grade valves. A schematic diagram of the gas flow system is shown in Figure 2.15.

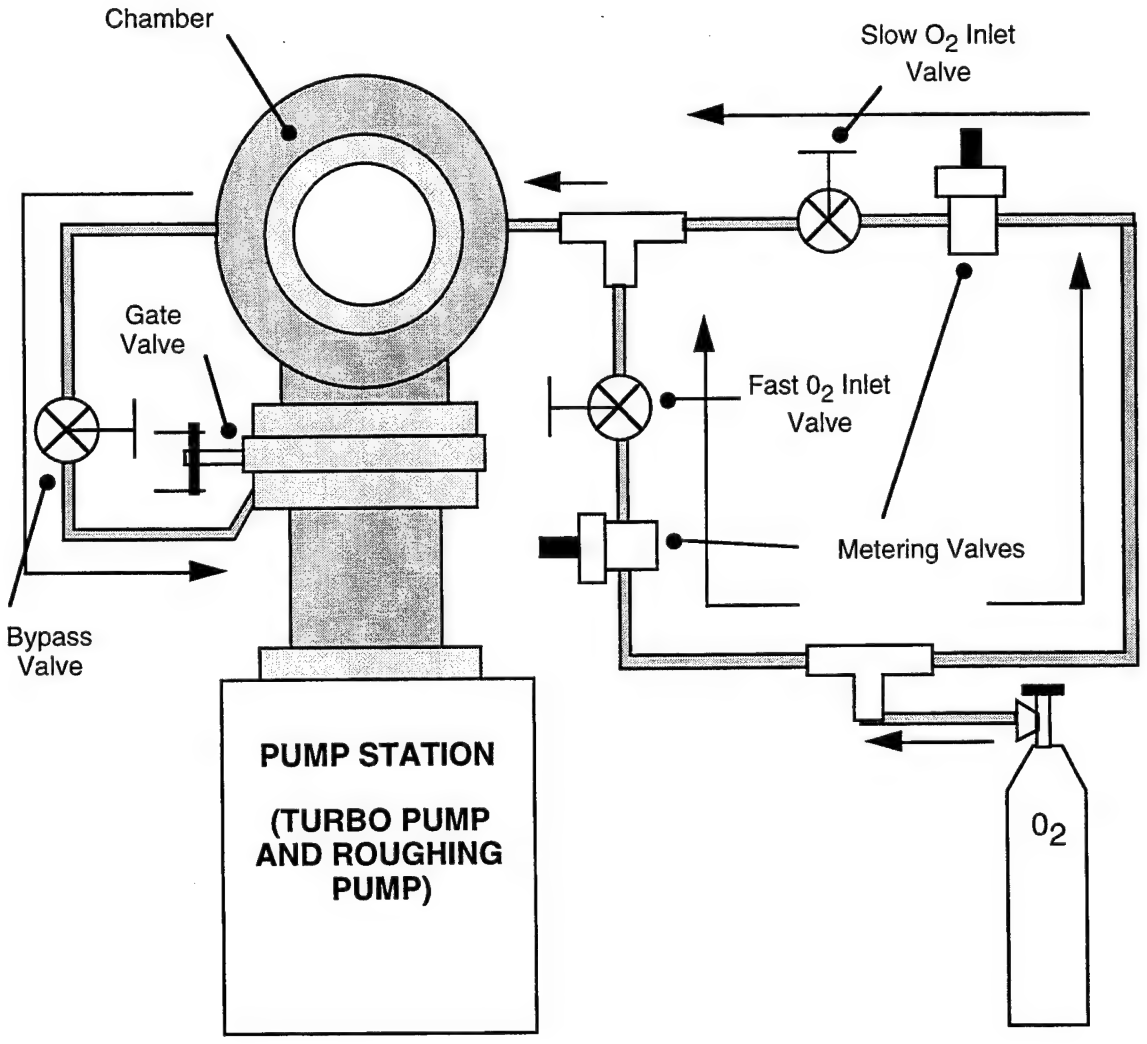

Figure 2.15 - *Gas Flow System*

[18]Arunava Gupta, "Novel Pulsed Laser Deposition Approaches", Pulsed Laser Deposition of Thin Films, (New York: John Wiley & Sons, Inc., 1994), 265-288.

Each pneumatic valve is itself actuated as a result of an electrically controlled solenoid valve being actuated. These solenoid valves act as nitrogen gates for the pneumatic valves.

Referring to Figure 2.15, it can be seen that oxygen flow to the chamber can come from either the Slow O_2 Inlet path or the Fast O_2 Inlet path (the software ensures that both valves are not open at the same time). Which path is used depends on the state of the deposition. The slow path is used *during* the deposition while the fast path is used to flood the chamber with oxygen immediately *after* the deposition. Note that each path has its own metering valve. These metering valves are used to manually adjust the oxygen flow-through rate. Once the oxygen reaches the chamber, it will stay there unless the Gate Valve or the Bypass Valve is open. In either case it will be sucked out through the pump station. The purpose of the GateValve is to quickly evacuate the chamber. It is normally closed during a deposition, leaving the Bypass line as the only vacuum path. Regulating the chamber pressure is then a matter of simply opening and closing the Bypass Valve (i.e. opening and closing the vacuum path).

The chamber pressure control structure is represented in block diagram form in Figure 2.16. The chamber pressure (P_{cham}) is provided by the Baratron pressure gauge, discussed in Appendix B.2.5. Since the pressure gauge output is analog (i.e. noisy), a simple hysterisis loop is used in the control algorithm, which simply determines the state of the bypass valve. The switching points for the control algorithm are determined by the tolerable percent error of the setpoint (P_s). During system setup, the percent error is typically set at 1% to avoid rapid switching of the bypass valve. It is set to 0% during the actual deposition. The system is stable, however, since the valve is updated only as fast as the pressure gauge can be read (approximately once a second).

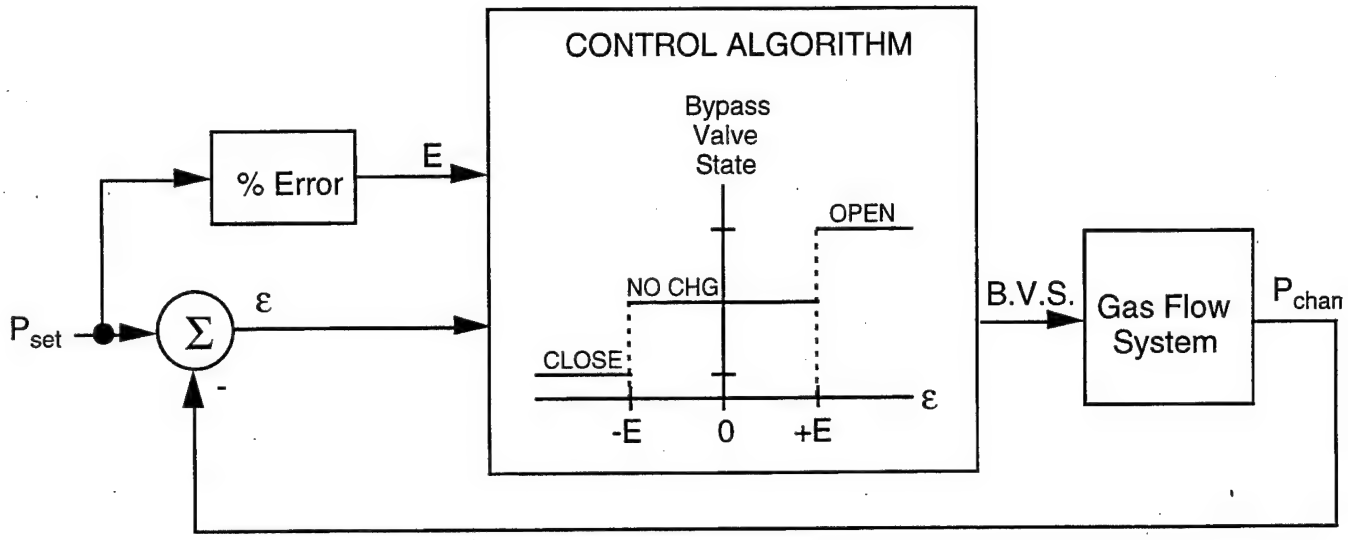

Figure 2.16 - *Pressure Control Structure*

2.3.4 Beam Position Control

In order to minimize the target damage due to prolonged laser ablation, the beam can be scanned across the surface of the target. Additionally, scanning the plume increases the ability of the plume to sufficiently cover the substrate (especially larger substrates). The plume is highly directional, with the most forward directed portion being stoichiometrically correct (i.e. the outer edges tend to be unstoichiometric).[19,20,21]

To minimize the target damage and increase the potential surface area that the system could accomdate, software was written to implement three scanning patterns as shown in Figure 2.17. The dimensions of each scan pattern can be specified as a function of the actual distances on the target. Note for the raster scan

[19]T. Venkatesen, X.D. Wu, A. Inam, and J. B. Wachtman, "Observation of Two Distinct Components During Pulsed Laser Deposition of High Tc Superconducting Films", *Applied Physics Letters* vol. 52, no. 14, 4 April 1988, 1193-1195.

[20]Jeff Cheung and Jim Horwitz, "Pulsed Laser Deposition History and Laser-Target Interactions", *MRS Bulletin*, February 1992, 30-36.

[21]Katherine L. Saenger, "Angular Distribution of Ablated Material", *Pulsed Laser Deposition of Thin Films*, (New York: John Wiley & Sons, Inc., 1994), 199-225.

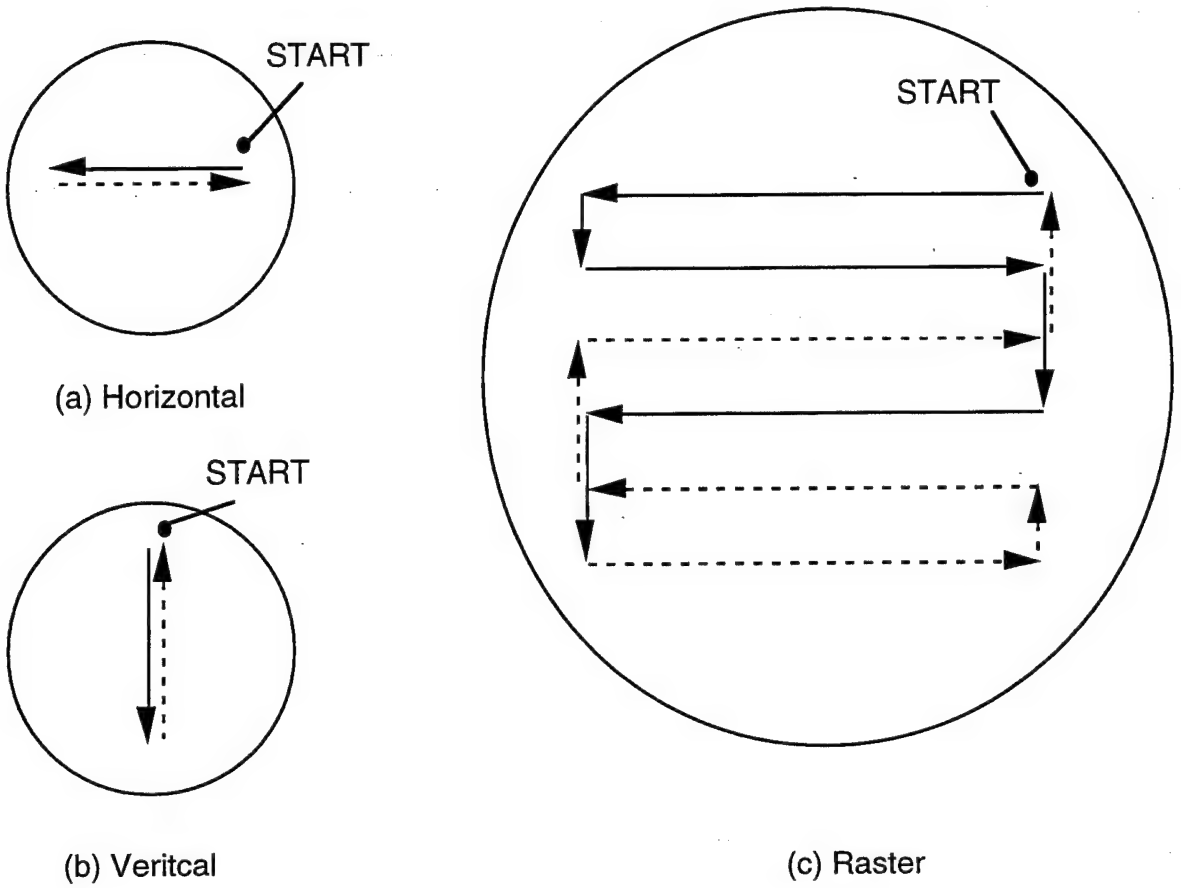

Figure 2.17 (a), (b), and (c) - *Laser Scanning Patterns*

pattern, the number of lines per scan can be increased as well. For a complete discussion of the software implementation, see Appendix B.2.3.

2.3.5 Insitu Level Sensor - Flourescence Spectroscope

After the various separate environmental variables were stabilized (i.e. pressure, substrate temperature, and laser energy) via individual feedback loops, it was necessary to test whether or not dynamic system changes were occurring which could affect the growth process. Some possible sources of these system changes are possible target damage and laser port window coatings (due to the

target material being scattered). Both of these will effectively decrease the growth rate. To see if system changes were occurring, some type of insitu measurement needed to be made. Chamber pressure and substrate pressure were measured insitu, and their values were found to be very stable due to the feedback loops used on each. The laser energy, however, was measured internal to the laser and not the chamber. Therefore, some way to measure the change in effective received energy (if any) was needed. Since the magnitude of the plume is a direct indication of the strength of the impinging laser beam, a device was needed that would somehow track the apparent strength of the plume. This measurement is accomplished via a 2-channel fluorescence spectroscope. The design of the instrument is based on a similar device constructed by Laube.[22]

Fluorescence is a material property that allows for the absorption and subsequent release of photon energy. In this case, the excited material is the target material while the excitation source is the 248 nm ultraviolet laser light. Due to the photoelectric effect, the absorbed energy is released at specific frequencies based on the material involved. As a given element transitions from a more to less excited state, it releases photons of known frequency.[23] It is this effect which can give an indication of the relative abundance or lack thereof of a specific plume constituent.

A diagram of the measurement setup is shown in Figure 2.18. Note that the spectroscope is actually external to the chamber. A collimating tube is located inside the chamber (actually two) so that a specific piece of the plume can be examined without seeing the whole thing. Note that the output of the spectroscope

---

[22]Samuel J.P. Laube, "Hierarchical Control of Pulsed Laser Deposition Processes for Manufacture", Doctoral Dissertation, Electrical and Computer Engineering, University of Cincinnati, 1993

[23]Robert M. Besancon, *The Encyclopedia of Physics*, 3rd ed., (New York: Van Nostrand Reinhold, 1990), 1157-1166.

is fed to a 2-channel digital storage scope. The scope is triggered externally by the laser.

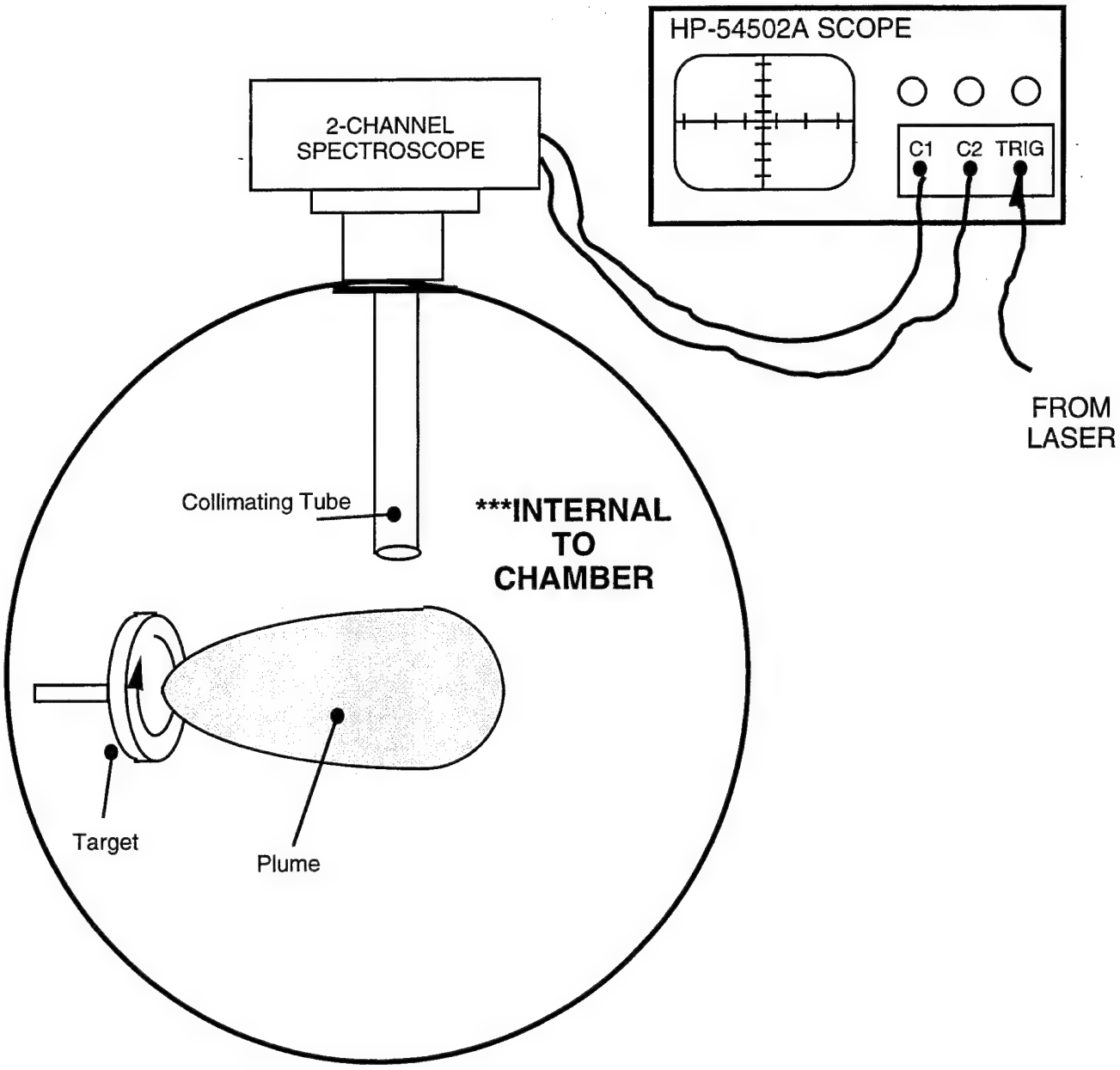

Figure 2.18 - *Spectroscope Setup*

By choosing the appropriate optical filter, it is possible to look at a given plume species (material). To determine whether or not the plume constituents were changing significantly during a deposition, the emission wavelength for Cu^0

(wavelength = 326 nm) and Ba^0 (wavelength = 550 nm) were looked at. Although a number of frequencies exist for various transitions (implying differing energy states), the most intense transitions were picked. These frequencies were chosen based on published data.[24]

[24]Robert C. Weast, Melvin J. Astle, and William H. Beyer, *CRC Handbook of Chemistry and Physics*, (Florida: CRC Press, 1987).

CHAPTER 3 - RESULTS, CONCLUSIONS AND FUTURE WORK

This section will discuss the effectiveness of the new PLD system based on the three initial goals of a new system assembly, real-time data acquisition/system automation, and system stabilization. Besides growing a number of films to demonstrate the effectiveness of the large amount of software, numerous tests were performed to determine the effectiveness of system stabilization. The last section, Section 3.4, will address the issue of whether or not more control is needed due to insitu system changes.

3.1 New System Assembly

The new system assembly is very effective. All of the instrumentation implemented functions properly, as does the rotatable target holder assembly. The system can hold a fairly good vacuum as well. As an added bonus, the new assembly is on wheels, enabling it to be easily moved if necessary.

3.2 Data Acquisition and Deposition Process Automation Software

The deposition software is very effective. Again, any instrument can be selected/deselected as required, and those devices which require some type of setup information can be configured either interactively or quickly through the use of disk-based device setup files. Instead of manually collecting the data with pen and paper, the operator simply supplies a file name for data storage. Additionally, all sensor measurements are displayed graphically in real-time. The data acquisition

is capable of collecting data from each instrument at the rate of about 1 sample per second.

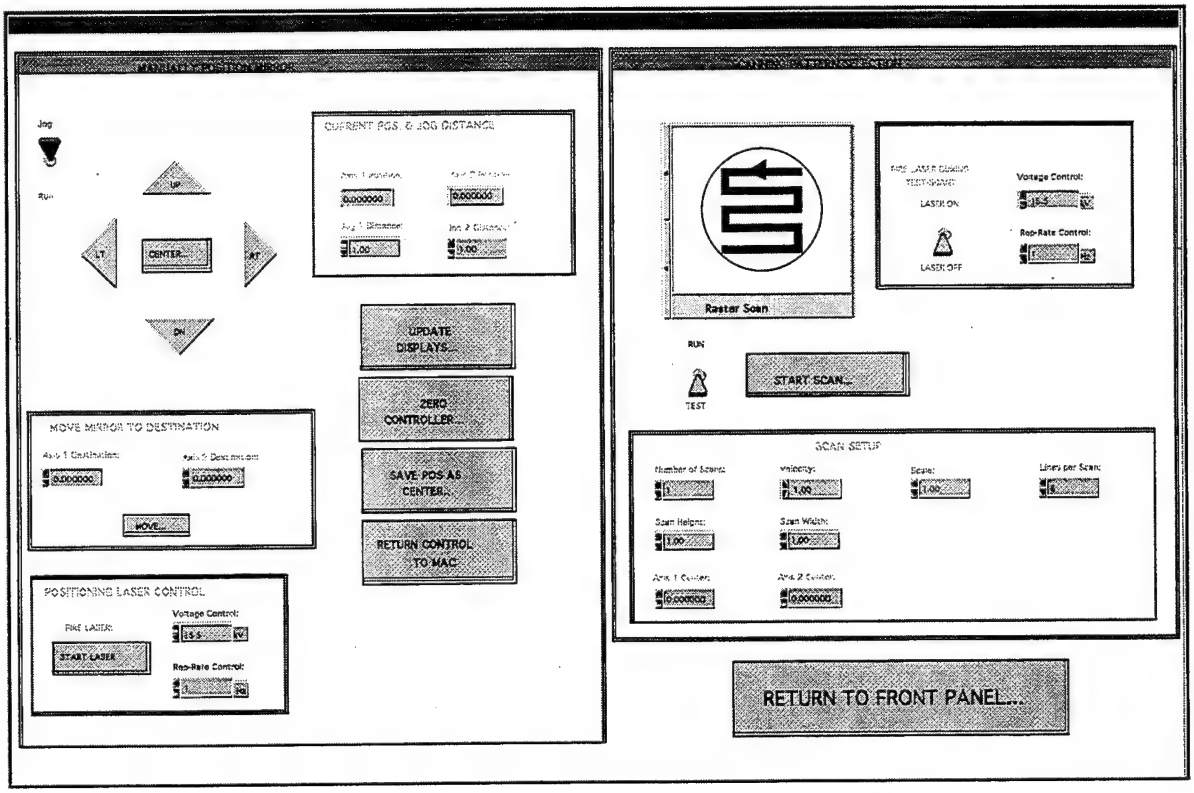

Figure 3.1 - *Newport Mirror Controller Front Panel*

Figure 3.1 shows a good example of the instrument setup screens available to the operator. This front panel is for the mirror controller. Setup and test screens such as this are available for each instrument. A through explanation of the different software modules is given in Appendices A and B.

The deposition procedure is completely automatic. After the deposition starts, system parameters are adjusted automatically if needed. The depositions are timed, and when the specified time elapses (also displayed), the laser is turned off automatically. The operator can optionally specify an additional length of time to collect data. If desired, an optional system shutdown sequence can be started, where the chamber is flooded with oxygen and the heater stage is turned off.

Essentially, the process can run on its own. However, any actuator setting can be changed at any time if necessary. The software lets the operator decide how much they want to be involved in the deposition.

3.3 System Environmental Control Results

3.3.1 Laser Control

The general performance of the lookup and PID laser control scheme seems to be quite good. Several tests were done to determine the effectiveness of the structure. Table 3.1 shows the format for one such test.

Time (s)	Desired Energy (mJ)	Frequency (Hz)
START	200	10
30	300	2
60	300	24
90	250	20
120	235	5
150	350	15
180	325	37
210	200	4
240	175	18
270	400	12

Table 3.1 - *Laser Control Test Format*

Essentially, the desired energy and frequency were changed in approximately 30 second intervals. Note that a number of frequencies were used so that the table update procedure could be tested. First, the control scheme was tested using a one day old lookup table. This was done to test the effectiveness of the PID controller

in correcting table errors. Figure 3.2 shows both the desired energy and the actual energy for this test. Even thought the table was one day old, it was still fairly accurate.

To see if the table update procedure was effective, the table was calibrated and the test was run again. Figure 3.3 shows both the desired energy and the actual energy for this test. When comparing these results to Figure 3.2, it can be seen that the controller performed better with the updated table version. As a final comparison, Figure 3.4 shows the voltage commands issued in both tests. This figure shows how the PID controller attempted to compensate for table errors.

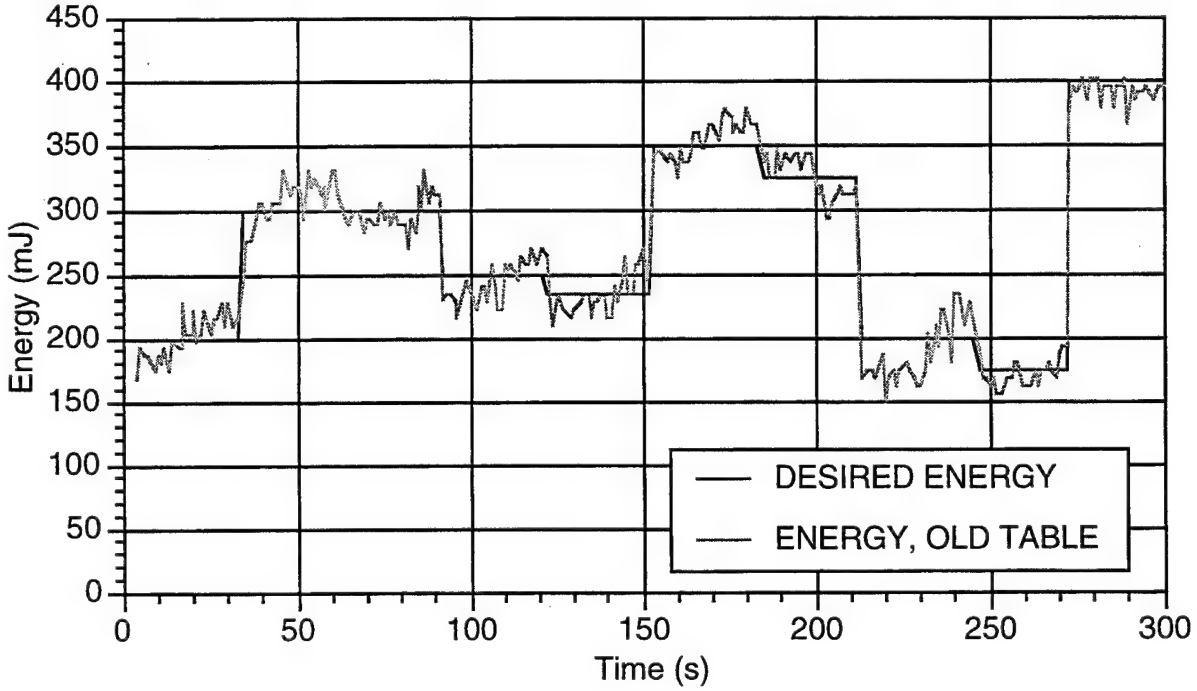

Figure 3.2 - *Laser Energy Response With Old Table*

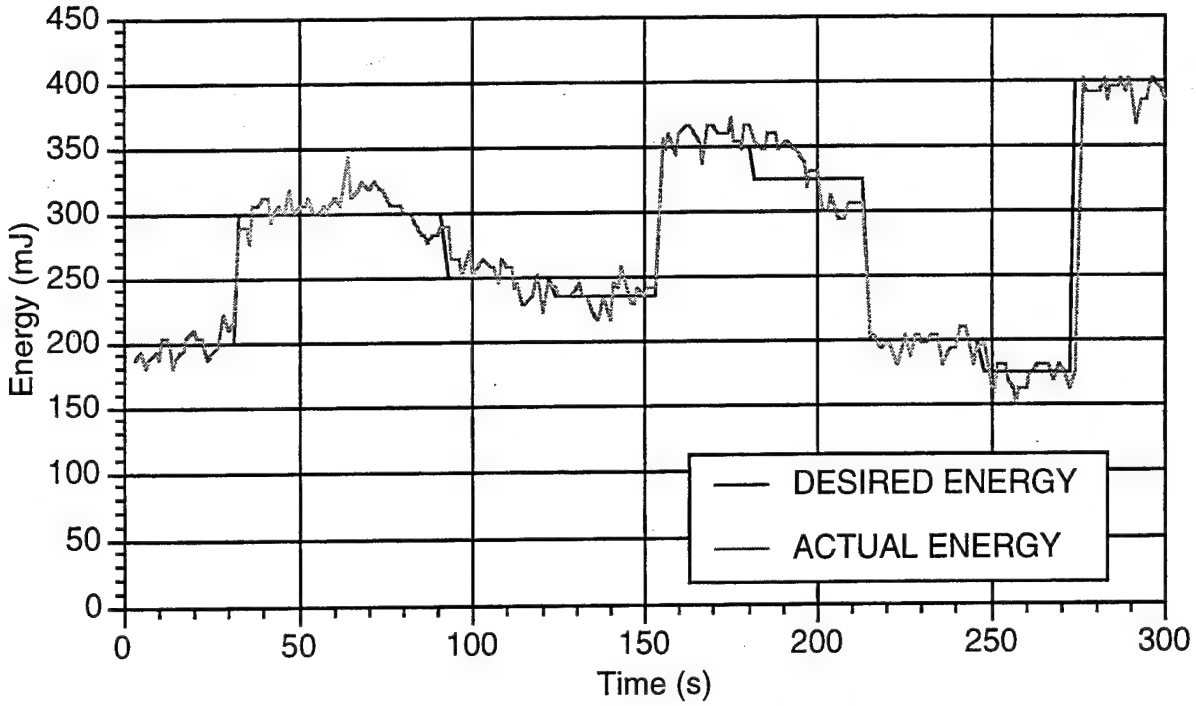

Figure 3.3 - *Laser Energy Response With Updated Table*

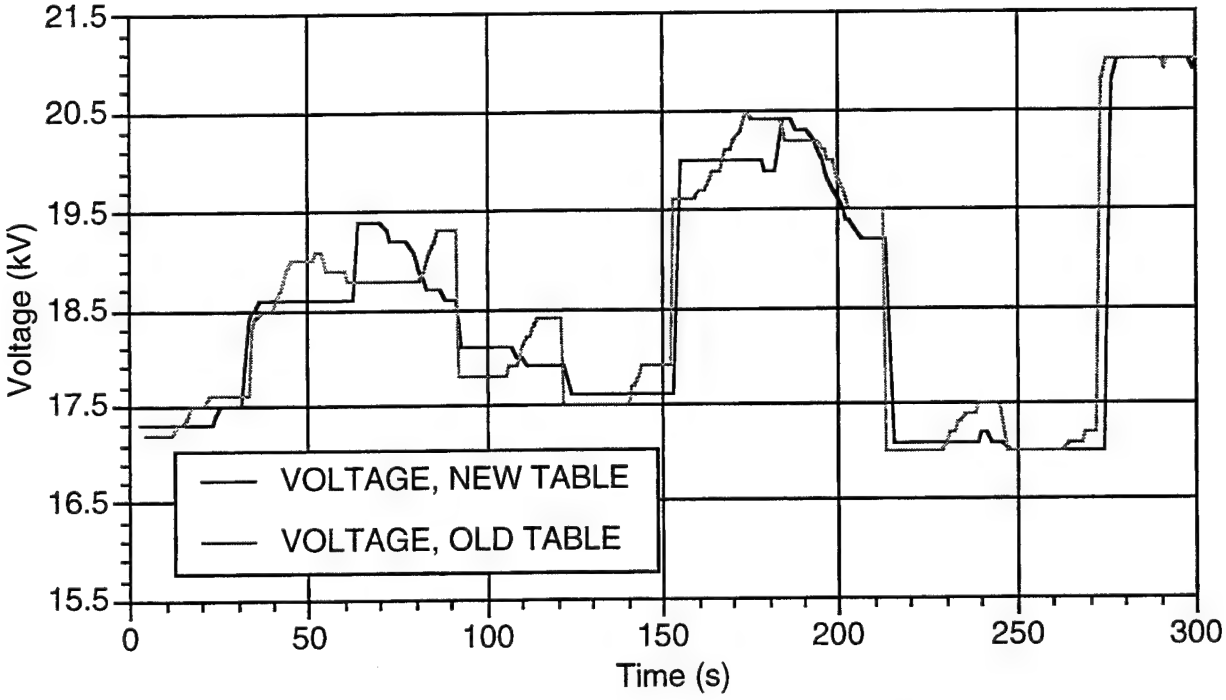

Figure 3.4 - *Voltage Commands for Laser Control Test*

The above tests indicate that the table lookup and update procedure works fairly well in predicting the required voltage for any desired energy at a given rep-rate. As a final test of the PID controller's stability, the step response was tested. Figures 3.5 (a) and (b) shows the results of this test. At the start of the test, the laser voltage was set to 15.5 kV, the lowest possible value. Then, the energy requirement was set at 350 mJ, much too high a requirement for only 15.5 kV. As Figure 3.5 (a) shows, the laser energy approaches 350 mJ around 15 seconds. Figure 3.5 (b) shows that the laser voltage does not change appreciably after this.

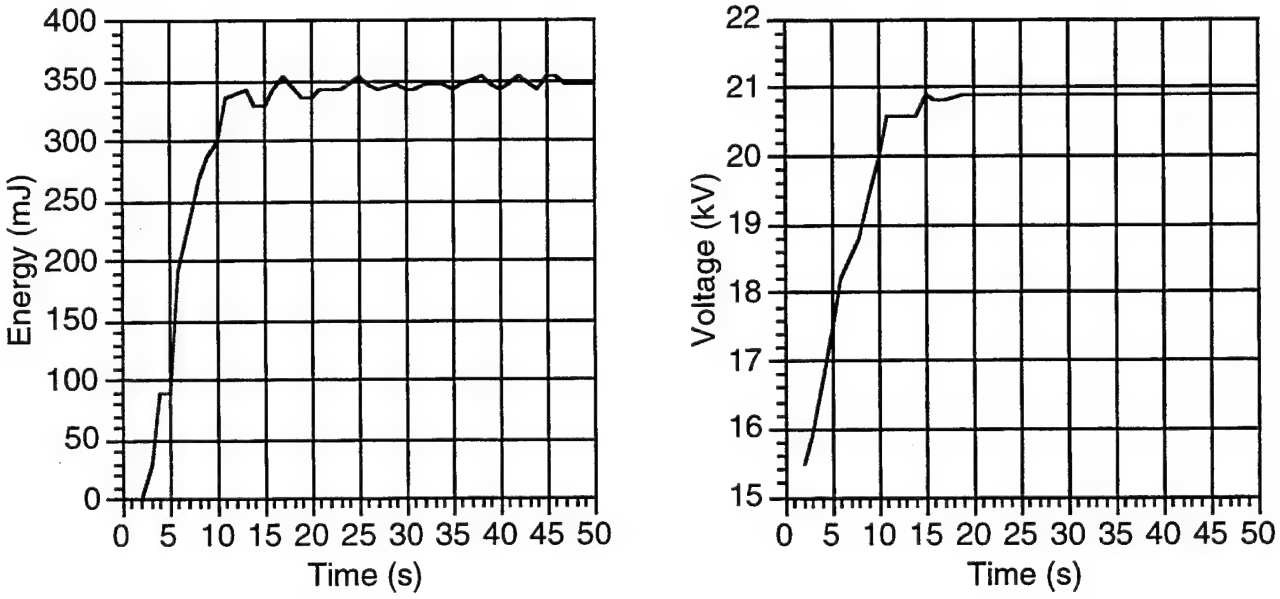

(a) Energy Response

(b) Voltage Commands

Figure 3.5 (a) and (b) - *Laser Step Response*

3.3.2 Substrate Temperature Control

The PID temperature control loop locks the substrate temperature at the desired temperature. Previously, the temperature was set through a variable

transformer (some percentage of 120 VAC). This approach was somewhat suspect because it failed to account for system changes. One such possibility was the output of the transformer could vary with line voltage. Also, varying oxygen flow-through rates would tend to either increase of decrease convection cooling, resulting in temperature gradients across the substrate with respect to time. More importantly than system changes, however, was the fact that there was no known relationship between a given transformer setting and the actual substrate temperature. Even if the operator tried to adjust the transformer setting based on an observed thermocouple reading, the setting could still be inaccurate since the thermocouple used to measure the temperature was frequently moved from one deposition to the next. Using the automatic feedback loop with a fixed thermocouple solved both the temperature drift problem and the accuracy of a given setting.

Figure 3.6 shows the temperature variation during a deposition after the heater has stabilized (T = 750° C in this case). Note that the small oscillation is the temperature changing from 750° C to 751° C. At about 260 seconds, the deposition was over and the heater was turned off.

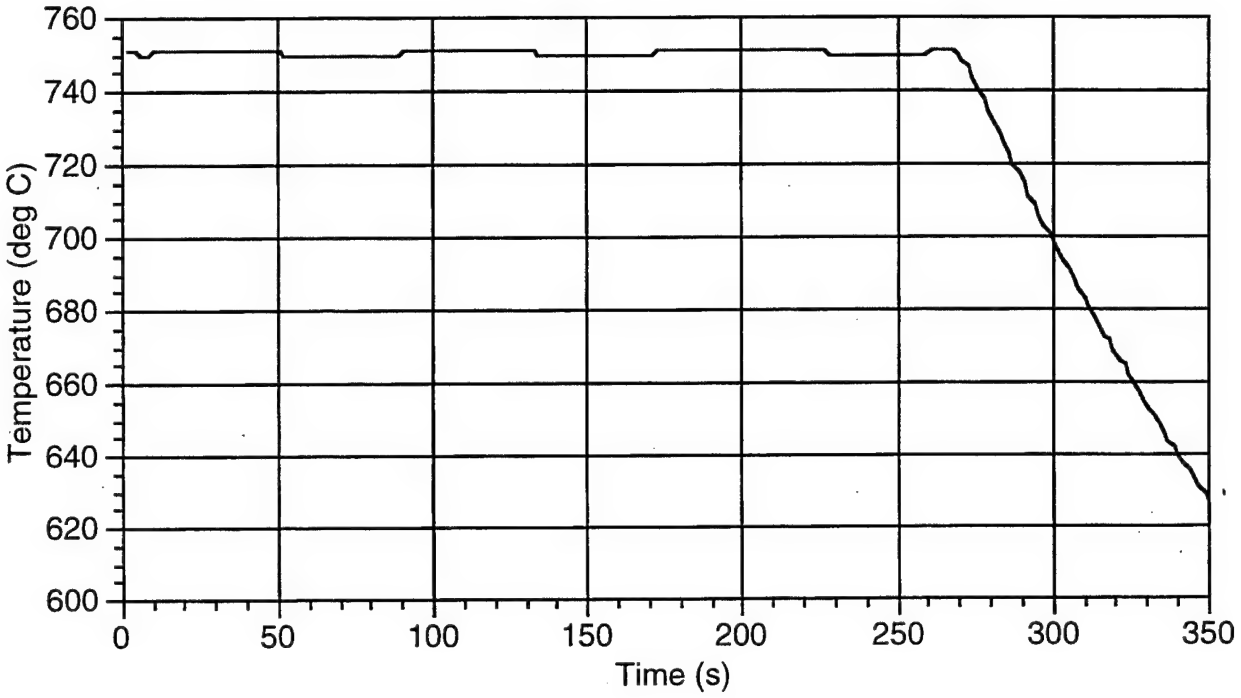

Figure 3.6 - *Temperature Control Performance*

3.3.3 Chamber Pressure Control

While the ON/OFF pressure control approach is simple, it does provide a very stable chamber pressure. The typical approach is to set a 'ballpark' pressure with the metering valve, and then let the controller narrow it down to the correct value. Figure 3.7 shows the effectiveness of this simple approach. In this case, the setpoint for this deposition was 150 mT. Note that the chamber pressure varies at most +/- 1° (it usually stays at 150 mT), while the pump pressure varies considerably, showing that the controller is opening and closing the Bypass line regularly.

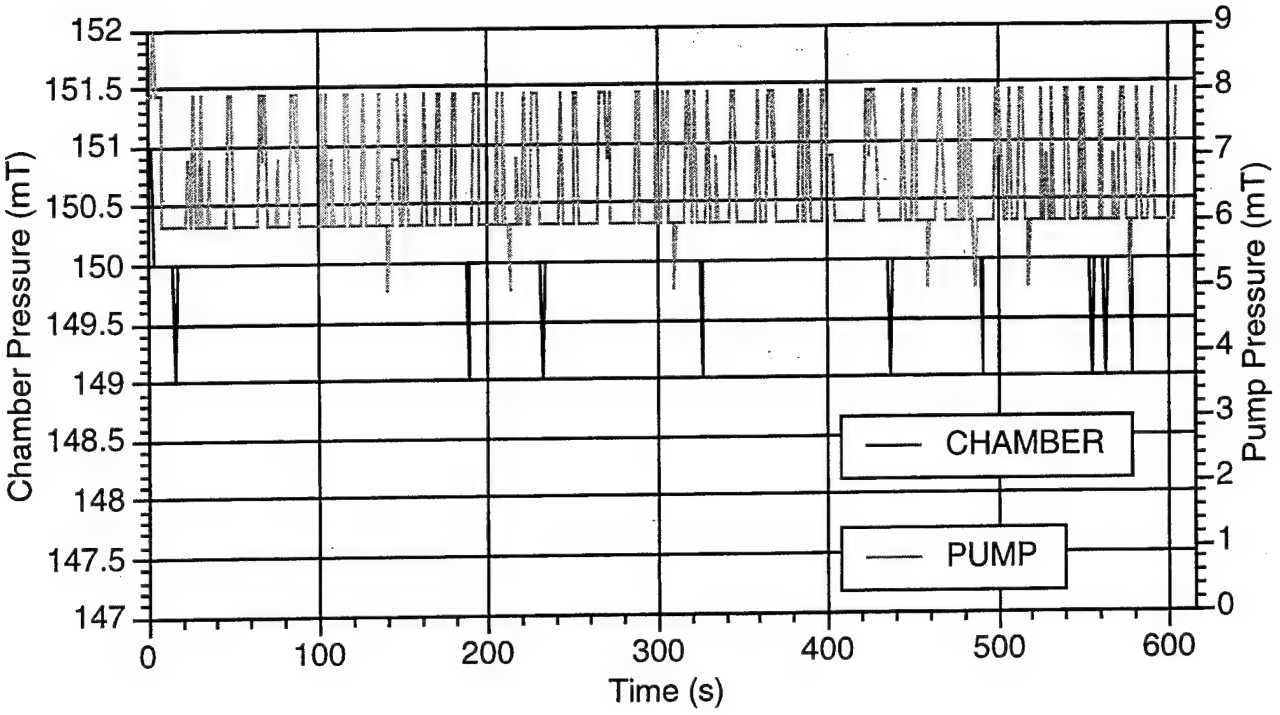

Figure 3.7 - *Chamber Pressure Control Results*

3.4 Insitu Sensor Results

Figure 3.8 shows a typical set of spectroscope responses for Cu^0 at varying oxygen pressures. Each signal has two important components. The first and most obvious one is the signal amplitude. It is the signal amplitude that gives an indication of the amount of material reaching the collimating tube (for a given species). Essentially, more energetic material will give off more light. The plots show that the amount of excited Cu^0 reaching the collimating tube decreases with increasing oxygen pressure. This effect is simply a matter of an increased number of atomic collisions between Cu^0 and oxygen. The increased number of collisions simply means that less Cu^0 will reach the collimating tube. The second important characteristic in the signals is their widths. The signal width (e.g. 10 -> 90% of the maximum value) is an indication of how long the material was in the vicinity of the

collimating tube. The plots show that the pulse width increases as the pressure increases. This result has a fairly simple explanation. Since there will be more collisions due to the increased oxygen pressure, the material flying past the collimating tube will be slowed significantly. This will tend to *lengthen* the time the spectroscope sees it. In an ultra-high vacuum, for example, the pulse has a large amplitude but the pulse width is extremely small. This is completely consistent with the above explanations. Both the large signal amplitude and small signal width are due to the lack of collisions.[25]

Figure 3.9 shows another set of spectroscope responses, this time holding the oxygen pressure constant while varying laser energy. Not surprisingly, the signal increases with increasing energy. Essentially, more material is ablated from the target at higher laser energies. Note that the 400 mJ signal is severely clipped due to the high-speed amplifier saturating.

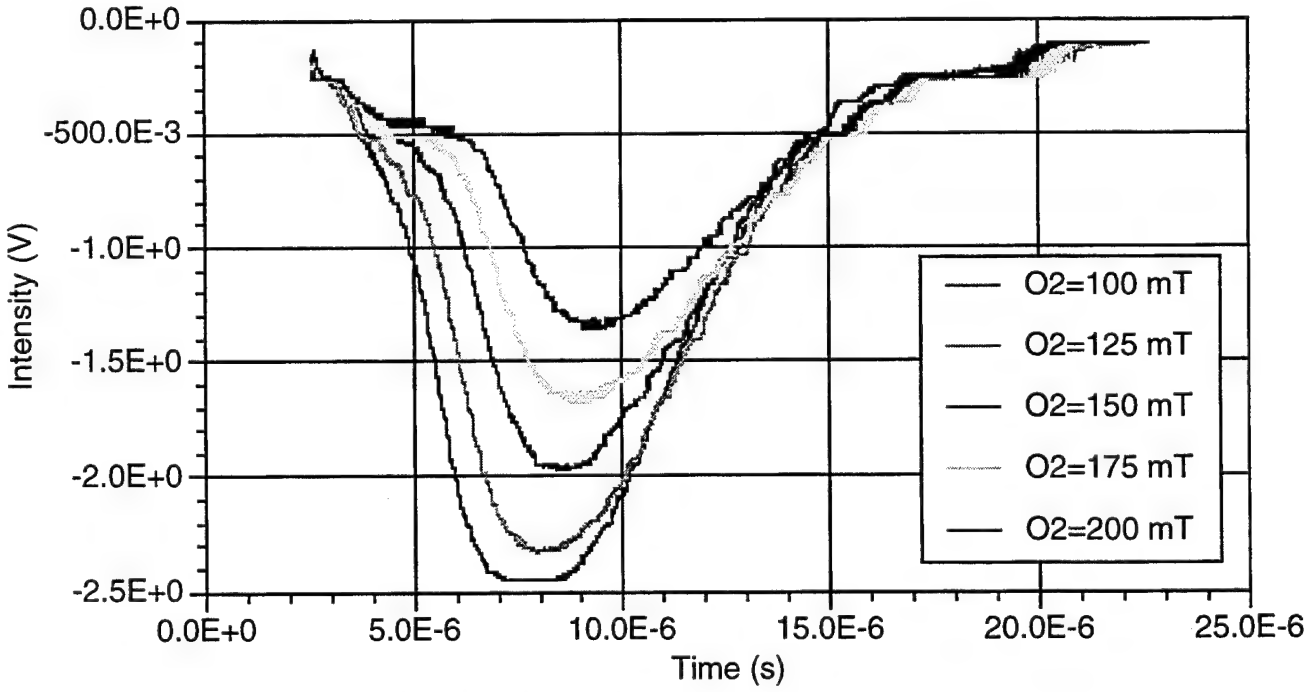

Figure 3.8 - *Cu^0 Signals With Varying Pressure*

[25]C. E. Otis and R. W. Dreyfus, "Laser Ablation of $YBa_2Cu_3O_{7-\delta}$ as Probed by Laser-Induced Fluorescence Spectroscopy", *Physical Review Letters,* Vol. 67, no. 15, 7 October 1991, 2102-2105.

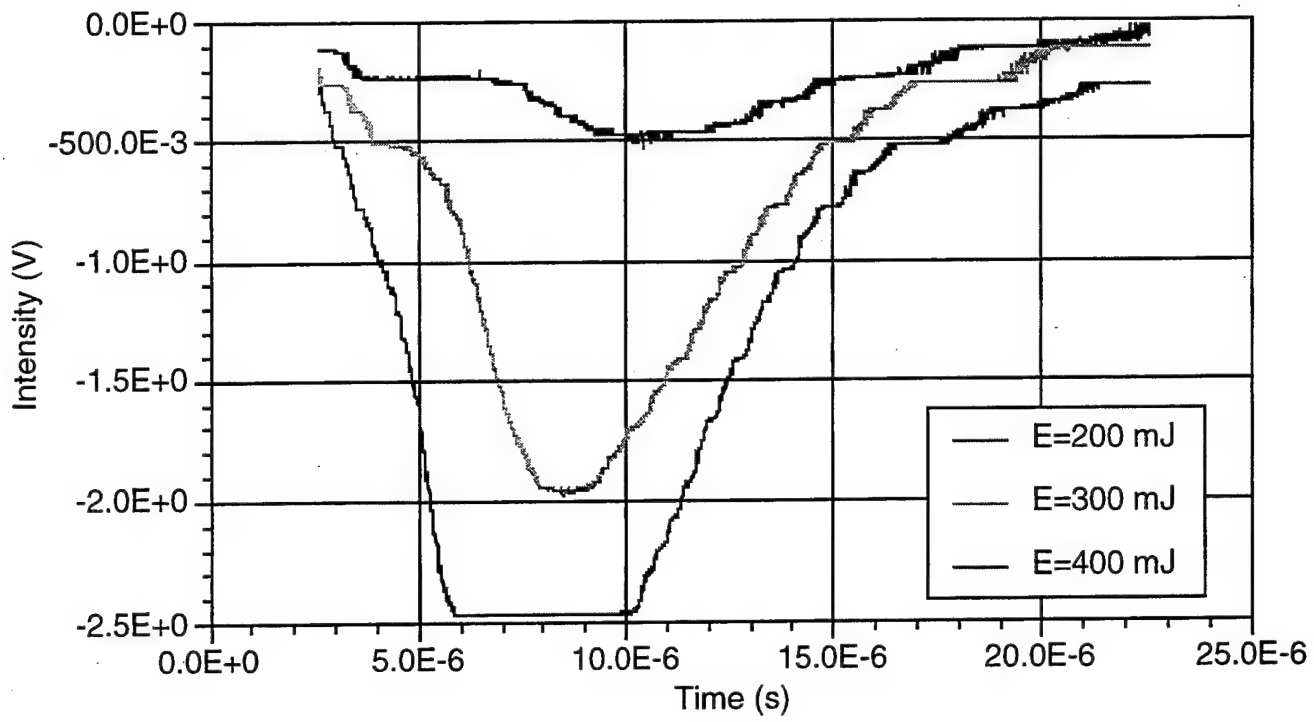

Figure 3.9 - *Cu^0 Signals With Varying Energy*

The above plots were analyzed to determine what type of effect oxygen pressure and laser energy had on the plume. In a real-time control situation, however, it would be nearly impossible for a computer to completely analyze a 2000 point waveform. To determine whether or not dynamic system changes were taking place, it was necessary to be able to quickly quantify a given spectroscope signal. This is done by automatically taking the average value (sum of values / number of values) of each pulse received at the oscilloscope. Whether or not this is a good way of characterizing the signal depends on the oxygen pressure dynamics. From the above results, it is known that increasing the oxygen pressure will simultaneously *decrease* the signal amplitude (less material) and *increase* the signal width. Conversely, decreasing the oxygen pressure will *increase* the signal amplitude and *decrease* the signal width. Obviously, a situation could exist where the behavior of a given plume constituent was changing but the *average value* of

the plume signal was constant. These problems are eliminated in the new system since the pressure is controlled. Deciding which direction, if any, a given constituent is moving (increasing/decreasing) is possible since the only parameter which should change is the maximum signal amplitude. In general, flourescence spectroscopy has been shown to give unreliable results when oxygen pressures varies considerably.[26]

Figure 3.10 shows the spectroscope response for a constant pressure and energy (E = 200 mJ, P = 100 mT). Although the plot appears to show that the spectroscope signal varies with frequency, this is not the case. Figure 3.11 shows the laser's energy output as a function of time for the same data. As can be seen, the absolute magnitude of the signal increases as the energy increases. The energy control was left turned off so that the results would be unbiased by any laser control action. These plots again show that the amount of material decreases with increasing oxygen pressure.

[26]S.R. Foltyn et. al., "Influence of Beam and Target Properties on the Excimer Laser Deposition of $YBa_2Cu_3O_{7-x}$ Thin Films", *Materials Research Soceity Symposium Proceedings*, vol. 191 (1990), 205-209.

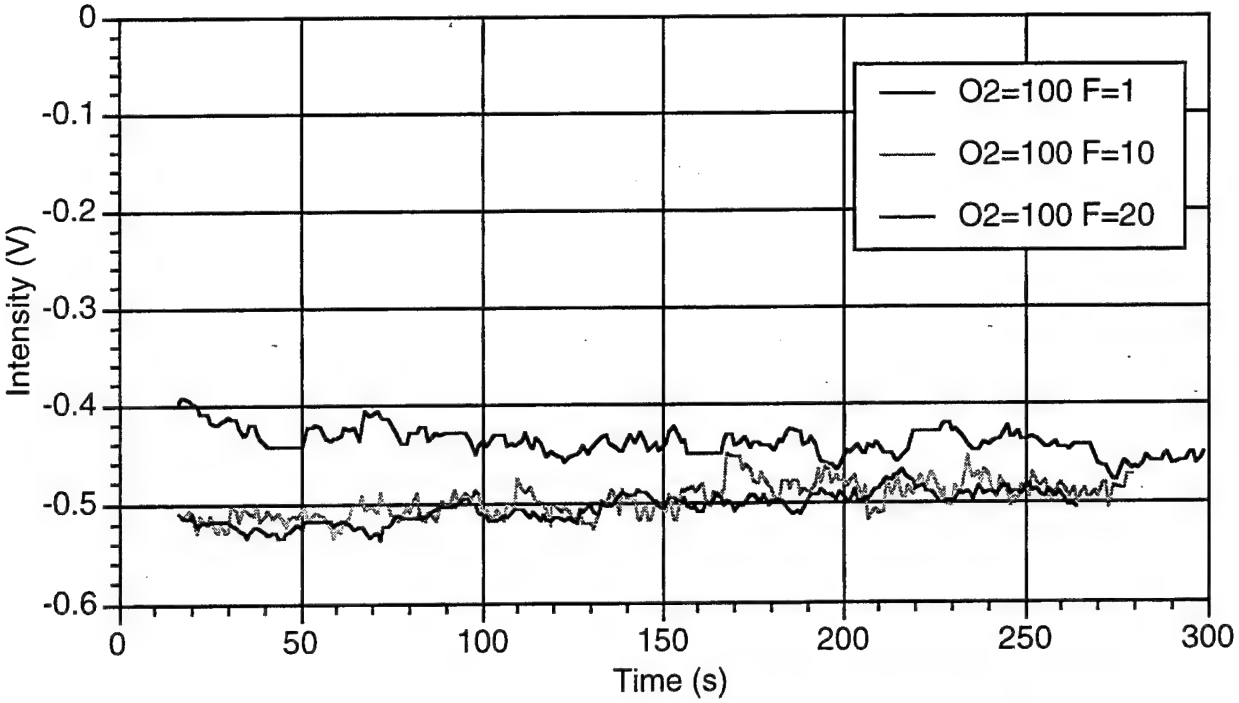

Figure 3.10 - *Average Value of Signal With Varying Frequency*

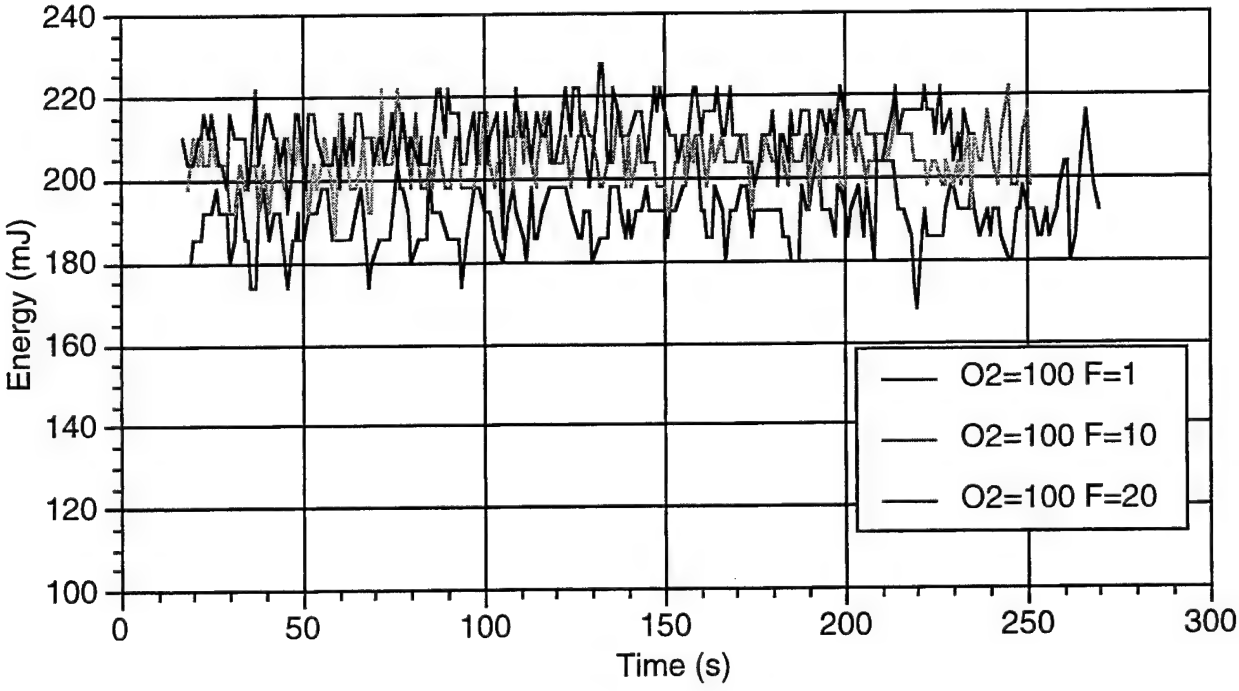

Figure 3.11 - *Laser Energy Corresponding to Figure 3.10*

The question that needs to be answered is whether or not system dynamics are affecting the growth process. As can be seen, the plume signals are very noisy. This is a direct effect of the shot-to-shot variation of the laser energy. However, some data collected shows very slow trends that are not apparent in the laser data. It is questionable whether or not these changes can be compensated for, or whether they matter since the magnitude of the changes are small. It may become important, however, to adjust the laser parameters if the deposition times are extended.

In an attempt to determine the effectiveness of reducing target damage by rotating and scanning the target, an additional test was completed using the spectroscope. In the first part of the test, data was collected for ten minutes with a stationary laser beam of constant energy and rep-rate (energy = 200 mJ, rep-rate = 20 Hz). The target, however, was rotated at about 20 rpm. Figure 3.12 shows a series of waveform plots taken at various times in the 10 minute test. As can be seen, the signal waveform intensity is decreasing as the length of time increases. Also, the signal does not begin decreasing in intensity until after the fourth minute waveform.

Next, the target rotation was turned off and data was collected for another 4 minutes. Figure 3.13 shows the spectroscope waveforms. Note that the waveform evolution picks up where it left off (before the rotation was turned off). Additionally, the decreasing intensity from waveform to waveform is more pronounced. This is obviously due to the fact that the damage at any given target location is a direct function of the number of times it is hit with the laser. With no target rotation, one location is hit continuously.

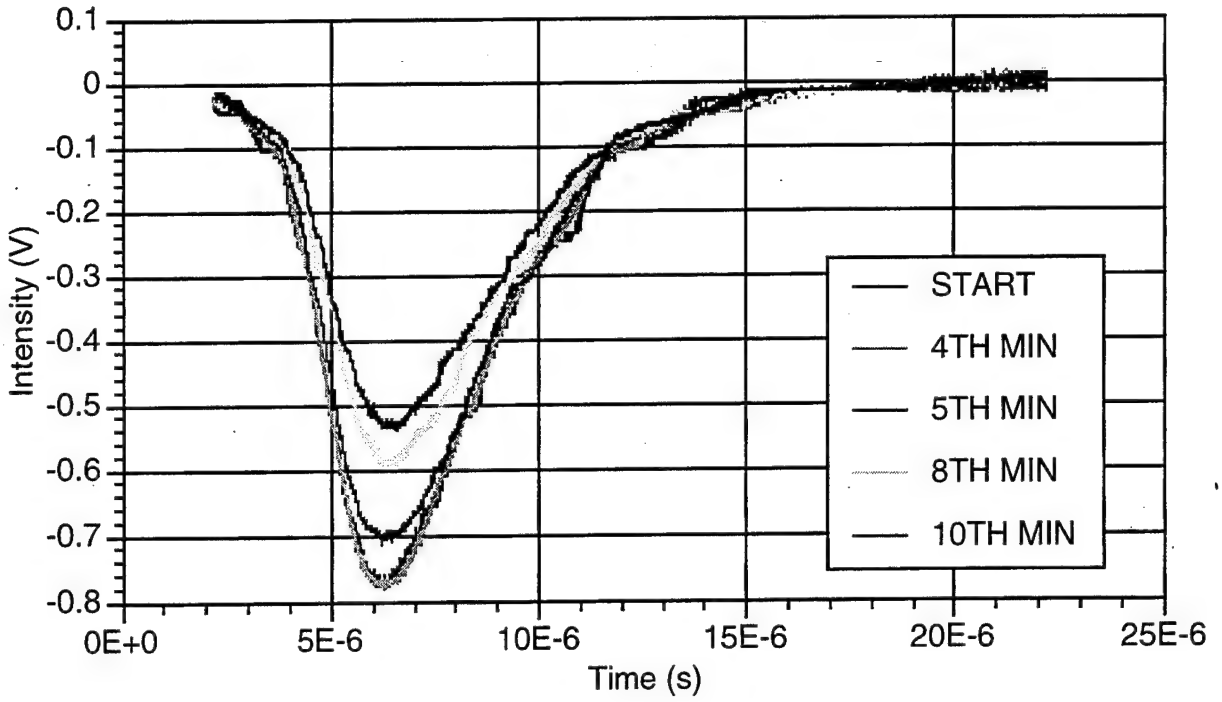

Figure 3.12 - *Cu^0 Signals With Target Rotation, No Scan*

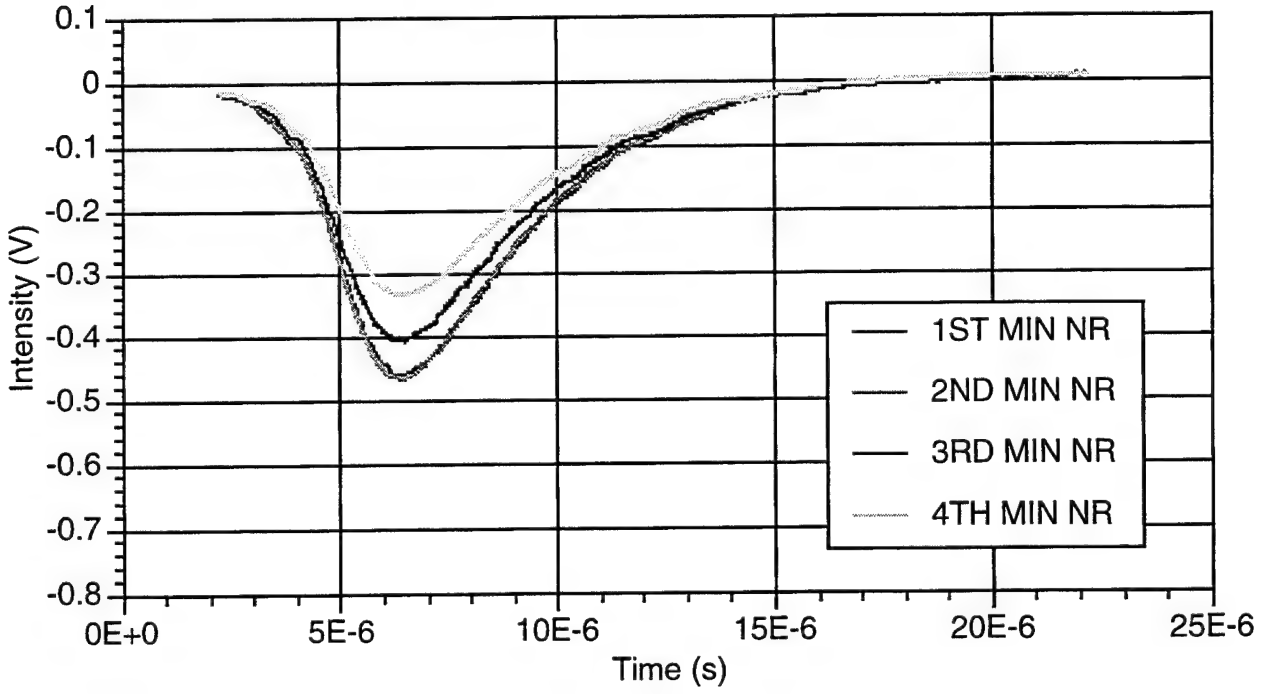

Figure 3.13 - *Cu^0 Signals With No Target Rotation, No Scan*

Figure 3.14 shows the average value of the signal received over time. Note that the average value does not begin increasing (*decreasing* intensity) until after 200 seconds. This agrees with the previous plots which show that the signal intensity begins to decrease around 4 minutes.

The above data again shows that with short depositions, no additional control is needed. Typically, deposition length are 250 seconds, which is well within the stable region if target scanning is included with target rotation. The important point is that dynamical system changes can be observed if the system is allowed to progress beyond a certain time limit.

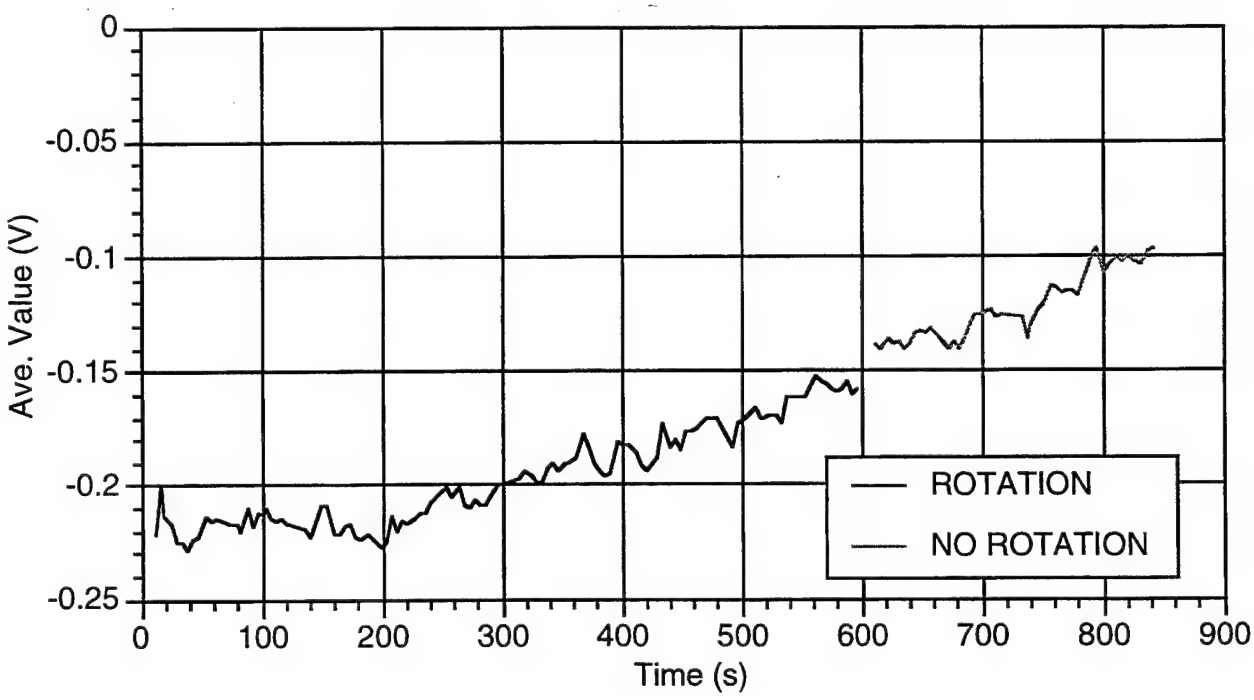

Figure 3.14 - *Average Value of Signal With No Scan*

3.5 Films Produced in the New System

In order to see if the new system was capable of growing good superconducting films, several film growth experiments were completed. Table 3.2 shows a table depicting both the test matrix used and the resulting film characteristics. The film parameters measured were the maximum transition temperature, or Tc, and the difference between the maximum and the minimum Tc, or ΔTc. This implies that the films have a range of possible Tcs. This is because the Tc varies depending on where on the film the measurement in taken. In general, the higher the maximum Tc measurement and the smaller the ΔTc, the better the film. The maximum Tc reflects the degree to which the grown film approaches perfect stocihiometry in its 'best' spot. On the other hand, ΔTc reflects the overall uniformity of the film.

The table indicates that the two environmental variables that were varied were the laser energy and the substrate temperature. Both the oxygen pressure and the pulse rep-rate were set and maintained, staying a constant 150 mT and 20 Hz respectively. Additionally, all depositions lasted 250 seconds.

The test results indicate that the films produced have Tcs above the temperature of liquid nitrogen, 77 K. The film grown at 750 °C with 250 mJ per laser pulse has a maximum Tc approaching the theoretical limit of 92 K. That film is also fairly uniform with a small ΔTc of 1.12 K. Note that increasing the temperature while holding the laser energy constant increased the maximum Tc in all films except for the one grown at 730 °C and 150 mJ per pulse. Regardless, the data seems to show that the film quality increases as both the energy and temperature are increased

O_2 = 150 mT T = 710-750 °C E = 150-250 mJ	T →		
	710 °C	730 °C	750 °C
E 150 mJ	T_c = 89.2 K ΔT_c = 3.8 K	T_c = 86.6 K ΔT_c = 4.5 K	T_c = 89.2 K ΔT_c = 2.2 K
200 mJ	T_c = 84.5 K ΔT_c = 2.3 K	T_c = 85.3 K ΔT_c = 4.1 K	T_c = 88.9 K ΔT_c = 1.0 K
250 mJ	T_c = 87.7 K ΔT_c = 2.9 K	T_c = 89.5 K ΔT_c = 2.6 K	T_c = 91.3 K ΔT_c = 1.12 K

Table 3.2 - *Film Quality Test Matrix*

3.6 Future Work

As the previous sections showed, adequate system stabilization has been achieved by controlling the system at the environmental level only. With short growth times, additional control is not needed since the plume signal does not appreciably change with time. However, deposition durations will need to increase to accomodate large area depositions. In this case, additional control may be needed to compensate for insitu system changes (most notably target damage). Since the spectroscope sensor is already built and functioning correctly, this should be fairly simple.

The most important task is to determine the optimum system parameter settings that maximize Tc and minimize ΔTc. Additional desirable film characteristics can be determined as well. Using the above film results as a starting point, it should be possible to design some experiments to determine what those parameter settings should be. The knowledge obtained from these tests can then be entered into film database. This database can then serve as the knowledge base for a qualitative rule-based controller. The controller will then generate insitu plume references based on the requirements for a given film. The PLD system can then produce films optimized for particular applications.

BIBLIOGRAPHY

Donald R. Askeland, *The Science and Engineering of Materials*, 2nd ed. (Massachusetts: PWS-KENT Publishing Company, 1989), 49-83.

Robert M. Besancon, *The Encyclopedia of Physics*, 3rd ed., (New York: Van Nostrand Reinhold, 1990), 1157-1166.

Kul Bhasin and Robert R. Romanofsky, "Superconducting Field-Effect Transistors", *NASA Tech Briefs*, Vol. 19, No. 7, July 1995, 38.

Rand R. Biggers et. al., "Microstructure and Properties of $YBa_2Cu_3O_7$ Thin Films Grown on Vicinal $LaAlO_3$ Substrates", 18 October 1994.

A. Bourdillon and N. X. Tan Bourdillon, *High Temperature Superconductors: Processing and Science*, (California: Academic Press, 1994), 44, 141.

Jeff Cheung and Jim Horwitz, "Pulsed Laser Deposition History and Laser-Target Interactions", *MRS Bulletin*, February 1992, 30-36.

Douglas B. Chrisey and Arun Inam, "Pulsed Laser Deposition of High Tc Superconducting Thin Films for Electronic Device Applications", *MRS Bulletin*, February 1992, 37-43.

Douglas B. Chrisey and Graham K. Hubler, *Pulsed Laser Deposition of Thin Films*, (New York: John Wiley & Sons, Inc., 1994).

J. H. Clark, G. B. Donaldson, and R. M. Bowman, "A Fully Automated Pulsed Laser Deposition System for HTS Multilayer Devices"

S.R. Foltyn et. al., "Influence of Beam and Target Properties on the Excimer Laser Deposition of $YBa_2Cu_3O_{7-x}$ Thin Films", *Materials Research Soceity Symposium Proceedings*, vol. 191 (1990), 205-209.

Patrick H. Garrett, "Insitu Subprocess Control: Advanced Automata for Process Industries", To be submitted to *IEEE Transactions on Systems, Man, and Cybernetics*.

Curtis F. Gerald and Patrick O. Wheatley, *Applied Numerical Analysis*, (Massachusetts: Addison-Wesley Publishing Company, 1994), 233-244.

Arunava Gupta, "Novel Pulsed Laser Deposition Approaches", Pulsed Laser Deposition of Thin Films, (New York: John Wiley & Sons, Inc., 1994), 265-288.

Jeff Hecht, *The Laser Guidebook*, (New York: McGraw-Hill, 1992), 59-89, 211-234.

Graham K. Hubler, "Pulsed Laser Deposition", *MRS Bulletin*, February 1992, 26-29.

W. Ito, Y.Yoshida, S. Mahajan, T. Morishita, "Effects of Film Thickness and Substrate on Superconductivity of Epitaxially Grown *a*-axis YBCO Films", *Physica C*, vol. 227 (1994), 313-320.

Roger Kelly and Antonio Miotello, "Mechanisms of Pulsed Laser Sputtering", Pulsed Laser Deposition of Thin Films, (New York: John Wiley & Sons, Inc., 1994), 55-85.

G. Koren, A. Gupta, R. J. Baseman, M. I. Lutwyche, and R. B. Laibowitz, "Laser Wavelength Dependent Properties of $YBa_2Cu_3O_{7-\delta}$ Thin Films Deposited by Laser Ablation", *Applied Physics Letters*, vol. 55, no. 23, 4 December 1989, 2450-2452.

Benjamin C. Kuo, *Automatic Control Systems*, (New Jersey: Prentice-Hall Inc., 1982), 468-540.

LabVIEW for Macintosh User Manual, Part Number 320591-01 (Texas: National Instruments Corporation, 1993).

Samuel J.P. Laube, "Hierarchical Control of Pulsed Laser Deposition Processes for Manufacture", Doctoral Dissertation, Electrical and Computer Engineering, University of Cincinnati, 1993

Douglas C. Moore, "Subprocess Control Design Methods For Advanced Materials Processing", Master's Thesis, Electrical and Computer Engineering, University of Cincinnati, 1994.

C. E. Otis and R. W. Dreyfus, "Laser Ablation of $YBa_2Cu_3O_{7-\delta}$ as Probed by Laser-Induced Fluorescence Spectroscopy", *Physical Review Letters,* Vol. 67, no. 15, 7 October 1991, 2102-2105.

Katherine L. Saenger, "Angular Distribution of Ablated Material", *Pulsed Laser Deposition of Thin Films*, (New York: John Wiley & Sons, Inc., 1994), 199-225.

Thomas P. Sheahen, *Introduction to High-Temperature Superconductivity*, (New York: Plenum Press, 1994).

Robert D. Strum and Donald E. Kirk, *First Principles of Discrete System and Digital Signal Processing*, (Massachusetts: Addison-Wesley Publishing Company, 1989), 529-608.

William M. Tong and R. Stanley Williams, "Kinetics of Surface Growth: Phenomenology, Scaling, and Mechanisms of Smoothening and Roughening", *Annual Review Physical Chemistry*, vol. 45 (1994), 401-438.

T. Venkatesan, X.D. Wu, R. Muenchausen, and A. Pique, "Pulsed Laser Deposition: Future Directions", *MRS Bulletin*, February 1992, 54-58.

T. Venkatesen, X.D. Wu, A. Inam, and J. B. Wachtman, "Observation of Two Distinct Components During Pulsed Laser Deposition of High Tc Superconducting Films", *Applied Physics Letters* vol. 52, no. 14, 4 April 1988, 1193-1195.

Robert C. Weast, Melvin J. Astle, and William H. Beyer, *CRC Handbook of Chemistry and Physics*, (Florida: CRC Press, 1987).

APPENDIX A - CONTROL HARDWARE/SOFTWARE

This section will further describe the software and/or hardware required to implement the three control loops implemented in the PLD system. These control loops are the laser energy control, substrate temperature control, and chamber pressure control.

A.1 Substrate Temperature Control

The control loop itself consists of an LFE PID Controller, a EUROTHERM SCR Driver (phase-angle fired), and the heater stage itself with an integrated thermocouple (type K - chromel/alumel). Figure A.1 shows the required wiring for the PID controller. Note that this schematic depicts the backside of the unit.

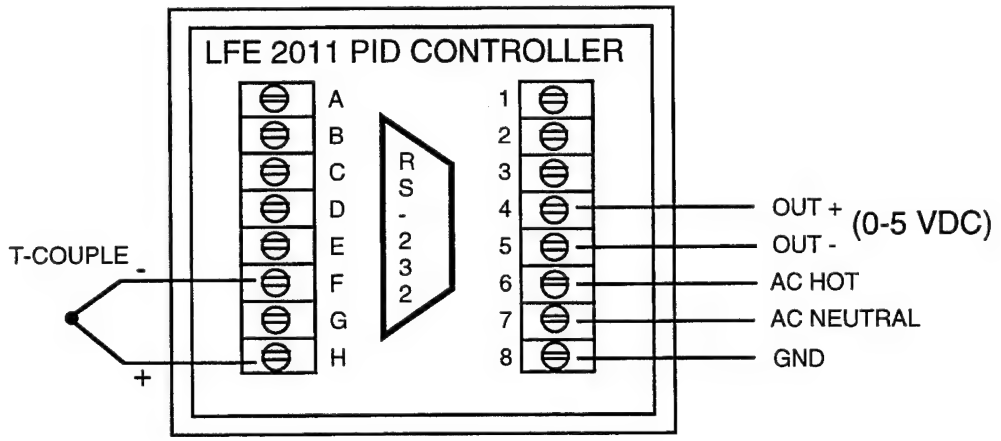

Figure A.1 - *LFE 2011 PID Controller Wiring*

The error signal out of the controller is a 0-5 VDC analog signal. It is this signal which is used to drive the SCR power controller, shown in Figure A.2. The

power controller has two separate connections to the AC line, one for it own internal electronics, and the other to drive the external load. Note that an external fuse kit must be provided. The power controller itself has no internal fusing for load shorts. Finally, it is important that the power controller be placed in a well ventilated area, as it will tend to dissipate large amounts of heat during operation.

Again, the purpose of the Macintosh is to issue temperature setpoint commands and collect heater stage temperature readings. This is done through the RS-232 port on the back side of the LFE 2011 PID controller, as shown in Figure A.1. The necessary cable for communicating between the Macintosh and the LFE 2011 is shown in Figure A.3. Note that the Macintosh serial port is actually RS-422 (differential). RXD+ must be grounded to allow for correct signal translation. The communication protocol is selected through back panel switches, with the factory defaults set as follows:

PARITY:	NO PARITY
BAUD RATE:	1200 bps
UNIT ADDRESS:	0
HANDSHAKE:	NO

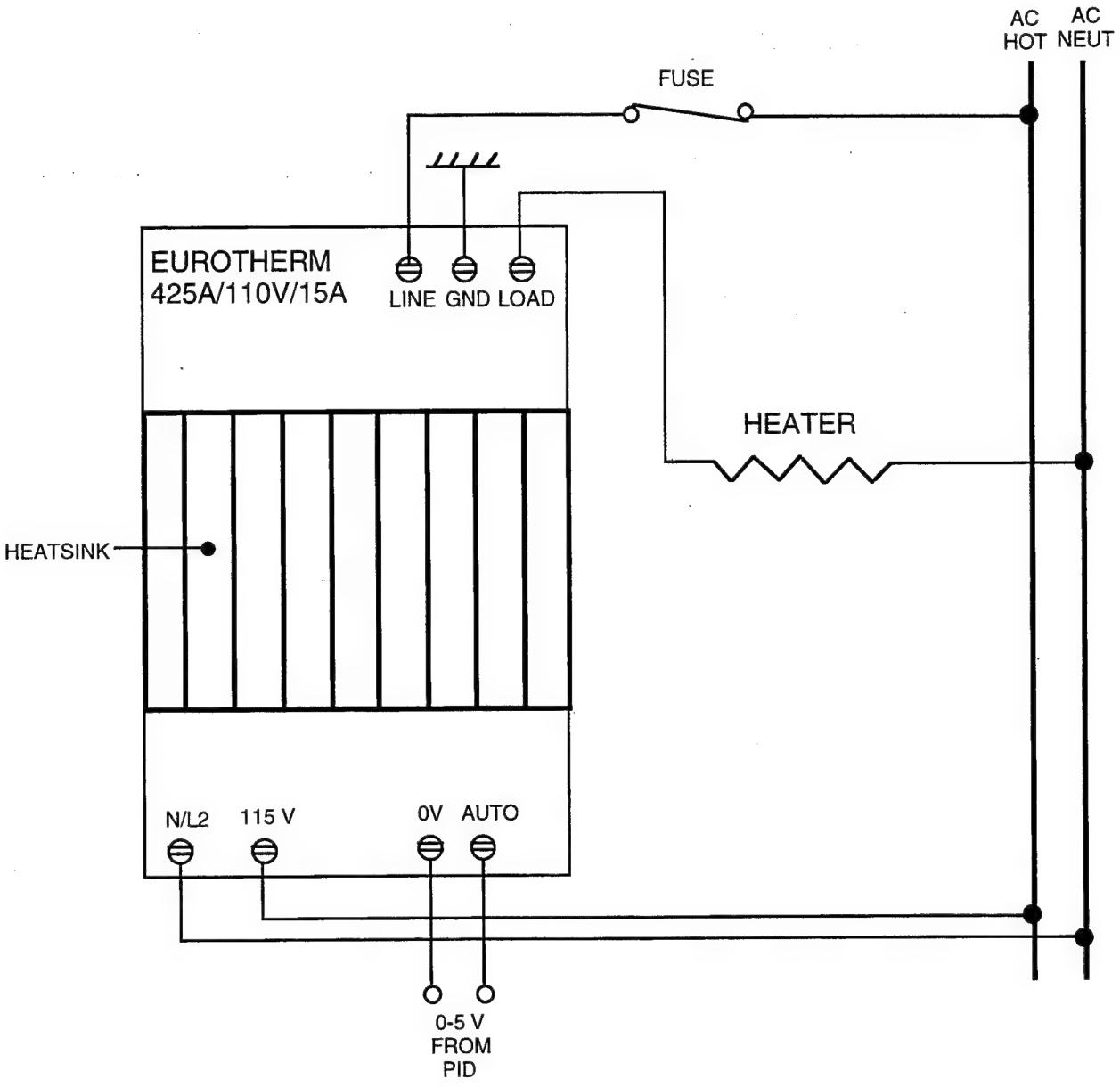

Figure A.2 - *Eurotherm SCR Power Controller Wiring*

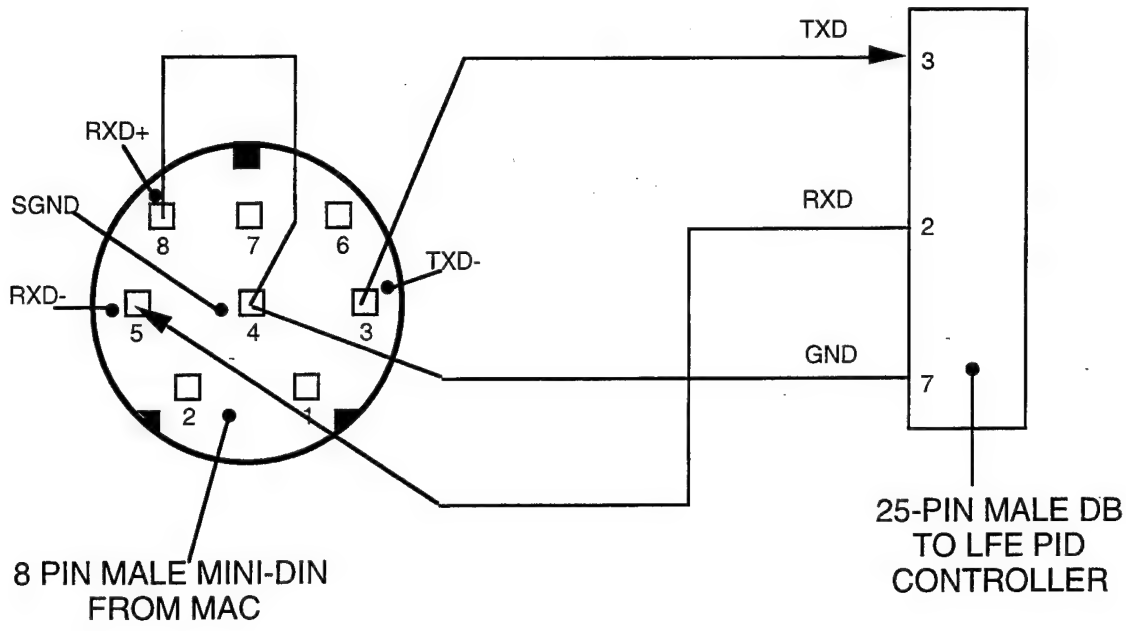

Figure A.3 - *LFE PID Serial Communications*

To program the PID controller, it is first necessary to turn on the PID controller (the controller has no power switch). This is done using a National Instrument's relay card. Note that AC power is simply applied to the PID unit. Next, a serial port is configured for the controller. The deposition software uses the modem port (port number 0) for this purpose. This port can be changed to the printer port by making a suitable software change to the PID controller configuration routine, PIDConfig.vi.

The Macintosh needs to issue two commands to control the device, a temperature setpoint command and a temperature read command. To write a new temperature setpoint to the device, the command *00:WCSP/(temp):<CR> is sent, where (temp) is the temperature in C°. The temperature setpoint command is indicative of the command structure for the PID unit. *00 addresses the 0th unit (default), while W indicates that the command is a write operation. Correspondingly, an R would indicate that the command issuer (the Macintosh) wanted to read some value. Finally, the variable to write or read follows W or R.

In this case, the variable is CSP (control setpoint). Note that every write operation to the controller will prompt a response from the controller (response contains checksum information). This response must be read in order for subsequent read operations to read the correct response, since any unread responses from previous write operations are stored in the serial input buffer. The simplest way to do this is to read the information at the serial port until there are no bytes left to read. This can be done by reading a single byte at a time until the <CR> character is read (<CR> represents the end of the message). To read the temperature, the command *00:RPV0:<CR> is issued (RPV0 = Read Process Variable number 0). Again, <CR> is checked for to determine the end of the message. If negative temperatures are expected, special precautions must be taken. First, the fifth character in the input string is checked to see it is an ASCII minus (-). If it is, the next five characters including the minus sign are converted to an integer (format is -####). If the number is positive, the four characters *following* the position checked for the minus sign are converted. This is necessary because the PID controller will insert a hex 00 (NULL) character in the position for a minus sign. If this character is passed to the string-to-integer conversion routine, the conversion will not work.

A.2 Chamber Pressure Control

The following list shows which Lab-NB lines drive which solenoid valves:

Slow O_2 Inlet	->	PC0
Fast O_2 Inlet	->	PB0
Bypass	->	PC1

Note that the relay assignments can be changed by changing the appropriate value in the global variable REALRUN.vi.

APPENDIX B - MACINTOSH INTERFACE

The first section of this appendix will explain the hardware details for the interface from the Macintosh IIfx to the PLD system. The second section will explain the user interface and data collection software that was written to direct the depositions.

B.1 System I/O Architecture

The deposition system is built around a Macintosh IIfx computer, three National Instruments' I/O cards, and a number of instruments/equipment. The following list gives a brief description of each piece of actual hardware used in the system.

1. LPX-305i Excimer Laser:

   This is obviously the main actuator in the PLD system. It operates at a wavelength of 248 nm and has a maximum output energy of 1 J. The output pulse width is approximately 25 ns. In addition to providing the energy for the deposition, the laser also contains an internal energy meter. This can be used during the deposition to monitor the output energy.

2. Newport Programmable Motion Controller PMC200-P (mirror controller):

   This device allows the laser beam to be 'steered' to whatever place is necessary. It accomplishes this through a controlled mirror.

3. 2 GRANVILLE-PHILLIPS Convectron Pressure Gauges:

One of these gauges is set to measure the pressure inside the chamber and the other is set for the pressure at the pump station.

4. MKS Baratron Pressure Gauge:

   This gauge is also set to read the chamber pressure. It is more accurate than the Convectron gauges listed above, but it has a limited range. It used to measure pressures less than 1 T.

5. HEWLETT PACKARD 54502A DIGITIZING OSCILLOSCOPE:

   The oscilloscope is used to record waveforms from the spectroscope sensor discussed in Section 2.3.4.

6. LFE PID Controller - RS-232 serial communications:

   This controller is used to regulate the substrate temperature, as discussed in Section 2.3.2. In addition, the heater thermocouple temperature can be read from the PID controller.

7. Nupro NVZ-110 Solenoid Valves:

   These valves are used to control the system oxygen pressure. Their use is discussed in Section 2.3.3.

A block diagram of the system communication architecture is shown in Figure B.1. As can be seen from the diagram, there are four types of communication interfaces used in the system. The type of interface used depends entirely on the capabilities of the instrument. Each of the four interfaces - GPIB, analog input, digital I/O, and serial port - will be discussed. These sub-sections will also contain a list of the instruments associated with each type of interface. The purpose of the following descriptions is to give the reader an understanding of

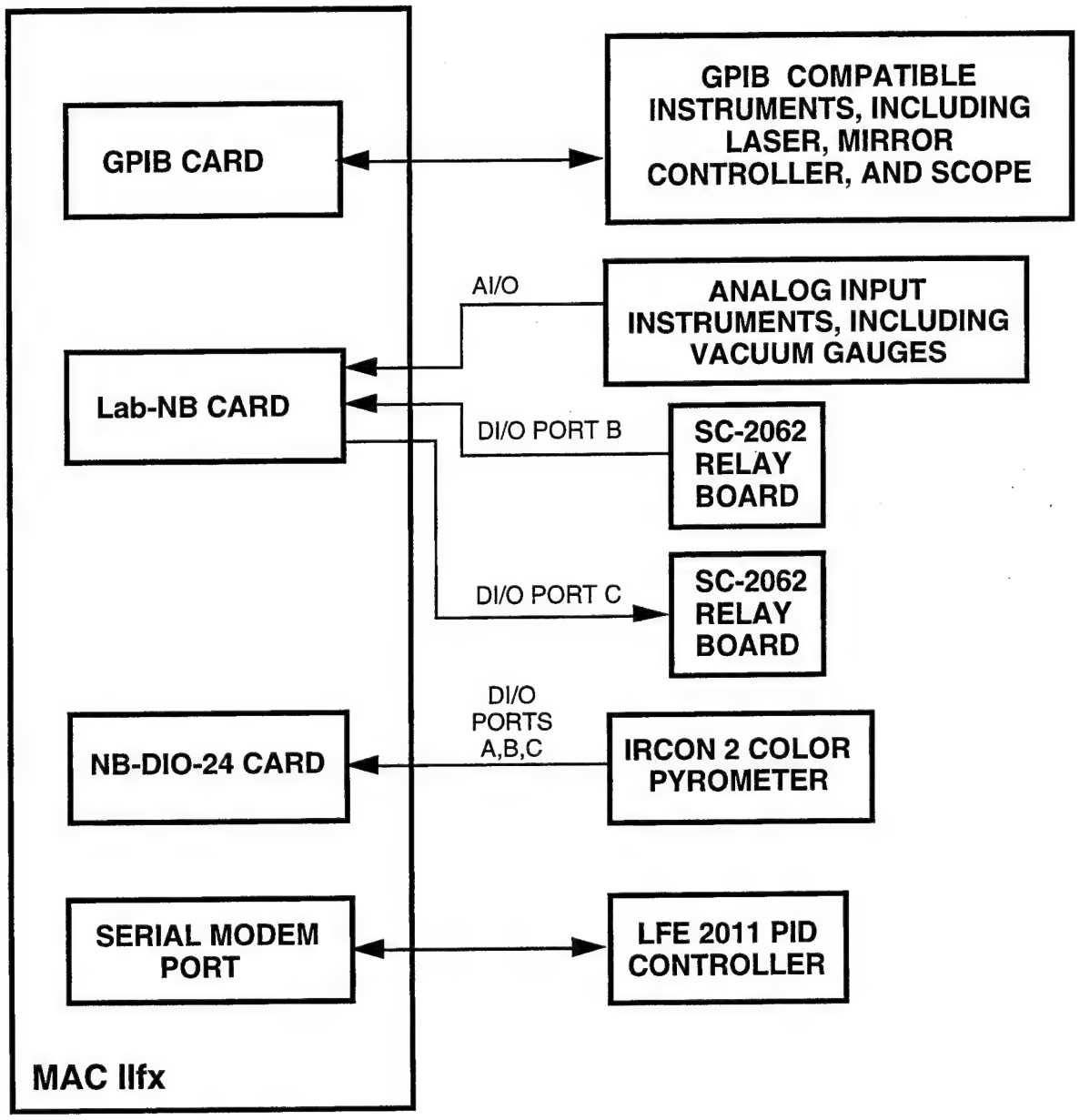

Figure B.1 - *System I/O Architecture*

what interface each instrument uses, and the general approach to using these different interfaces.

B.1.1 GPIB Communications

The GPIB Instrumentation Protocol (General Purpose Interface Bus), also known as I.E.E.E. 488 and HPIB, allows for fast data transfer accross a cable 'bus'. The device that controls all of the instruments connected to the GPIB is the GPIB card. The details of GPIB are unimportant, as the protocol is fairly transparent to the programmer. Regardless, GPIB compatible devices tend to be easier to program remotely because of the 'common commands' available to most instruments that implement GPIB. The GPIB compatible instruments used in this system are the LPX-305i laser at address 2, the Newport PMC200-P motion controller at address 4, and the HP 54502A Digitizing Oscilloscope at address 7. Note that the instruments can be connected in any fashion desired, since instruments are commanded to 'talk' or 'listen' (accept data from or provide data to the bus) only when their address is selected. Otherwise, any data that may be on the bus is ignored.

B.1.2 Analog Input Data Acquisition

Obviously, an analog input connection allows for one-way 'communication' only (instrument -> computer). The 'communication' is simply a voltage that represents some measured parameter. Handling the various analog instruments connected to the computer is one job of the Lab-NB card. This card has the capability of accommodating eight analog input channels, of which four are used. The instruments that supply an analog output are the chamber and pump pressure Convectron gauges and the Baratron Pressure Gauge. Figures B.2 and B.3 show

the connections for each gauge type. Note that these figures also show which analog channel these devices are connected to.

Before an instrument's analog voltage can be read, the specific channel associated with the instrument must be configured. This is done through the AIConfig.vi subroutine. This subroutine first looks for the Lab-NB board in each of the slots of the Macintosh. Provided the card is found, one specific channel is configured. This is done through the AI Group Config.vi, which returns a 'task id' specifier. This task id is a number which identifies a given channel input on a given card. Each input channel (analog or digital) has a specific task id. Note that any subsequent reads/writes to a channel are directed based on the channel's task id. The task ids for each input are stored in the global variable REALRUN.vi. In this way, all functions have access to each instrument. Figure B.4shows the front panel for REALRUN.vi. Note that this panel is not user visible.

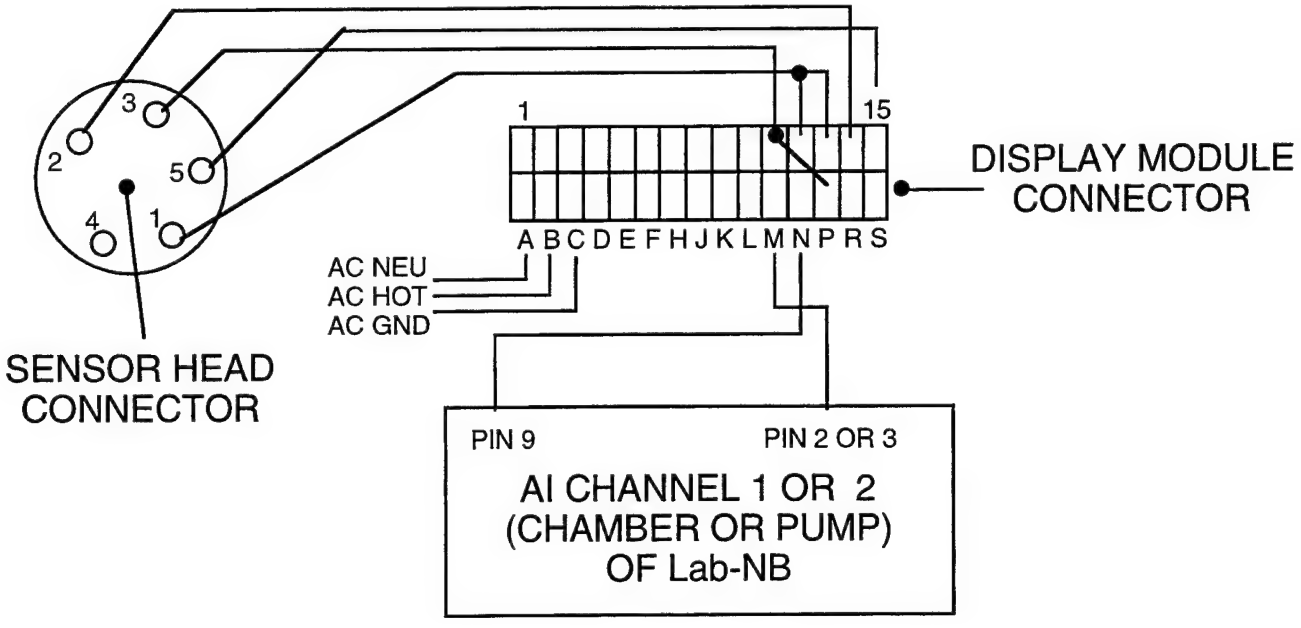

Figure B.2 - *Convectron Gauge Wiring (Chamber and Pump)*

In the case of an analog input channel, the actual channel characteristics need to be set after a task id is generated. For an analog input, the channel attributes are the range, polarity and gain. These are set through the sub-routine AI Hardware Config.vi. The following settings are possible:

range -- +/-5 Vor 0 -> 10 V, jumper selectable

polarity -- Bipolar or Unipolar, software selectable

gain -- 1, 2, 5, 10, 20, 50, 100, software selectable

B.1.3 Digital I/O

As Figure B.1 shows, both the Lab-NB card and the NB-DIO-24 card have digital I/O capabilities. In fact, the Lab-NB card has all the capabilities of the NB-DIO-24 card (three byte-wide ports). Therefore, configuring both of these devices uses the same function, DIO Port Config.vi. DIO Port Config.vi configures the width of a specified port (usually a byte) and the direction (input/output). A task id is then assigned to this port, which will specify the port in subsequent reads/writes, exactly like the analog input case.

For the Lab-NB card, digital ports B and C are used to drive two relay cards. Note that each card requires an external +5 V supply to drive the relay circuitry. Also, eight LEDs are provided to indicate the state of a given relay (ON/OFF).

Ports B and C of the Lab-NB card are used to drive the two relay cards (i.e. one port line per relay). These relays are used to switch 120 VAC on and off. Figure B.5 shows a schematic representation of the relays connected to Port C. Note that six relays are connected to standard line receptacles. Instruments without power switches can be plugged into these receptacles. In this way, these instruments can be powered up under software control by simply turning on the

associated relay. Note that a relay is turned on by pulling its control line high -- for example, to turn on R0, PC0 would be pulled high. The following list shows which instruments are connected to which receptacle (receptacle#, relay#).

S1, R7 -- Convectron pump pressure gauge

S2, R6 -- Convectron chamber pressure gauge

S3, R5 -- Omega thermocouple gauge

S4, R4 -- LFE PID Controller

S5, R3 -- open

S6, R2 -- open

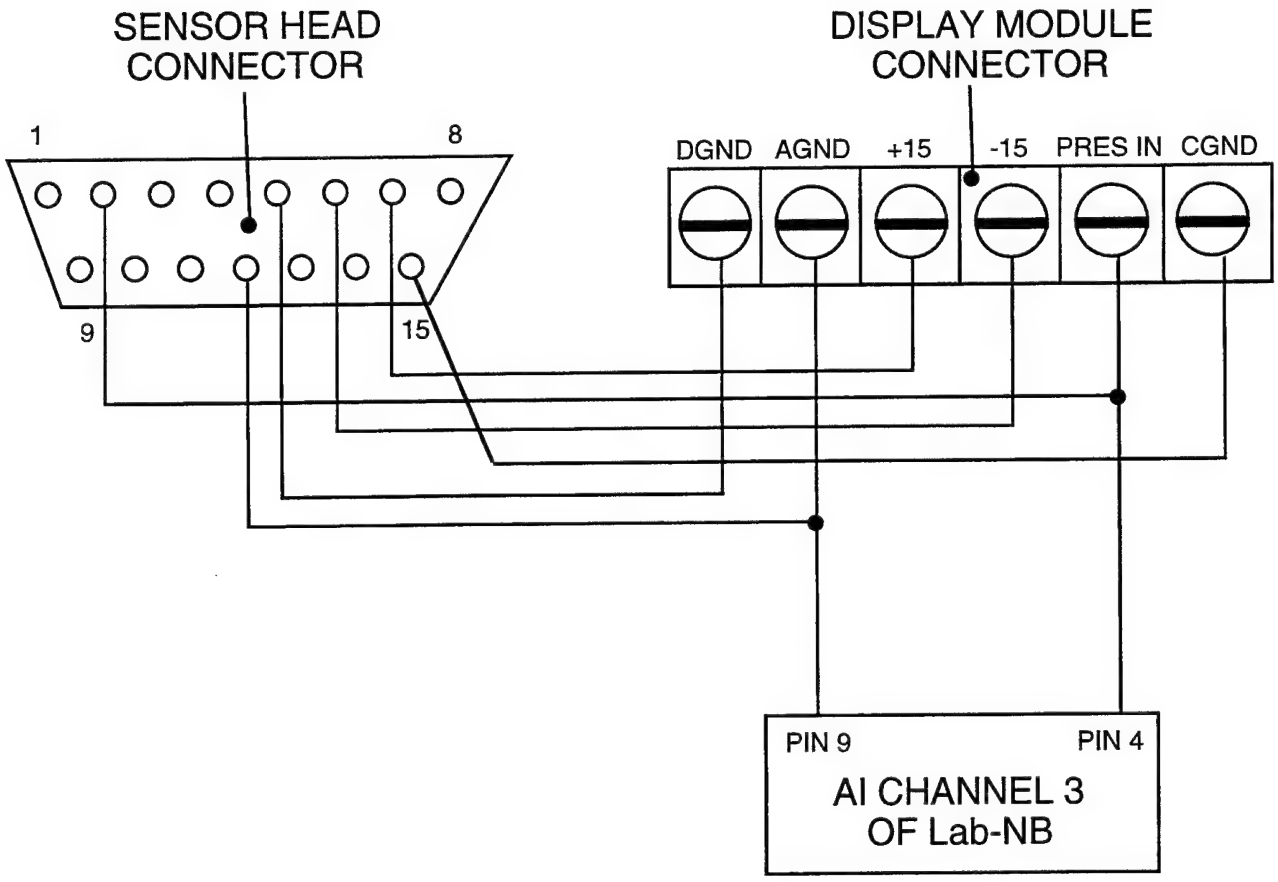

Figure B.3 - *Baratron Gauge Wiring*

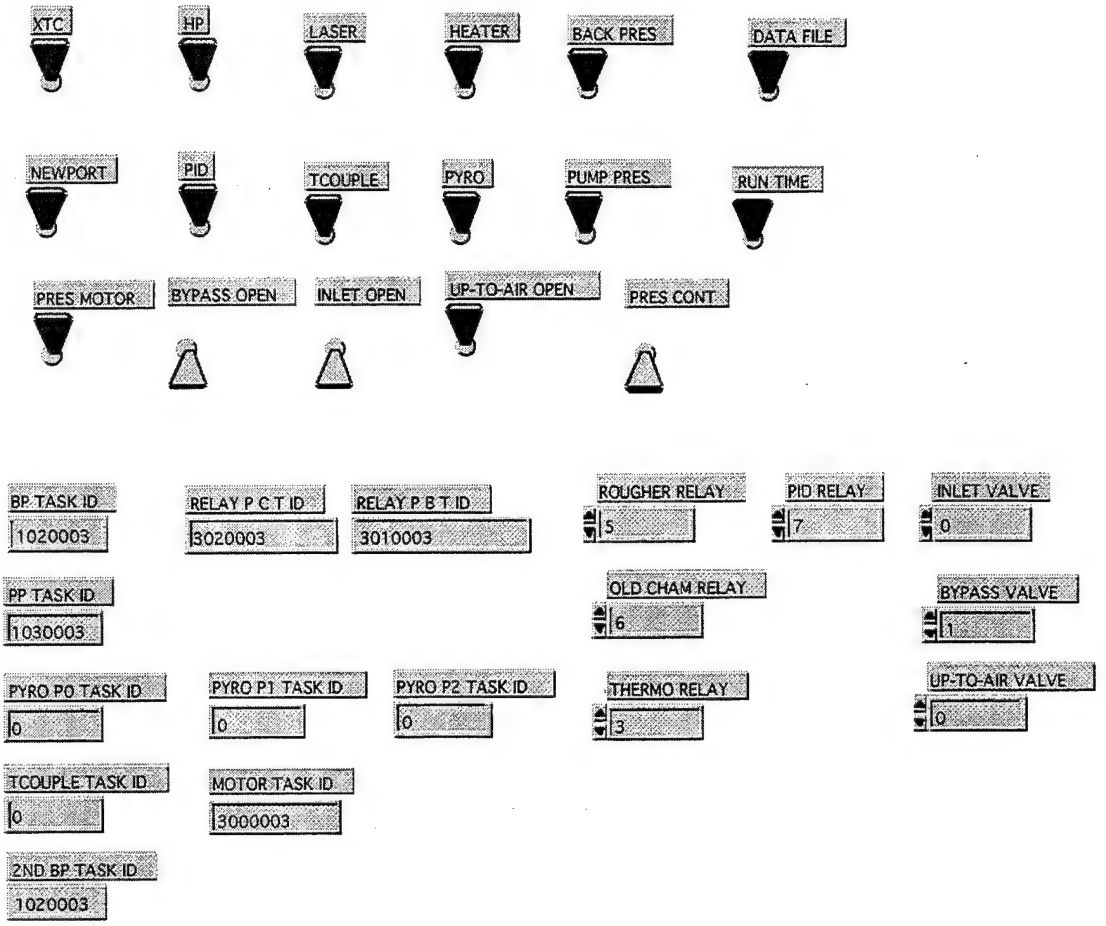

Figure B.4 - *REALRUN.vi Front Panel*

If needed, the open receptacles can be used on new instruments. Note that each relay assignment is given in REALRUN.vi. These assignments can be changed if needed. The remaining two relays of the Lab-NB Port C (R1 and R0) are used to switch pressure regulation valves. Their use will be discussed in the pressure control section. For now, however, a list of which valves are connected to which relays is given below.

PC, R1 -- bypass valve

PC, R0 -- inlet valve

PB, R0 -- up-to-air valve

Again, these assigments are given as default values in REALRUN.vi. Their values can be changed if necessary.

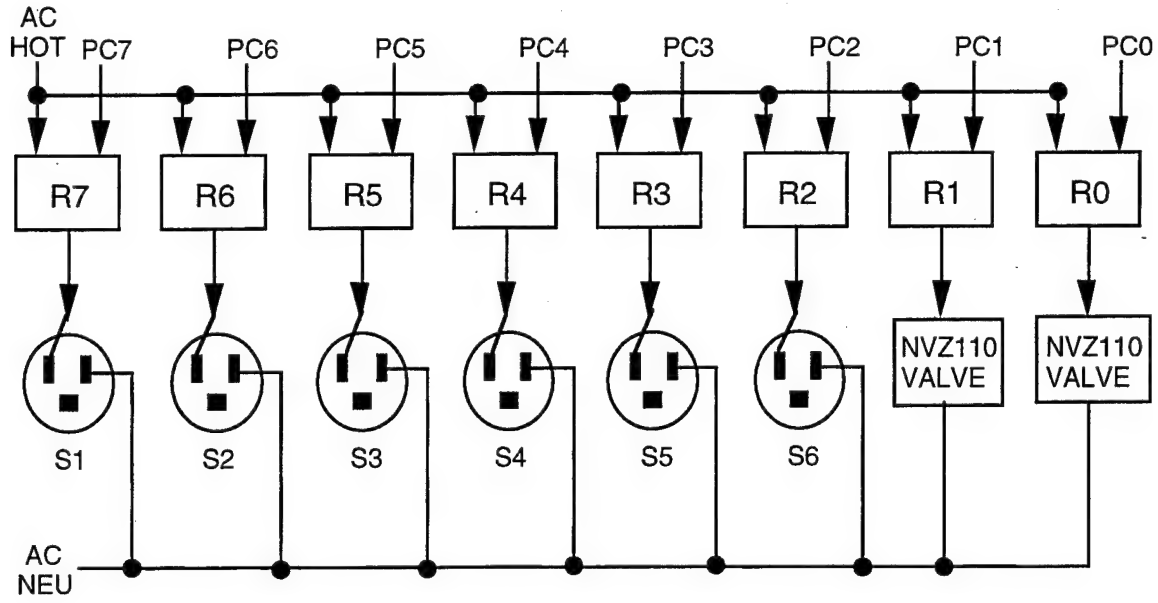

Figure B.5 - *LabNB Port C Relay Wiring*

The NB-DIO-24 card contains three digital I/O ports, all of which are used with the IRCON Pyrometer. The pyrometer was used in the old deposition system to measure temperatures. It may be transferred to the new system, however, so software was written to handle its BCD output. Figure B.6 shows the connections from the NB-DIO-24 card to the pyrometer.

B.1.3 Serial Port Communications

As Figure B.1 shows, the LFE PID Controller is connected to the modem port. Both this and the GPIB interface are the only bi-directional interfaces. Before communications can take place between the Macintosh and the controller, the serial port must be setup. This is done through Serial Port Init.vi, which sets

the baud rate and the communications protocol. Note that the port can be changed to the printer port by changing the port value in REALRUN.vi.

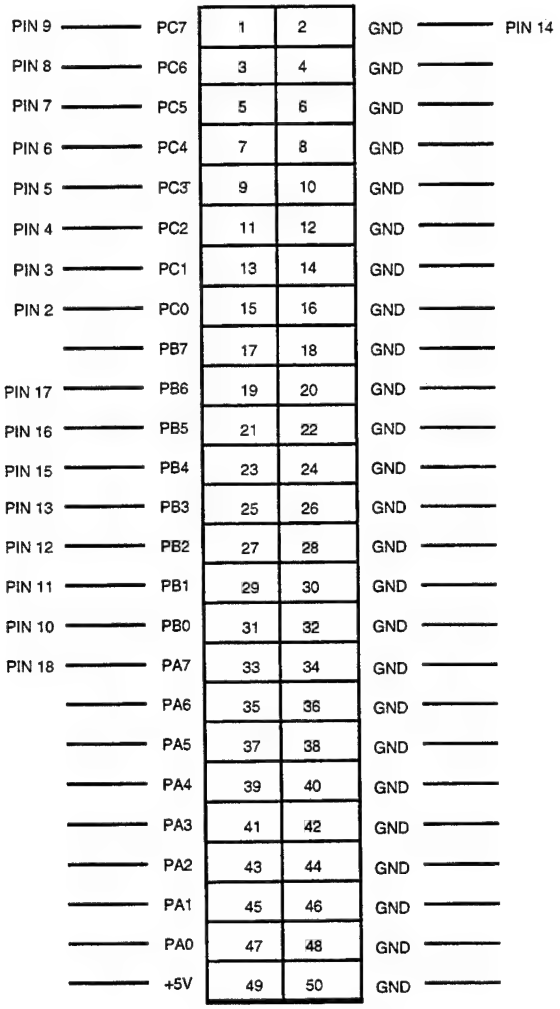

(a) DB-25 to 50-PIN NB-DIO-24

DB Pin #	Function
2	w=1
3	w=2
4	w=4
5	w=8
6	w=10
7	w=20
8	w=40
9	w=80
10	w=100
11	w=200
12	w=400
13	w=800
14	GND
15	w=1000
16	w=2000
17	w=4000
18	DATA READY

(b) DB-25 Signal Names

Figure B.6 (a) and (b) - *NB-DIO-24 Card to Pyrometer Wiring*

B.2 Deposition System Software

The following list contains a short description of each software module used in the system software. The modules are arranged based on their intended

function. For example, all the software needed to control the laser is grouped together.

1. System setup and deposition software:

   Data log setup ver 2.vi - deposition data file setup

   Data log.vi - write data file header information

   PLDDeposition ver 4.vi - deposition observation

   PLDFront Panel.vi - deposition setup

   PLDWrite data ver 2.vi - write data collected during deposition to data file

   PostDepComm.vi - append post-deposition comments to data file

   REALRUN.vi - global variable containing system setup information

2. Lambda Physik LPX-305i laser software:

   LPXFront Panel ver 2.vi - laser setup

   GET OPMODE AND PRESS.vi - get the laser operating mode and the current cavity pressure

   LPXDLoad Hz.vi - write the rep-rate to the laser

   LPXDLoad V.vi - write the cavity voltage to the laser

   LPXDLoad V,Hz.vi - write both the cavity voltage and the rep-rate to the laser

   LPXGet Energy - read the current energy output from the laser

   LPXGet Settings - read the current voltage and rep-rate from the laser

   LPXNew File.vi - create a new laser file containing the currently selected voltage and rep-rate

   LPXRead File.vi - read a laser file

LPXRead.vi - read the response generated from a LPXWrite.vi command

LPXWr-Re loop.vi - write a command and read the response from the laser

LPXWrite.vi - write a command to the laser

3. Laser control software:

GEN MATRIX VER 3.vi - generate the lookup table

LPX PI Control.vi - control the laser energy

PICK HV.vi - pick the laser operating voltage based on the energy and the rep-rate

READ MAT FILE.vi - read the lookup table file

SPLINE FIT.vi - spline-fit the table errors.

4. Newport PMC200-P mirror controller software:

gNPCenter Data.vi - global variable containing scan parameters

NPCalib final ver 4.vi - scan calibration

NPConv num to NP.vi - convert target coordinates to Newport coordinates

NPConv num to string.vi - convert a target coordinate to a Newport coordinate string

NPConv num - convert a Newport coordinate to a target coordinate

NPFront Panel final ver 3.vi - mirror setup

NPInit final ver 3.vi - mirror initialization

NPJog down.vi - instruct controller to step mirror down

NPJog up.vi - instruct controller to step mirror up

NPNew File.vi - create a new mirror controller file containing the current scan parameters

NPOpc ver 2.vi - OPERATION COMPLETE detection

NPPos1 ver 3.vi - read Newport axis 1 position

NPPos2 ver 3.vi - read Newport axis 2 position

NPRead File.vi - read a mirror controller file

NPRead with Error.vi - read a response to an NPWrite.vi and indicate any errors

NPReset.vi - reset the mirror controller to a known state

NPSave Center 1.vi - save the axis 1 position as the axis 1 scan center

NPSave Center 2.vi - save the axis 2 position as the axis 2 scan center

NPScan final ver 7.vi - generate the scanning instructions for the mirror controller

NPStop.vi - stop any mirror motion

NPWr-Re loop ver 2.vi - write a command and read the mirror controller's response

NPWrite.vi - write a command to the mirror controller

5. Measurement software:

AIConfig.vi - configure an analog input channel

BACKPRESTest.vi - test the chamber pressure gauge

BPRESRead.vi - read the chamber pressure gauge

PPRESRead.vi - read the pump pressure gauge

PUMPPRESTest.vi - test the pump pressure gauge

PYROConfig.vi - configure the pyrometer input channel

PYRORead.vi - read the pyrometer output

PYROTest.vi - test the pyrometer

TCRead.vi - read the thermocouple gauge

TCTest.vi - test the thermocouple gauge

HPGetData ver 2.vi - read the spectroscope measurments

HPRead with Error.vi - read a response from the oscilloscope

HPWr-Re loop ver 2.vi - write a command and read a response from the oscilloscope

HPWrite.vi - write a command to the oscilloscope

GET PID TEMP.vi - read the substrate temperature

PID TEST.vi - test the PID temperature controller

PIDConfig.vi - configure the PID temperature controller

TEMP PID SETPOINT.vi - set the substrate temperature

6. Pressure control software:

   PressContRTime.vi - control the chamber pressure

7. Relay control software:

   RELAY CONFIG.vi - configure the relay cards

   RELAY WRITE.vi - write a state (TRUE/FALSE) to a relay

B.2.1 System Setup and Deposition Software

The purpose of the first front panel, PLDFront Panel.vi, is to configure the deposition system. As can be seen from Figure B.7, the panel has setup buttons for each instrument in the system. This scheme allows the user to configure only the instruments they wish to use. Depending on the data collection

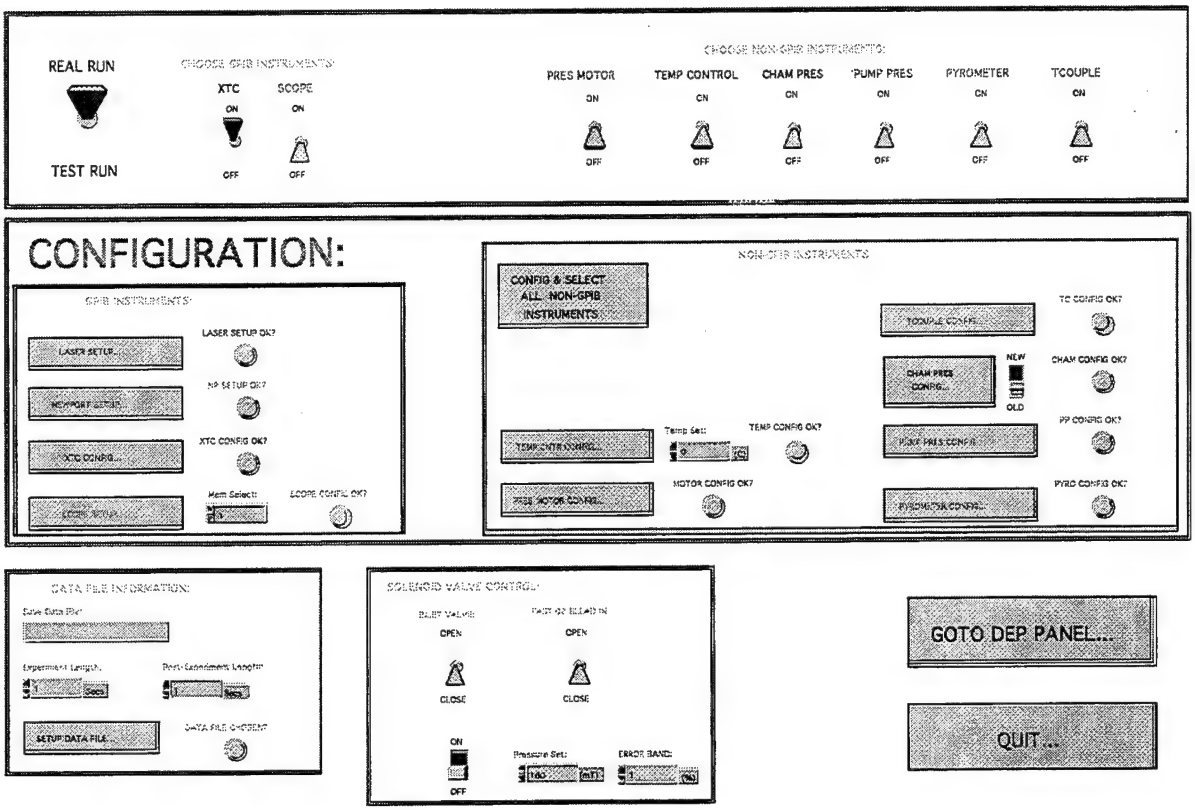

Figure B.7 - *PLDFrontPanel.vi User Interface*

requirements, certain instruments might not be selected. If a given instrument is configured successfully (this depends on the instrument selected), it is then selected to be used in the deposition. This selection is indicated by the toggle switches in the upper half of Figure B.7. Previously selected instruments can be de-selected if needed. Note that the configuration routines called when these

buttons are pushed are described in other sections. Any configuration information required for reading a given instrument is contained in the global variable REALRUN.vi. This vi also contains the state of the system in terms of which instruments have been selected.

The other purpose this front panel serves is to start a data file for the data collected during the deposition. Before the deposition front panel is called (PLD Deposition Front Panel.vi), a list is presented to the operator instructing him/her as to what instruments have been selected and whether or not a data file has been selected. This is done so that. any changes to the setup can be made before the actual deposition panel is called.

When the user wishes to start the deposition (i.e. the system is ready), PLDDeposition ver 4.vi is called. As the name suggests, the purpose of this piece of software is to direct the deposition procedure. In addition to collecting all the data requested, this sub-routine allows the user to set any system parameters. Figure B.8 shows the front panel presented to the user when this subroutine is called. As this figure shows, all of the instrument readings are displayed graphically. Also, controls are provided to set deposition parameters.

The operation of this piece of software is fairly straightforward. Essentially, when the 'START DEP...' key is pressed, every instrument that was selected is read and each measurement is displayed in the appropriate graph. Also, the deposition parameter controls (laser energy, rep-rate, etc.) are monitored for activity. In this way, each parameter can be changed as necessary. The laser is automatically stopped when the length of time specified in the 'Deposition Length:' has expired. After the laser is stopped, the program continues to read the selected instruments until the length of time specified in the 'Post-Dep Length:' has expired. In this way, the software can track system changes after the actual deposition has

ended. When both time lengths have expired, the data collected is written to the data file specified previously.

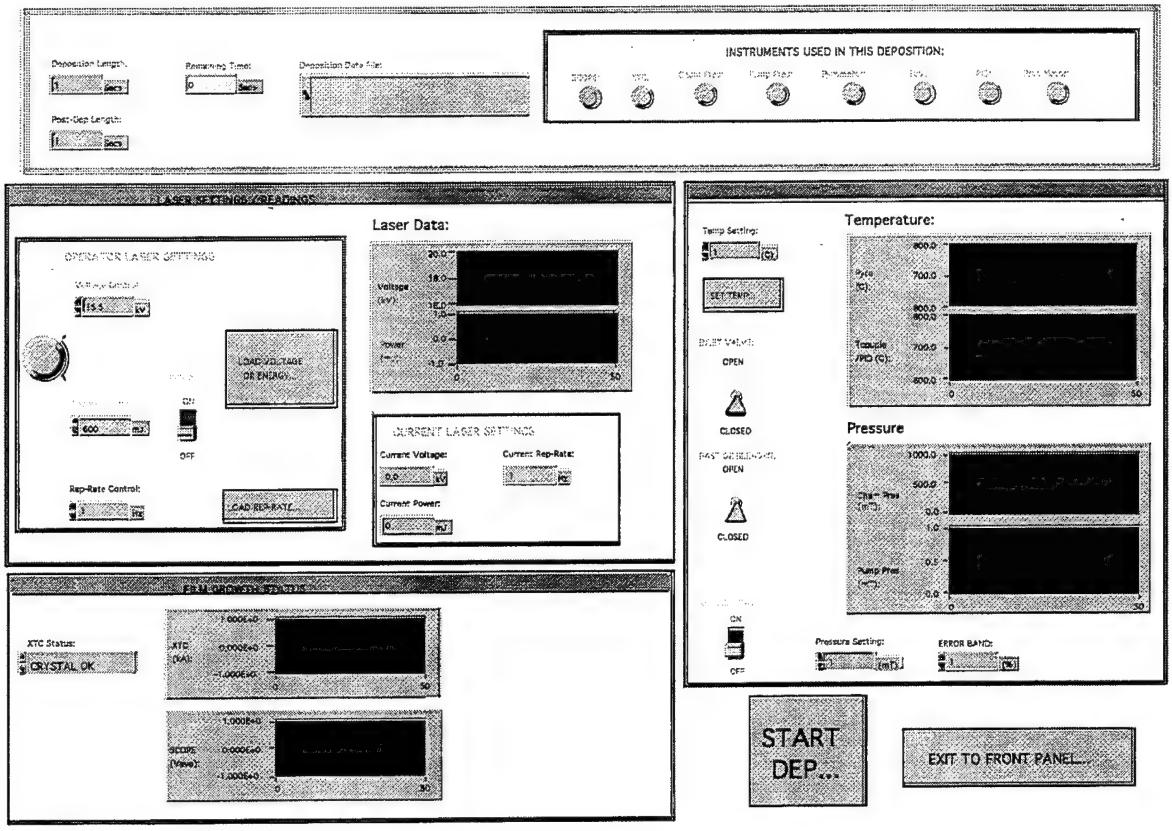

Figure B.8 - *PLDDeposition ver 4.vi User Interface*

B.2.2 Lambda Physik Laser

The Macintosh communicates with the laser via the GPIB bus. Since the laser is the main actuator in the system, a large portion of the deposition software is written for it. All of the software functions can be accessed through the user-visible laser front panel, called LPXFront Panel ver 2.vi. Note that this major piece of software performs five basic functions, each of which will be discussed in detail. Figure B.9 shows the actual graphic display visible to the user.

Before anything can be done with the laser, a self-test procedure must be initiated by pressing the SELF-TEST... key. Note that all of the other buttons on the panel will be dimmed unless this test passes. As part of the test, the laser will

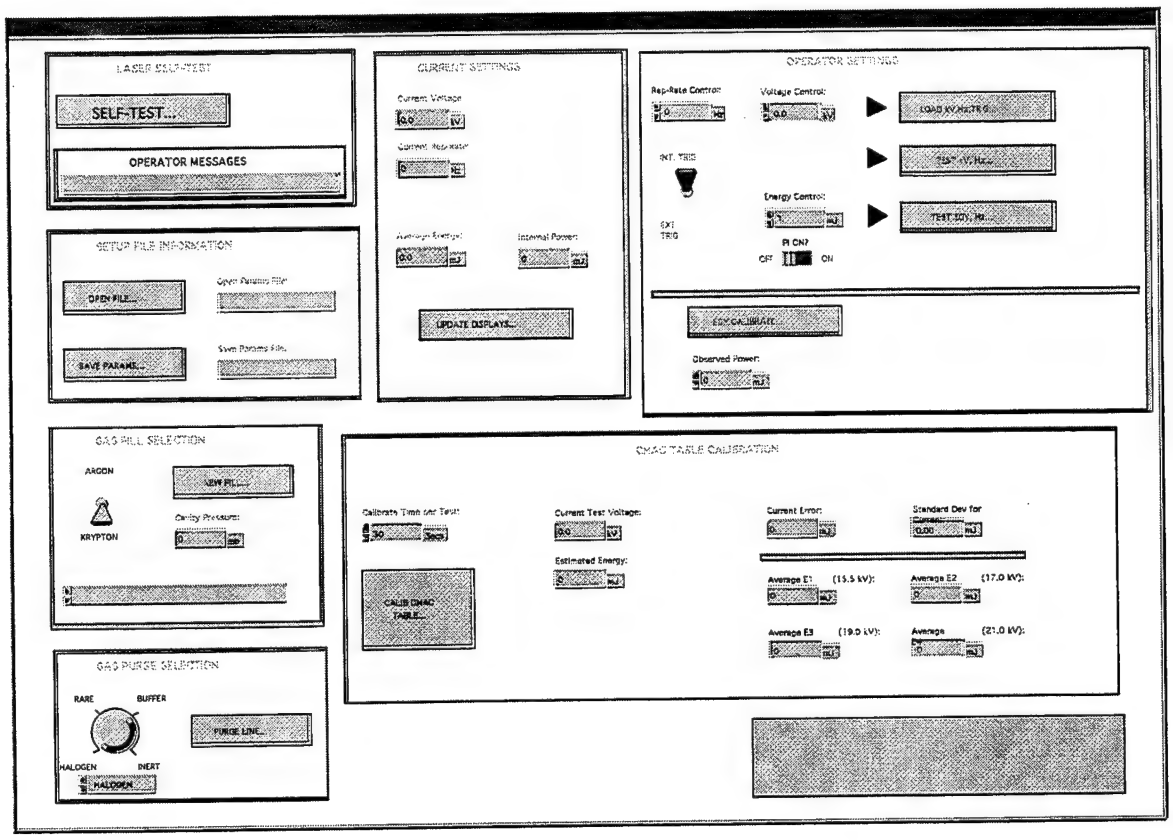

Figure B.9 - *LPXFrontPanel.vi User Interface*

be warmed up for eight minutes, during which time no commands will be accepted. If the laser fails the self-test for any reason, an error message reflecting the failure cause will be displayed in the OPERATOR MESSAGES indicator.

One of the main purposes of this front panel is to determine the current state of the laser. Since the laser output energy is a function of gas fill age, it is possible that the internal energy measurements may not agree with the actual output energy. This leads to one specific function of this piece of software, calibration of the

internal energy monitor. This function is invoked by pressing the EGY CALIBRATE... key on the front panel. Pressing this key downloads the current voltage (located the Voltage Control: box) and a rep-rate of 2 Hz (rep-rate is the number of laser pulses per second) through the subroutine LPXDLoad V,Hz.vi. Note that this function is used whenever the voltage or rep-rate or both are changed. Next, the laser is placed into the calibration mode by issuing the command "OPMODE=ENERGY CAL". The laser will then automatically turn itself on at the prescribed voltage and rep-rate. The software then repeatedly queries the laser's operating mode (OPMODE?) until the response "ENERGY CAL CONT" is received. Then, the operator is instructed to enter the externally observed power. When the EGY CALIBRATE... key is released (it is still stuck in the down position from the original push), the energy value in Observed Power: will be downloaded to the laser. This value will automatically calibrate the power meter.

The internal power meter is calibrated so that energy measurements from the laser will agree with energy measurements made at the chamber entrance. In this way, the laser output can be adjusted in real-time if needed. Since the parameters that can be varied are laser voltage and rep-rate, it is necessary to be able to relate the energy output of the laser to the voltage and rep-rate inputs. This is done through the lookup table, the operation of which is discussed in Appendix A.1.1. Appendix A.1.2 describes how the table is updated, which is accomplished by pressing the CALIB LOOKUP TABLE... key. The software then proceeds through four timed tests (user selectable time length) as discussed in Appendix A.1.2. The purpose of these tests, incidentally, is to determine the accuracy of the old table. For this reason, the average error for each test is displayed. Note that a negative average error indicates that the table value was too low for a given test.

Once the lookup table is calibrated, the operator may wish to test its effectiveness. This is done through the TEST EGY, HZ... key. When this key is pressed, the software takes the energy value in the Energy Control: box together with the rep-rate value in the Rep-Rate Control: box and picks a voltage to give the specified energy at the specified rep-rate. The software picks the required voltage through the subroutine PICK HV.vi and downloads this value to the laser along with the specified rep-rate. The laser is then started and continues to run until the TEST EGY, HZ... key is released. Note that as the laser is running, all of the laser parameters are being collected and displayed in appropriate indicators (rep-rate, voltage, and energy). If the PID ON? switch is in the ON position, the PID energy control is activated. As discussed in Section 2.3.1, the purpose of the energy PID controller is to correct errors in the table.

Since the energy output will degrade as the gas-fill ages, it will become necessary to periodically refill the laser. This is done automatically by pressing the NEW FILL key. The filling procedure is then started by first telling the laser which type of fill will be completed. This is based on the selection of the ARGON/KRYPTON switch. The statement "MENU=#" is issued to the laser, where # = 1 if ARGON is selected, or # = 2 if KRYPTON is selected. Next, each of the gas lines is purged. Note that an individual gas line can be purged by pressing the PURGE LINE... button. Finally, after all the gas lines have been purged, the filling procedure commences. The cavity pressure is continuously updated during the fill so that the operator has some visual feedback as to the state of the operation.

The final function of the front panel is to either load previous settings from or save current settings to a data file. The parameters read/saved are voltage and rep-rate. Files are opened and saved through LPXRead File.vi and LPXNew File.vi, respectively.

B.2.3 Newport Mirror Controller

Before proceeding to the software description, it is necessary to first describe the coordinate systems used in the software. The mirror itself is controlled by two actuators; one drives it horizontally and the other vertically. The position of the mirror is therefore described by two numbers, called the axis 1 position and the axis 2 position. This is obviously a simple two-dimensional coordinate space where the x-axis is axis 1 and the y-axis is axis 2. This coordinate system the mirror controller uses is referred to in the software as the Newport coordinate system. In other words, any movement commands issued from the software must be in this coordinate system. The other coordinate system is the target coordinate system, which is simply the x-y coordinate space on the target. Since the mirror is separated from the target by some distance, the two coordinate systems are not equivalent. In order that the operator have some idea how large a given scan pattern is on the target, it is necessary to convert back and forth between the two systems. Note that there is no way to define the coordinates the mirror controller uses. Therefore, all conversions must be done in software.

To illustrate the projection problem, consider Figure B.10. This figure shows a schematic representation of the projection involved in the translation from mirror controller coordinates to target coordinates. From simple trigonometry,

$$\tan(\theta) = \frac{X_{NP}}{r}$$

and

$$\tan(\theta) = \frac{X_{TARG}}{L}$$

where X_{NP} and X_{TARG} are the coordinates for the mirror controller and the target, respectively, L is the distance between the mirror and the target, and r is the

distance from the mirror center to the axis 1 actuator (x-axis). X_{TARG} and X_{NP} are then given by

$$X_{TARG} = \frac{L \bullet X_{NP}}{r}$$

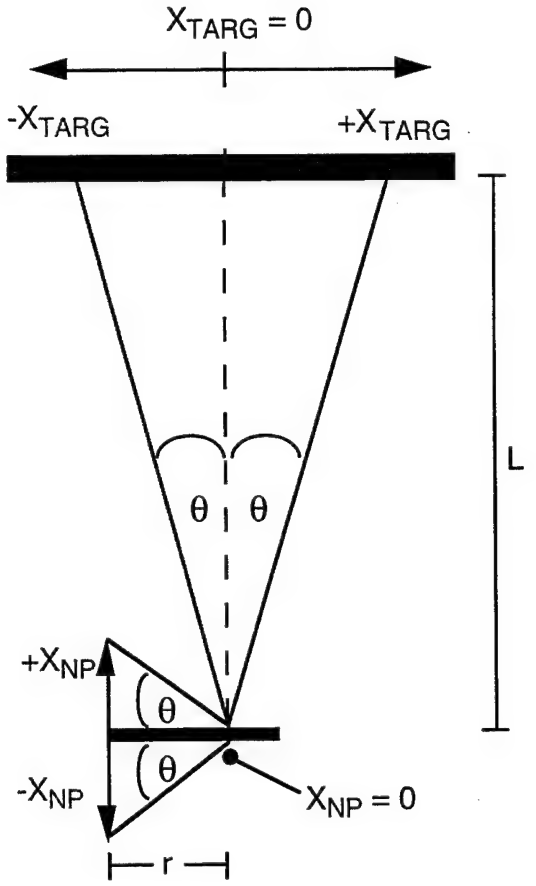

Figure B.10 - *Translation From Mirror to Target Coordinates for Axis 1*

and

$$X_{NP} = \frac{r \bullet X_{TARG}}{L}$$

For axis 2 (y-axis), the calculation is a little more complex due to the fact that the target is not perpendicular to the impinging beam. Consider Figure B.11.
As can be seen, the target is at a 45° angle with respect to the beam path. Note that a negative Y_{NP} gives a positive Y_{TARG}. For a negative Y_{NP}, θ is given by

$$\theta = \tan^{-1}\left(\frac{|Y_{NP}|}{r}\right)$$

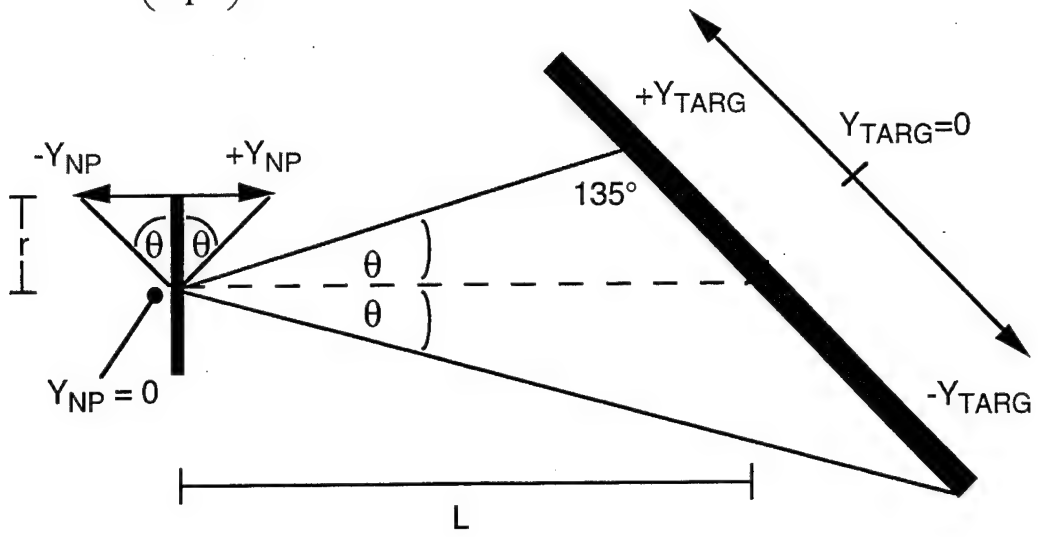

Figure B.11 - *Translation From Mirror to Target Coordinates for Axis 2*

where r is the distance from the mirror center to the axis 2 (y-axis) actuator. Note that the r for axis 1 is not the same value as r for axis 2 for the mirror in the new system. From the law of sines,

$$\frac{Y_{TARG}}{\sin(\theta)} = \frac{L}{\sin 135^{o}}$$

Y_{TARG} is therefore

$$Y_{TARG} = \frac{\tan^{-1}\left(\frac{|Y_{NP}|}{r}\right) \bullet L}{\sin 135^{o}}$$

For a positive Y_{NP}, Y_{TARG} is found in the same manner except that the 135° angle is now a 45° angle. To find Y_{NP} from Y_{TARG}, the same procedure is used except that θ is solved for.

The software is written so that either of these coordinate systems can be used. The operator typically uses target coordinates, since the mirror controller's coordinates are essentially meaningless. Therefore, the software must be able to easily switch between the two coordinate systems.

NPFront Panel ver 3.vi is the first panel shown to the user when the operator wishes to control the mirror (called from the main PLD program). Figure B.12 shows the interface visible to the user to the user. First note that this panel also allows for the selection of both the coordinate system to use and the chamber to use. The chamber selection switch is needed because the coordinate system translations are not the same in both the new system and the old system (i.e. the distances involved are different, as well as the orientation of the chambers). This panel allows the user to load a data file containing a list of scan parameters, such as the scan type, the height and width of the scan, and the scan center coordinates. Pattern scans can also be generated, optionally firing the laser during test scans.

The main purpose of this panel is to serve as the launcher for the other two visible front panels, NPInit final ver 3.vi and NPCalib final ver 4.vi. NPFrontPanel final ver 3.vi communicates with these other panels (as well as additional pieces of code) through the use of a global variable called gNPCenter Data.vi. This global variable is actually a collection of parameters, such as the coordinate system used, the scan height and width, and the scan center coordinates.

NPInit final ver 3.vi is used to return the mirror controller to a known position prior to the actual deposition. Figure B.13 shows the user interface. When the mirror controller is turned on, it has no way to determine what coordinates the mirror is at, so it simply zeros the display. Due to the requirement that the system operators know the scanning dimensions on the target itself, it is necessary to reset the controller's coordinates so that the two sets of coordinates will agree (the controller's coordinates and the actual target coordinates).

Essentially, this subroutine's function is to run the mirror to the limit on both axes in both directions (positive and negative values for both axis 1 and axis 2). The initialization subroutine contains code which illustrates some of the basic functions

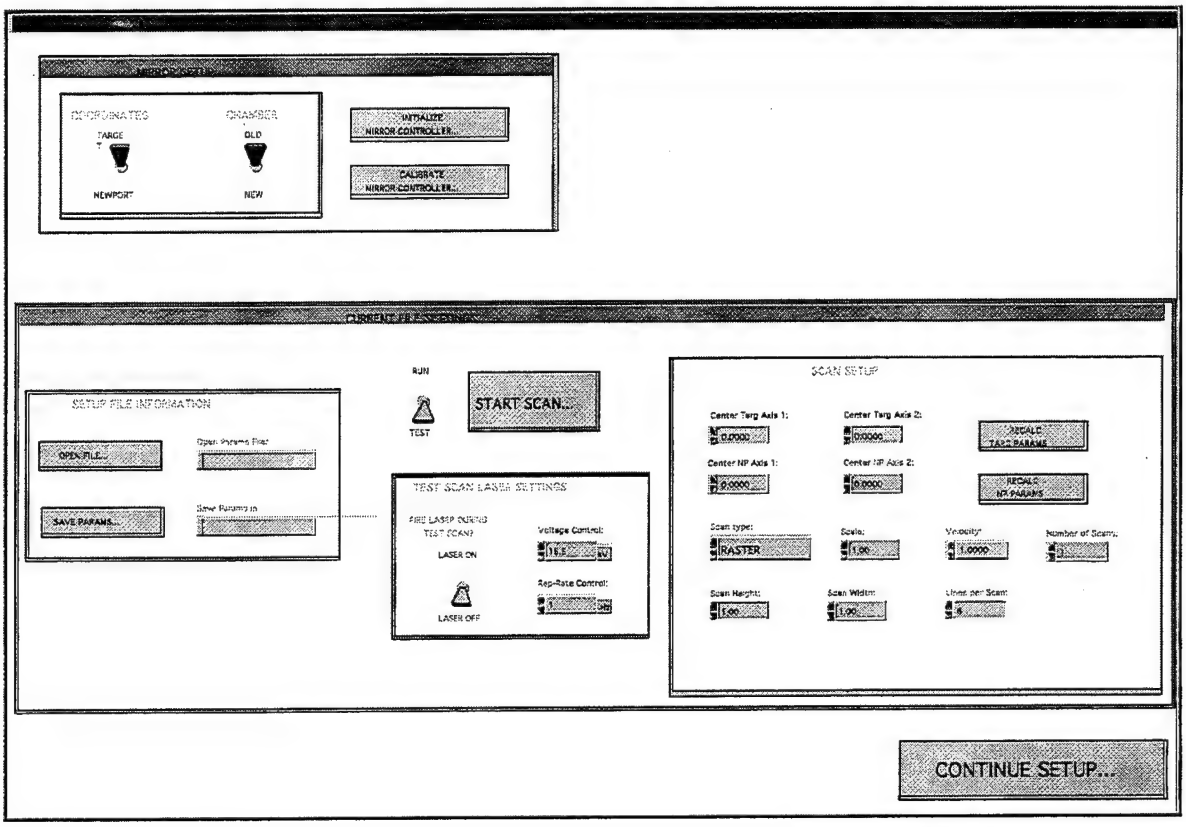

Figure B.12 - *NPFront Panel final ver 3.vi User Interface*

and abilities of the mirror controller. In order to understand the requirements of programming the mirror controller, this subroutine will be described in some detail.

Again, the function of this subroutine is to move the mirror to some known position on the target, ideally the target center. After the INIT button is pressed on the front panel, the initialization sequence is started. First, a controller reset routine is called. This routine defines initial parameters for the controller, such as the actuator types connected to the scanning mirror and the units used for distance measurements (typically mm). The next step is to run the mirror in a specified

direction until the mechanical stops are hit. To initiate this action, the command "*CLS;RUN1 -100;*OPC" is used. This command actually contains three separate commands, all separated by semicolons (*CLS, RUN1 -100, and *OPC). Of these three commands, RUN1 -100 has the most obvious meaning. It essentially starts

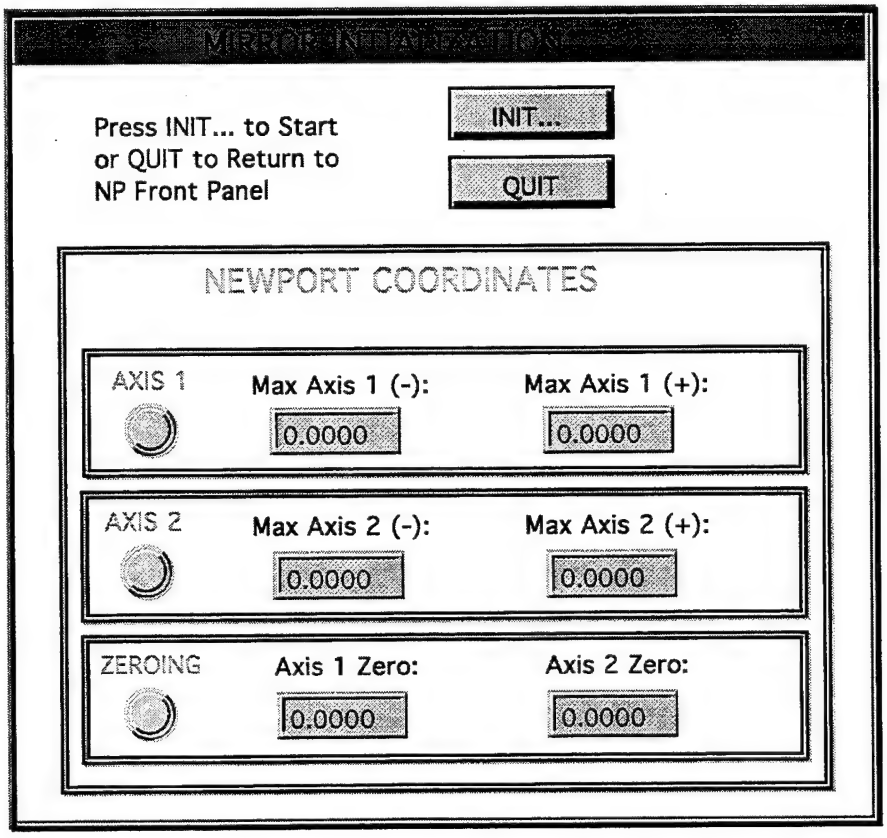

Figure B.13 - *NPInit final ver 3.vi User Interface*

moving axis 1 in the negative direction with a velocity of 100 mm/sec. Note that this value is not actually the speed the actuator moves at, although the controller will *attempt* to move it at this speed. The other two commands, *CLS and *OPC are used together to determine when the axis 1 actuator has reached the 'negative' stop (note that commands prefaced with an asterisk are commands common to all GPIB instruments). *CLS clears all of the status registers internal to the mirror controller prior to the RUN1 command. These registers contain status information

for the actuators. Please refer to the manual for a schematic representation of the register structure (footnote). The register of interest in this case is the Standard Event Status Register (ESR), which contains an Operation Complete bit (bit 0). *OPC forces the controller to set this bit true when the actuator stops due to the mechanical stops. The code then continuously checks this bit until it is set, indicating the operation is complete. When the operation is complete, the current position of the axis 1 actuator is read. This procedure of clearing the ESR, issuing the command, and waiting for the OPC bit to be set is used for all movement instructions. This is necessary so that the program knows when to ask for actuator positions.

The program then instructs the mirror controller to move the axis 1 actuator until the 'positive' stop is hit, and again reads this position. This sequence is repeated for the axis 2 actuator (y-axis) so that the program now has four position values: axis 1 max negative, axis 1 max positive, axis 2 max negative, and axis 2 max positive. The center coordinates are then found by

$$\text{axis 1 mid} = \frac{\text{axis 1 max neg} + \text{axis 2 max pos}}{2}$$

$$\text{axis 2 mid} = \frac{\text{axis 2 max neg} + \text{axis 2 max pos}}{2}$$

The actuators are then moved to this position using the MOVE command. The display is then zeroed using the ZERO command.

The NPCalib final ver 4.vi function serves two purposes. It is used to manually position the mirror and to generate scanning instructions for the mirror controller. With regards to simple mirror positioning, Figure 3.1 shows that there are four possible movement directions (two for each axis). The controls to initiate each of these directions are labeled as UP, DOWN, LEFT, and RIGHT. The CENTER button moves the mirror to the currently defined center position, given in

the SCAN SETUP sub-window. Note that the switch with the labels Jog and Run determines the type of motion of the actuators. When the switch is set in jog mode, the actuators will step the specified distance indicated in either Jog 1 Distance or Jog 2 distance (these distances depend on the coordinate selection), depending on movement direction. Note that pressing the UP button will actually

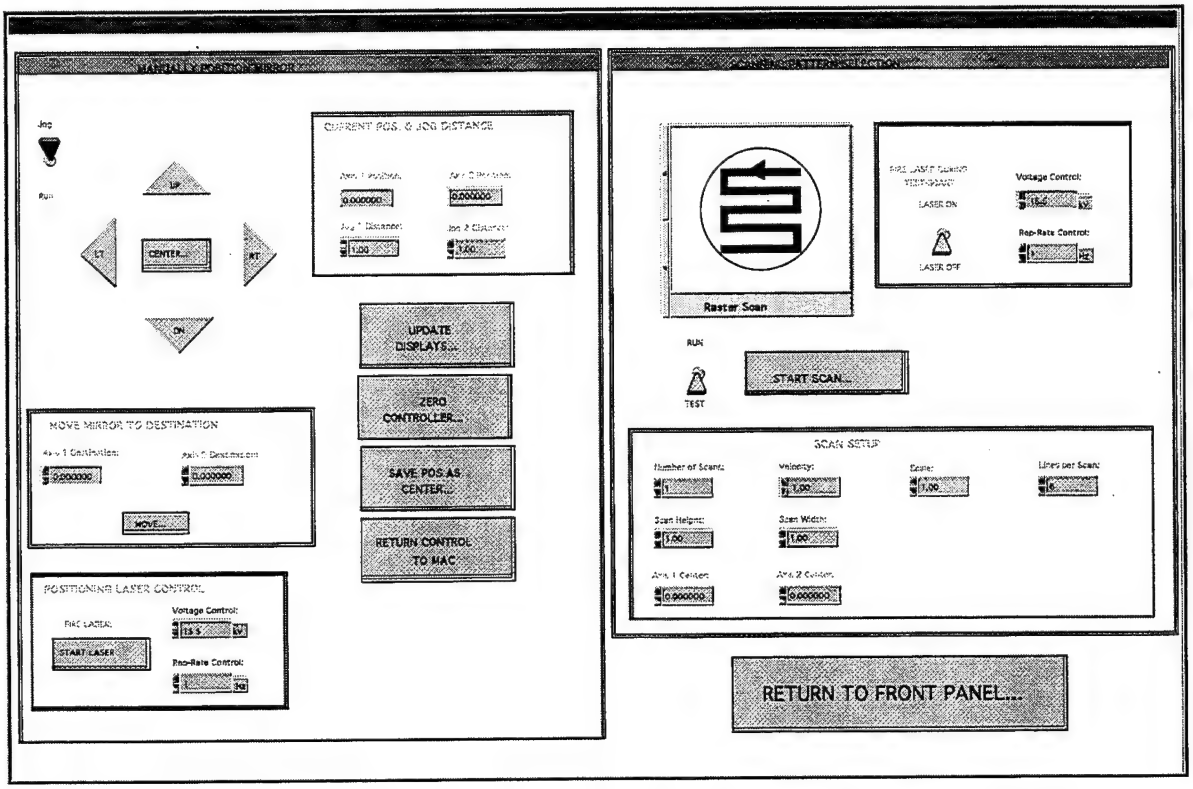

Figure 3.1 - *Newport Mirror Controller User Interface*

retract the axis 2 actuator even though the projected beam will move upwards on the target (i.e. the mirror controller axis 2 coordinate will decrease). Pressing the DOWN button will correspondingly extend the actuator. In the Run mode, the direction keys are touch sensitive in the sense that holding them down will move the mirror continuously. Only when they are released will the corresponding actuator stop. In both the Jog and Run modes, the position at the end of the action is updated. It will again reflect the user's choice of coordinate systems. The other

command used to move the mirror is the MOVE command, which will move the mirror to the coordinates given in the Axis 1 Destination and Axis 2 Destination controls. Note that the control labeled START LASER in the POSITIONING LASER CONTROL sub-window is used to allow the user to simultaneously fire the laser and move the mirror. This enables the user to see exactly where the beam will hit the target given specific coordinates.

The other purpose of this subroutine is to set up the mirror for a given scan pattern. The mirror control software was developed to allow the user three possible scanning patterns: horizontal, vertical, and raster. Figure 2.19 is repeated here to aid in the scanning software discussion. Note that the circles represent the target surface. Figure 2.19 (c) is enlarged to show the additional detail for a rastered scan. The solid lines and dashed lines in all the patterns indicate the initial top-to-bottom and the return bottom-to-top paths of the beam. Additionally, forward and reverse paths actually overlap. They were drawn adjacent to each other for ease of understanding. Referring back to Figure 3.1, the parameters in the SCAN SETUP sub-window affect the various scan patterns. However, Scan Height is meaningless for horizontal scans as is Scan Width for vertical scans. Also, Axis 1 Center and Axis 2 Center indicate the center of the scan and not the starting point. Note that Lines per Scan is meaningless except in raster scans. The minimum number of lines is six, and this value can be incremented by multiples of four. The Velocity control indicates how fast the beam will scan, while the Scale control gives the user the ability to conveniently increase or decrease the size of the scan.

The Number of Scans control is only active during a test scan, selected by the RUN/TEST switch above it. In RUN mode, the software generates the necessary scan instructions and downloads these to the mirror controller. The mirror controller is then placed in an infinite loop where it continuously executes

these instructions. In a test scan, the software will instruct the mirror controller to execute a defined scan pattern a given number of times, specified in the Number of Scans control. Note that the laser can also be fired during a test scan. This helps to ensure that the scan pattern will stay on the target over the complete pattern.

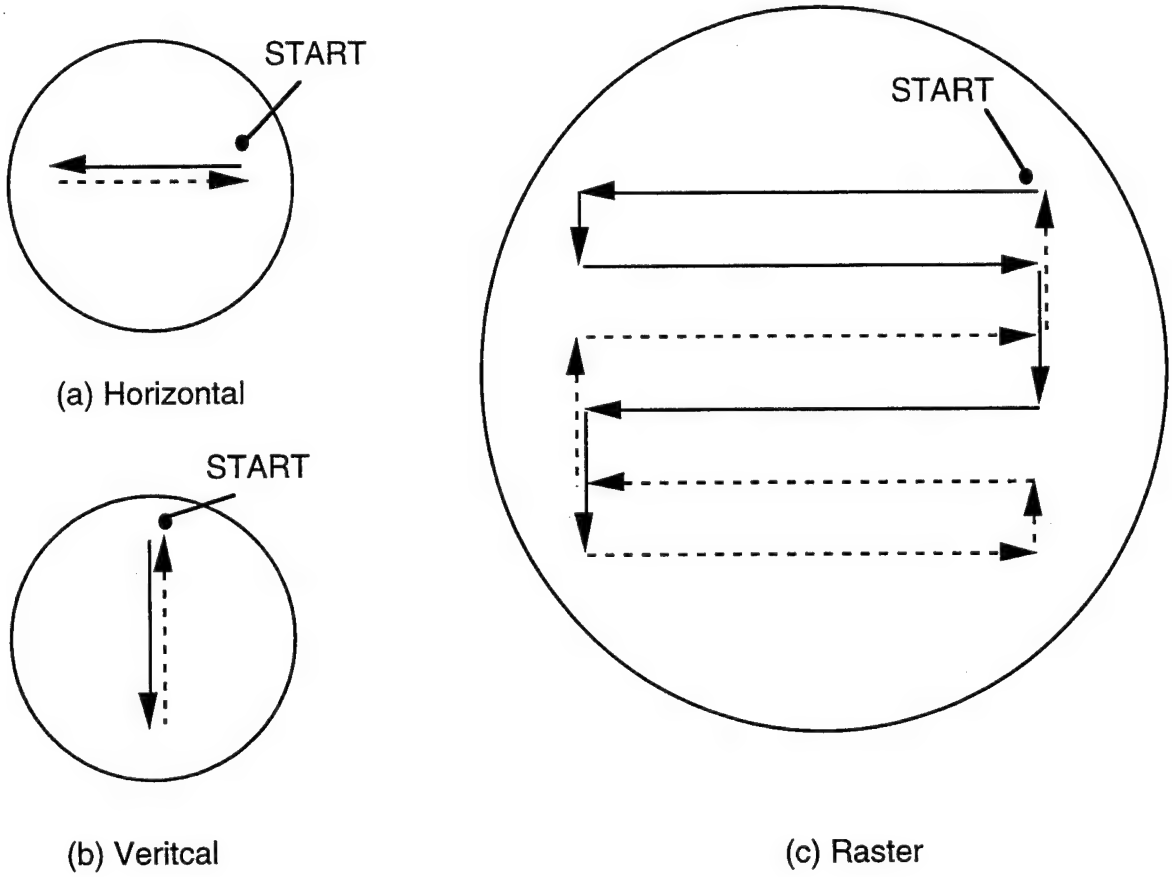

Figure 2.17 (a), (b), and (c) - *Laser Scanning Patterns*

NPScan final ver 7.vi is both the most important and the most difficult to understand piece of mirror control software. It is therefore necessary to fully explain the operation of this piece of code. It is obvious that both the horizontal and vertical scans are much simpler than the raster scan. These two examples will be discussed first before an explanation of the raster scan is given.

Obviously, the scan width parameter (as discussed before) affects a horizontal scan pattern while the height scan parameter affects a vertical scan pattern. Note from Figure B.15 that all of the important parameters from NPCalib final ver 4.vi are passed to this program through the cluster named SCAN DATA.

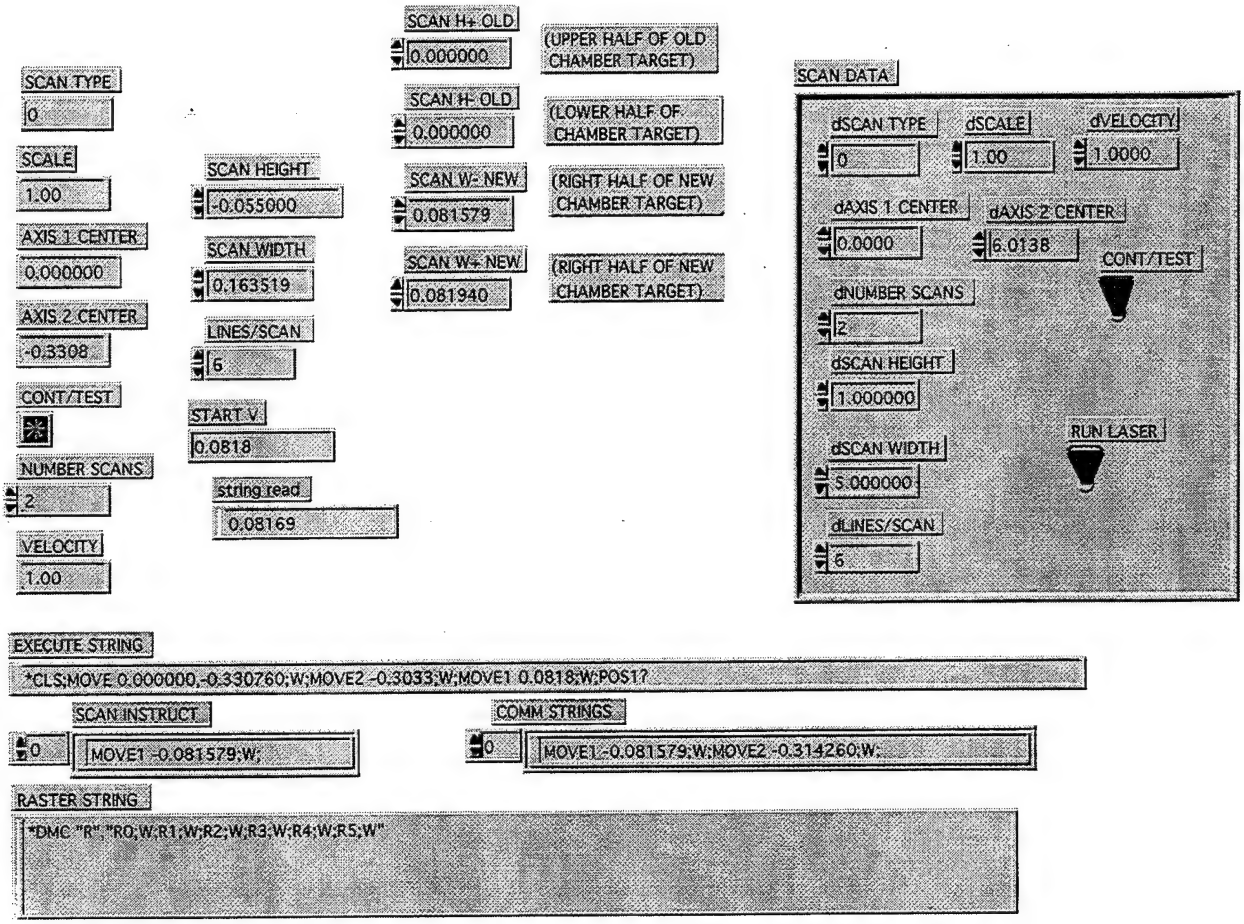

Figure B.14 - *NPScan final ver 7.vi Front Panel*

The individual elements of this cluster are then copied to their own individual controls. This is done so that the program has easy access to these variables (through the use of local variables). Regardless, the three parameters important for generating the scan instructions are the height/width (depending on vertical or horizontal scan) and the axis center coordinates. Note that NPScan ver

7.vi knows the selection of coordinates based on the global variable GCOORDS, part of gNPCenter Data.vi. The first task done is to convert both the center coordinates and the height/width into controller coordinates (unless they already are controller coordinates). The first statement written to the controller is "SCALE 1,1;*PMC;*EMC 1;*DMC "W";*WAI". SCALE 1,1 sets the scale to unity - this is necessary because the program must move the mirror to the scan center before the scan starts. *PMC erases any macro commands while *EMC enables macro expansion. Finally, *DMC "W","*WAI" defines a macro called W, which is equivalent to the *WAI command (GPIB *WAI = wait). The use of macros is very important, especially for raster scan patterns. For now, it is sufficient to say that without their use, raster patterns could not be implemented.

Next, the program prepares the controller to begin executing the scan pattern requested. If a horizontal scan was selected, the controller moves the mirror to the center coordinates plus 1/2 the scan width (adds to axis 1 displacement). For vertical scans, 1/2 is added to the axis 2 center coordinate. Note that in these instruction sequences, the *WAI command is used. This command is used to pause the next operation (after the semicolon) until the current operation is completed. In addition, the last command in the string is POS1?, which queries the controller for the current axis 1 position. Since this command follows a *WAI command, it will not be executed until all pending operations have been completed. Therefore, the program can continuously wait until a message is available on the GPIB bus, indicating the mirror controller has responded to the query (i.e. it executed the query requested, which means the commands before it were completed). Finally, the scale requested and the velocity are loaded. The program then generates the scan instructions based on the scan requested. In the case of horizontal and vertical scans, these instructions contain the starting and ending points (two sets of coordinates). Note that these instruction sequences are

defined as macros ("H" = horizontal, "V" = vertical). The reason they need to be defined as macros is because the max length for a single instruction is eighty characters. By combining macros into statements, the eighty character limitation can be bypassed. Note that the last instruction in the macro sequence is a position query if TEST mode is selected (recall that test mode will execute the scan a given number of times while RUN mode will run the scan pattern indefinitely). If TEST mode is selected, the program will check for a response query before issuing the next scan command. The RUN mode simply sets the controller in a continuous loop. This is done by defining a new macro called LOOP, which first calls the associated scanning macro, waits for it to complete, then calls itself. The command string to do this is *DMC "LOOP","H;*WAI;LOOP".

It is possible that macros might not be needed for horizontal and vertical scans, provided that the scan instruction for a complete scan (move forward and then return) is no longer the eighty characters. With raster patterns, this is no longer possible since there are at least twelve sets of coordinates (number of lines = 6), each requiring a MOVE statement. The raster diagram shows that it is necessary to move only one actuator on each move step (i.e. either axis 1 or axis 2 will stay fixed during each move). Therefore, the code sequence will be an alternating sequence of MOVE1 and MOVE2 commands. However, building this list of commands is somewhat complicated. As an example, assume that the center coordinates for axis 1 and axis 2 are (0,0), the scan width is 5 mm, and the scan height is 5 mm. To make the code sequence easier to understand, a sequence of steps will be listed that automatically generate the required instructions. This sequence is exactly the steps the program uses to generate the required instructions.

1. *Create two string arrays called SCAN INSTRUCT and COMM STRINGS.* Initialize SCAN INSTRUCT with ';W;', where W is the macro for wait.. SCAN INSTRUCT's length is the number of lines per

scan requested x 2. COMM STRINGS's length is the number of lines per scan. Note that the minimum number of lines per scan is six. The permissible number of lines per scan increases in increments of four (i.e. 6, 10, 14, 18, 22, . . .).

2. *Generate the axis 1 coordinates for the scan instructions and place these in the correct sequence.* From the raster diagram, it is obvious that there will be only 2 possible values for axis 1. These two values correspond to the left and right edges of the scan pattern. This set of coordinates is generated by adding (right side of forward path) or subtracting (left side of forward path) half the width from the axis 1 center coordinate. Note that these values will alternate as the beam scans first from right to left (assuming the scan is starting at the START point) and then from left to right. The SCAN INSTRUCT array is now becomes

ELEMENT #	STRING
0	-2.5;W;
1	;W;
2	+2.5;W;
3	;W;
4	-2.5;W;
5	;W;
6	+2.5;W;
7	;W;
8	-2.5;W;
9	;W;
10	+2.5;W;
11	;W;

3. *Generate the axis 2 coordinates for the scan instructions in the forward path and place these in the correct sequence for the scan instructions.* From the raster diagram, it can be seen that the first change in the axis 2 coordinate occurs after the initial movement on axis 1 (to the left). Remembering that positive values on the target correspond to negative controller values, the axis 2 coordinate at the ending point of this change is given by

$$A2 = A2_{SC} + \left(\frac{SH}{L/S - 1} \right)$$

where $A2_{SC}$ is the axis 2 coordinate of the scan center, SH is the scan height, and L/S is the number of lines per scan. In general, the axis 2 coordinate in the forward path is given by

$$A2 = A2_{SC} + \left(\frac{SH}{L/S-1}\right) \bullet (2i+1),\ i = 0,1,2,...$$

where i is the transition number - 1 (i.e. i = 0 for the first transition after the START point). This equation can be easily implemented in software. Given that there are three transitions for 6 lines per scan, the SCAN INSTRUCT array now becomes

ELEMENT #	STRING
0	-2.5;W;
1	-1.5;W;
2	+2.5;W;
3	+0.5;W;
4	+2.5;W;
5	-2.5;W;
6	+2.5;W;
7	;W;
8	-2.5;W;
9	;W;
10	+2.5;W;
11	;W;

5. *Generate the axis 2 coordinates for the scan instructions in the backward path and place these in the correct sequence for the scan instructions.* When the beam has reached the bottom of the scanning pattern, it is necessary to perform the steps to bring it back to the START point. The equation that performs this function is given by

$$A2 = A2_{SC} + \left(\frac{SH}{L/S-1}\right) \bullet (-2i+L/S-2),\ i = 0,1,2,...$$

where i is the transition number on the backward pass, again with i=0 on the first transition. The SCAN INSTRUCT array is now

ELEMENT #	STRING
0	-2.5;W;
1	-1.5;W;
2	+2.5;W;
3	+0.5;W;
4	+2.5;W;
5	-2.5;W;
6	+2.5;W;
7	+1.5;W;
8	-2.5;W;
9	-0.5;W;
10	+2.5;W;
11	-2.5;W;

5. *Classify each element in SCAN INSTRUCT as a MOVE1 or MOVE2 instruction.* Elements 0, 2, 4, 6, 8, and 10 are MOVE1 instructions, while elements 1, 3, 5, 7, 9, and 11 are MOVE 2 instructions. This gives

ELEMENT #	STRING
0	MOVE1 -2.5;W;
1	MOVE2 -1.5;W;
2	MOVE1 +2.5;W;
3	MOVE2 +0.5;W;
4	MOVE1 +2.5;W;
5	MOVE2 -2.5;W;
6	MOVE1 +2.5;W;
7	MOVE2 +1.5;W;
8	MOVE1 -2.5;W;
9	MOVE2 -0.5;W;
10	MOVE1 +2.5;W;
11	MOVE2 -2.5;W;

6. *Divide the instruction into six groups, each group having two adjacent instructions from SCAN INSTRUCT. Place these groups in COMM STRINGS.* Since there are twelve elements in SCAN INSTRUCT, there will be six elements in COMM STRINGS. COMM STRINGS is then

ELEMENT #	STRING
0	MOVE1 -2.5;W;MOVE2 -1.5;W;
1	MOVE1 +2.5;W;MOVE2 +0.5;W;
2	MOVE1 +2.5;W;MOVE2 -2.5;W;
3	MOVE1 +2.5;W;MOVE2 +1.5;W;
4	MOVE1 -2.5;W;MOVE2 -0.5;W;
5	MOVE1 +2.5;W;MOVE2 -2.5;W;

The individual elements of COMM STRINGS can now be passed to the mirror controller as macro commands. Then, another macro can be defined which then calls each of these macro commands in sequence (remembering to place a ;W; command between each instruction macro).

B.2.4 IRCON Pyrometer

The pyrometer was used in the old deposition system where reliable thermocouple measurements were very difficult to obtain. Since this instrument may be incorporated into the new system as well, software was written to read the digital output of the pyrometer. As stated in Appendix B, the pyrometer is connected to the Macintosh via a NB-DIO-24 card. The digital output is a modified version of Binary Coded Decimal (BCD). The table in Figure B.7 (b) gives descriptions for each DB-25 pin connected. The 'w=#' statements in the DB Pin Descriptions box specify the decimal weight of that specific line. Note that unlisted pins in the table are either unused or ignored.

To read values from the NB-DIO-24 card, the PYRORead.vi sub-routine is used. First, logic-1 to logic-0 is detected on Pin 14 to indicate that data is ready. Next, the BCD data is converted to decimal using the equation

$$TC° = 1 \bullet PC0 + 2 \bullet PC1 + 4 \bullet PC2 + 8 \bullet PC3 + 10 \bullet PC4 + 20 \bullet PC5 + 40 \bullet PC6 + 80 \bullet PC7 + 100 \bullet PB0 + 200 \bullet PB1 + 400 \bullet PB2 + 800 \bullet PB3 + 1000 \bullet PB4 + 2000 \bullet PB5 + 4000 \bullet PB6$$

Note that the PCs and PBs are the digital lines attached to those pins of the NB-DIO-24 card. Each value is read as either a 1 or a 0, depending on the logical state of that line.

B.2.5 MKS Baratron Pressure Gauge

This type of gauge is based on a simple capacitance principle. As the pressure on a sensor head is increased or decreased, the distance between two plates of a capacitor is decreased or increased in turn. The resulting change in capacitance of the parallel plate capacitor is therefore indicative of the pressure on the sensor head. This type of pressure gauge is extremely accurate, and it is therefore used as the sensor in the pressure control loop. However, the operating range of the sensor is sacrificed to obtain this high accuracy. This type of device is limited to measuring pressures that are less than 1 T During a deposition, this is well within the range of possible background gas pressures.

The sensor head is itself mounted on the chamber, while the signal itself is displayed on a readout unit mounted in the instrumentation rack. The sensor head contains all of the conversion electronics; the readout unit is simply used to display the electrical signal numerically. It also supplies power to the sensor head electronics. The connections between the sensor head, the display unit, and the Lab-NB board are shown in Figure B.3.

Pressure measurements are made by reading the voltage on Channel 3, which represents the pressure in Torr (a full-scale reading of +10.0 V is equal to 1 Torr). The read operation is performed by BPRESRead.vi. Note that this subroutine is capable of reading either a Baratron gauge or a Convectron gauge. The decision of how to interpret the voltage read at a given channel is determined

by the value for the WHICH CHAMBER variable. The old chamber used a Convectron gauge for the chamber pressure measurement (WHICH CHAMBER = 0) while the new chamber uses the much more accurate Baratron gauge. To convert the pressure measurement to a mT reading, the software multiplies the voltage at Channel 3 by 100.

B.2.5 Granville-Phillips Convectron Gauges

Again, the Convectron gauges measure both the chamber pressure and the pressure at the input to the roughing pump. Although the Convectron is less accurate than the Baratron, it can read pressures up to and beyond atmospheric. After a deposition, the chamber is filled with pure oxygen to a pressure of around 600 T. The Convectron gives the operator an idea of how much oxygen is in the chamber so that he/she can turn it off when the pressure is at the required amount.

The Convectron gauges work on the principle of convection cooling of a temperature sensitive resistor located in the sensor head. Increasing/decreasing the pressure will increase/decrease the convection cooling rate which will in turn decrease/increase the resistance of the temperature sensitive resistor. This change in resistance can be converted to a change in pressure.

Unlike the Baratron pressure gauge, the electronics to convert the voltage reading from the sensor head are contained in the display unit. The only components in the sensor head are the resistors required for the Wheatstone Bridge, including the temperature sensitive resistor. The connections between the sensor head, the display unit, and the Lab-NB board for both the chamber pressure gauge and the pump pressure gauge are shown in Figure B.2. Note that both Convectron gauges are connected to relays on the relay cards. This is because the gauges have

no power switch on the front panel. Therefore, it is necessary to turn them on via the Macintosh.

As with the Baratron gauge, the voltage at the channel input is converted to a pressure in mT through the conversion sub-routines BPRESRead.vi and PPRESRead.vi (chamber pressure and pump pressure, respectively). The conversion, however, is more complicated than the simple multiplication by a constant in the Baratron case. The conversion is based on output voltage vs. pressure plots. These curves are broken up into eight segments, with each segment described by a third-order polynomial of the form

$$P = c_3 \bullet V^3 + c_2 \bullet V^2 + c_1 \bullet V^1 + c_0$$

where P is the pressure, V is the voltage at the given channel input, and c_3 - c_0 are the polynomial coefficients for the given curve segment. The coefficients for each segment of the curve are given in the Table B.1 below. Each row in the table corresponds to a set of coefficients for the fit polynomial. The conversion subroutines decide which set of coefficients to use based on if the measured voltage is less that the voltage in the 'V less than ...' column.

V less than...	c0	c1	c2	c3
1.8457	0.00E+00	6.50E-02	1.16E-04	4.14E-08
3.1641	-1.22E+02	4.44E-01	-2.71E-04	1.71E-07
4.3945	5.00E+02	-7.62E-01	5.12E-04	3.37E-18
6.54785	-1.72E+04	2.50E+01	-1.21E-02	2.06E-06
7.3828	-3.27E+06	3.24E+03	-1.07E+00	1.18E-04
7.6465	-2.47E+07	2.27E+04	-6.95E+00	7.10E-04
7.9102	8.24E+08	-6.87E+05	1.91E+02	-1.76E-02
9	-1.10E+08	8.73E+04	-2.32E+01	2.07E-03

Table B.1 - *Convectron Gauge Curve Fit Coefficients*

APPENDIX C - DEPOSITION SOFTWARE FLOWCHARTS

The flowcharts following this introduction attempt to show program flow. However, since the user interface is graphical, the sequential nature of some of the flow charts is misleading. For example, consider flowchart Figure 15 on page . It can be seen that this flowchart is essentially a series of question diamonds with paths leading to appropriate actions based on the question response. This part of the flowchart deals with the mirror controller user interface (Figure 3.1).

Each button on the mirror controller user interface is tested for in one of the question diamonds. Although the code tests each button in a sequential manner, this action is transparent to the user. In other words, the operator is not prompted at each question block for a response. This is one of the main reasons for the graphic interface. In most cases, any operator requested action can be initiated at any time simply by pressing the associated button. Essentially, the flowcharts are included for the sole purpose of showing how the actual code is written. This is done to aid in debugging or future software additions.

Certain conventions were used in the flowcharts to make their interpretation easier. As mentioned previously, question blocks are indicated with diamonds. If the question refers to a panel button (operator input), the question text will be italicized. Otherwise, the box refers to a question the program must answer. For example, during certain laser operations, the computer will need to ask the laser for its current status to determine whether or not a given operation is complete. These types of questions require no operator input and are thus not italicized. Various other symbols are used to denote specific types of code operations. Parallelograms are used to denote code operations while rectangles are used for pop-up operator dialog boxes. Ovals are used for subroutine start/return indicators while circles indicate subroutine continuation markers (subroutine continues on the next page).

The subroutines themselves are indicated by 3-D rectangles with boldface type. The text inside the rectangle will contain the reference figure number. As a final note, the flowcharts distinguish between 'front panel' routines and actual subroutines. Front panel routines have the additional characteristic that a graphic screen is displayed when these routines are called.

PLD Program Flow, Fig. 1

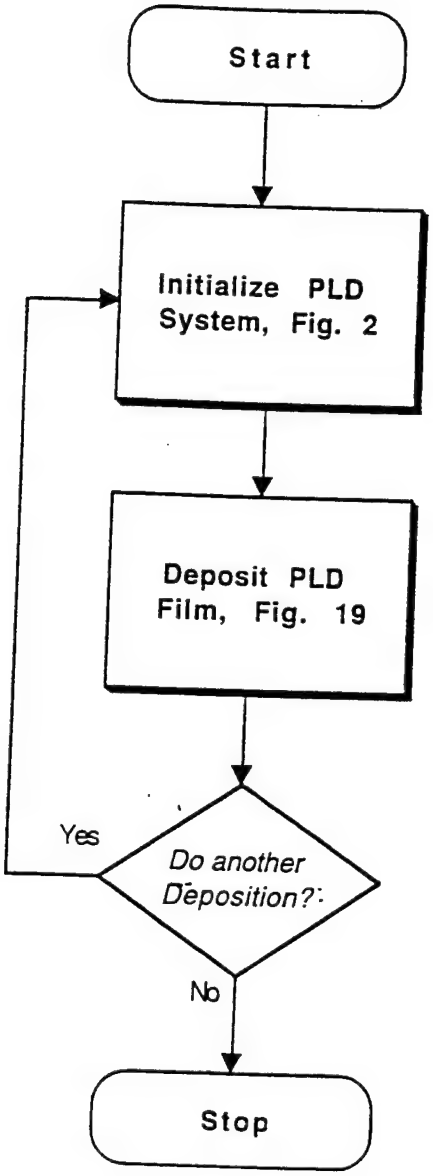

Initialize PLD System Panel, Fig. 2

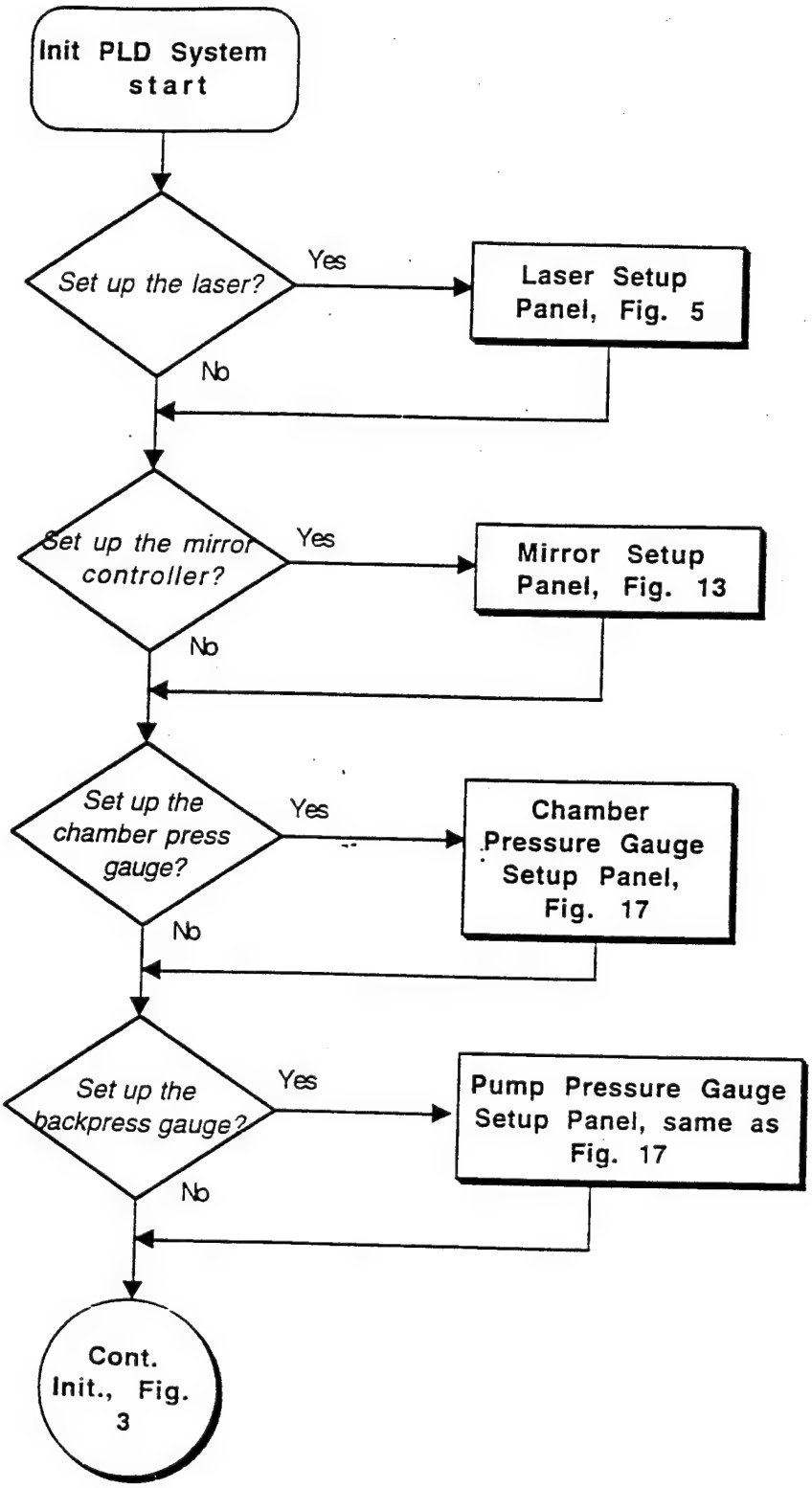

Cont. Initialize PLD System Panel, Fig. 3

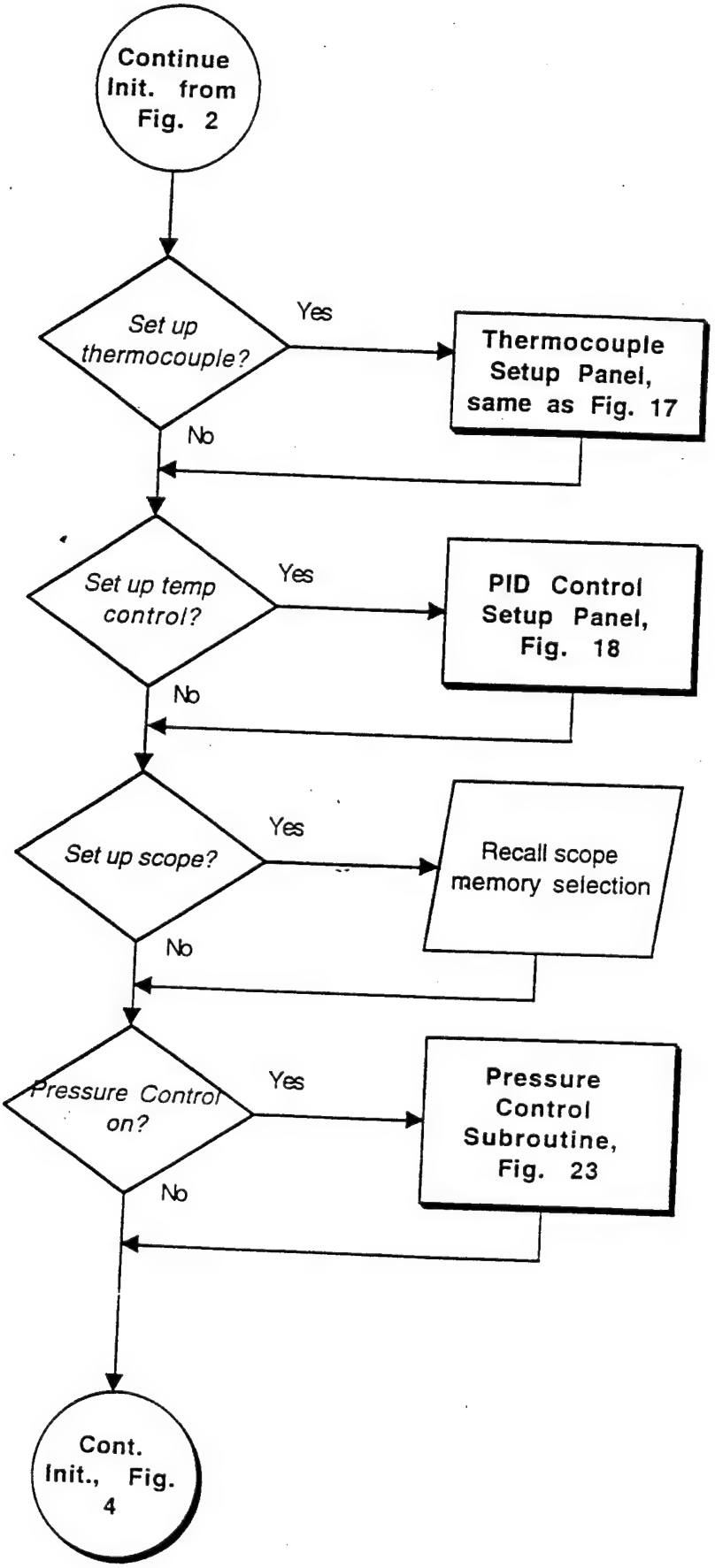

Cont. Initialize PLD System Panel, Fig. 4

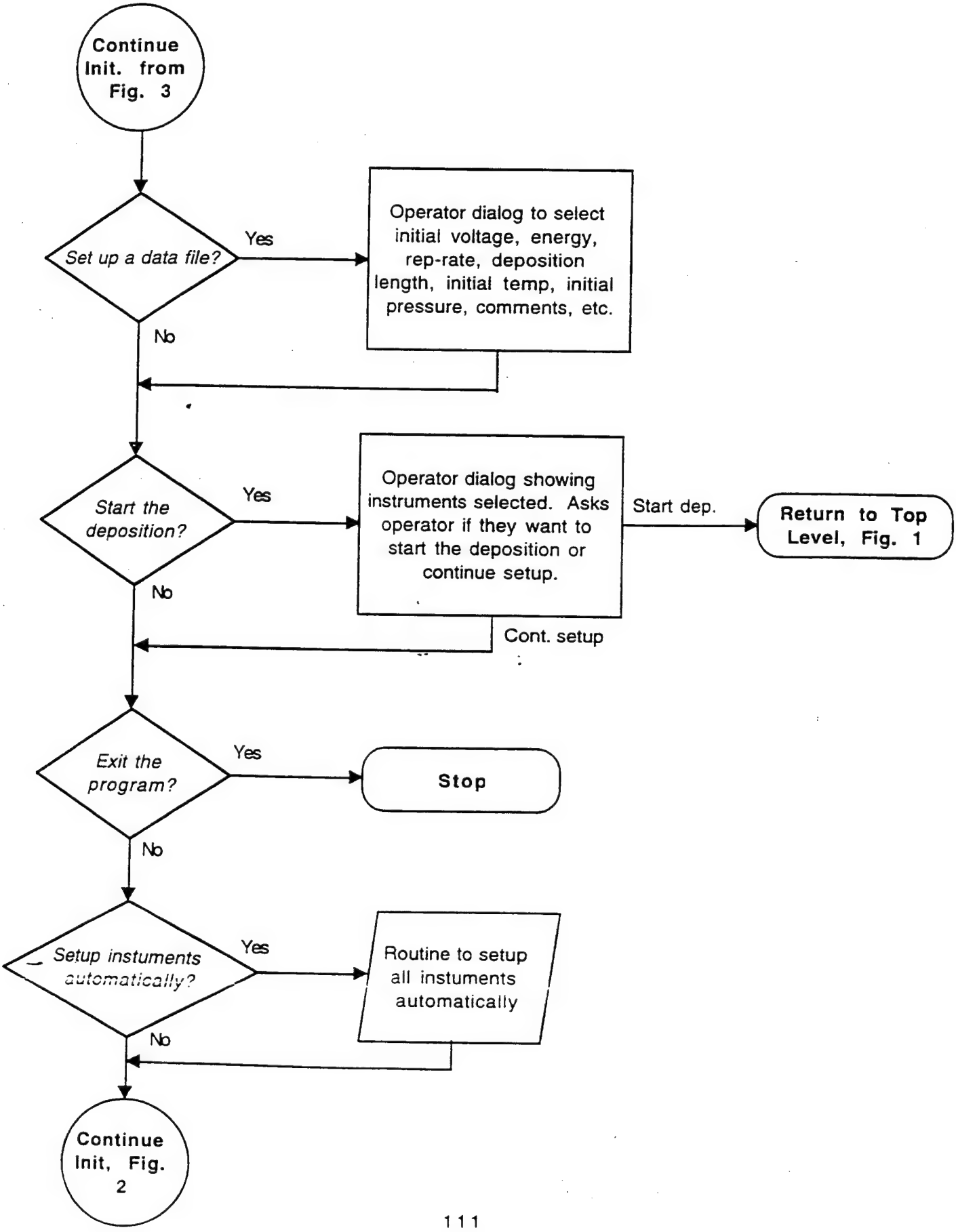

Laser Setup Panel , Fig. 5

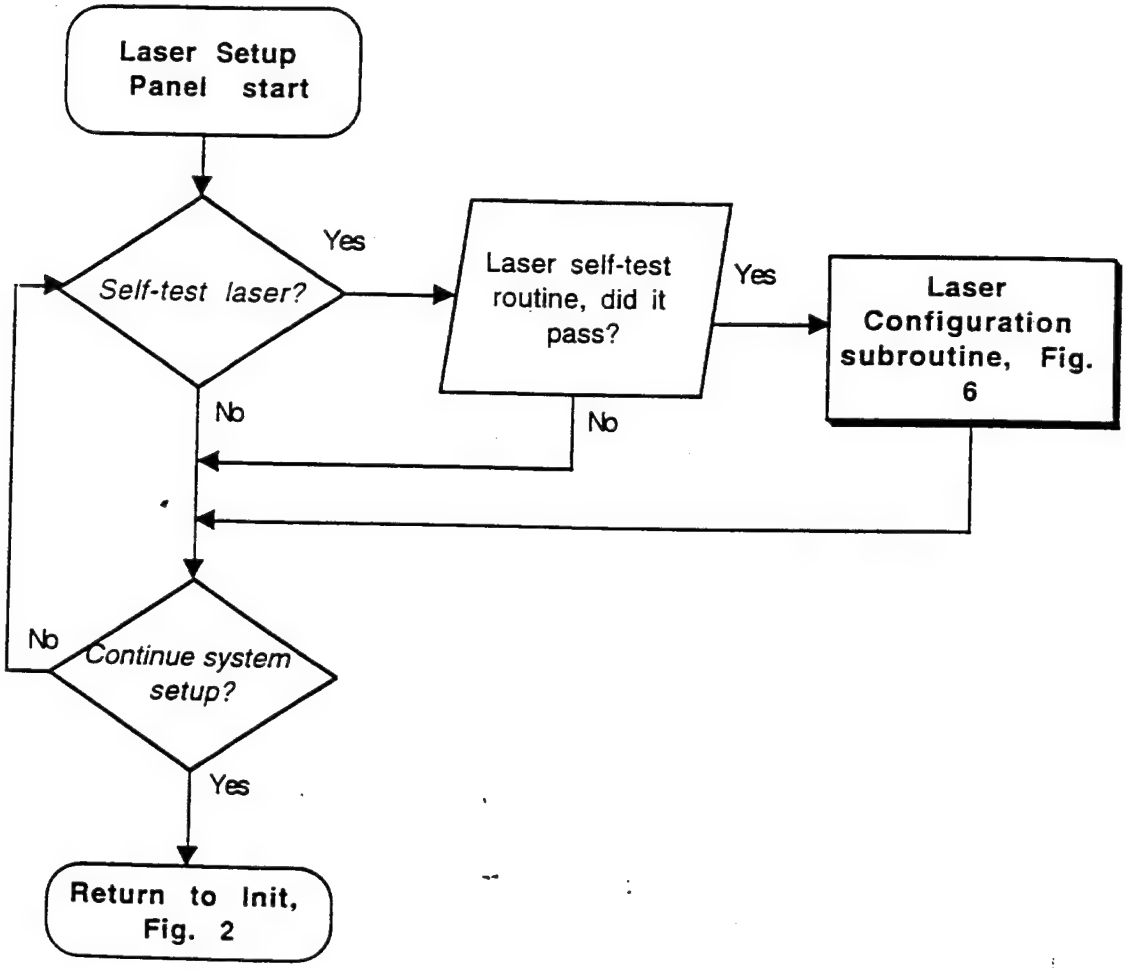

Laser Configuration subroutine, Fig. 6

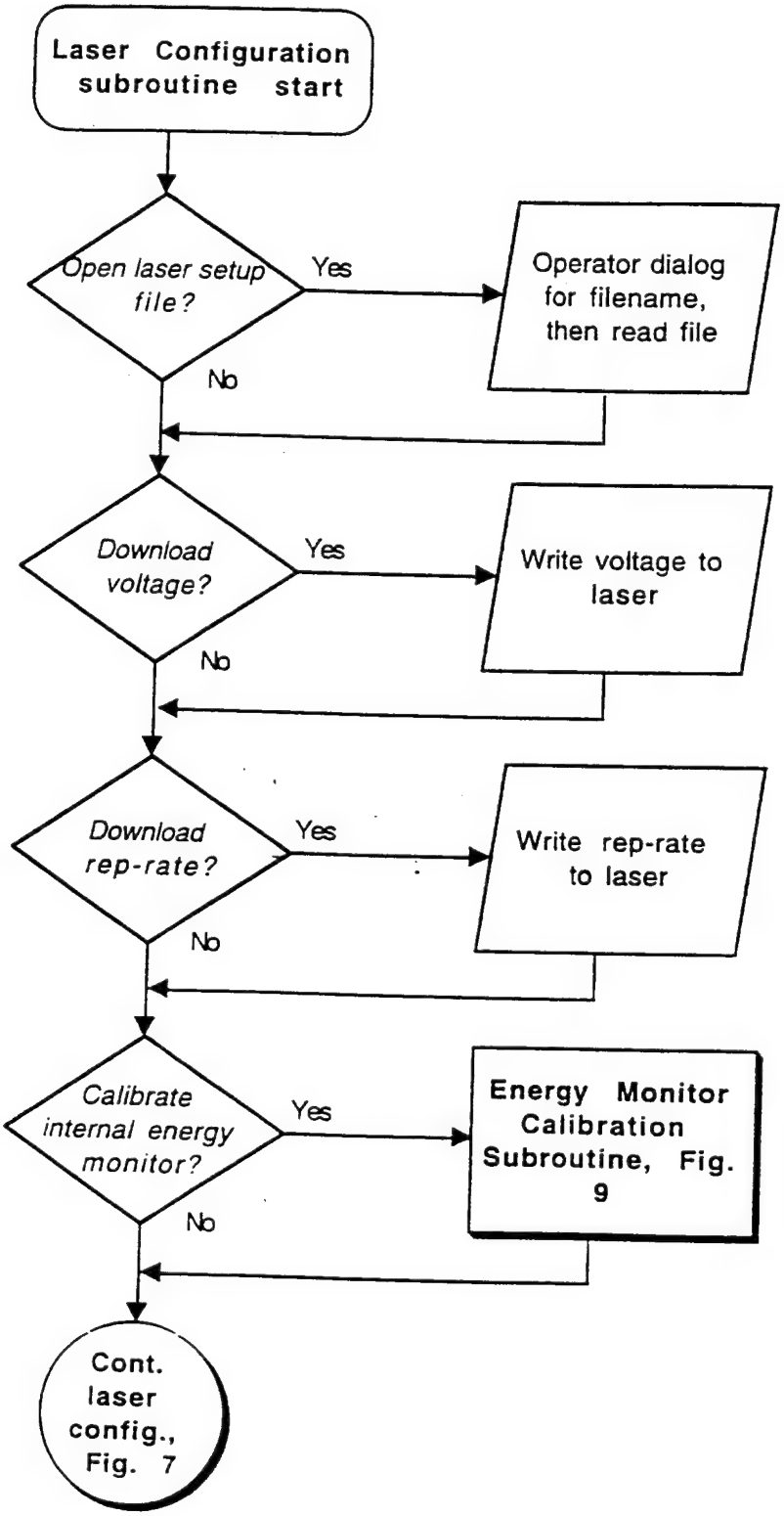

Cont. Laser Configuration subroutine, Fig. 7

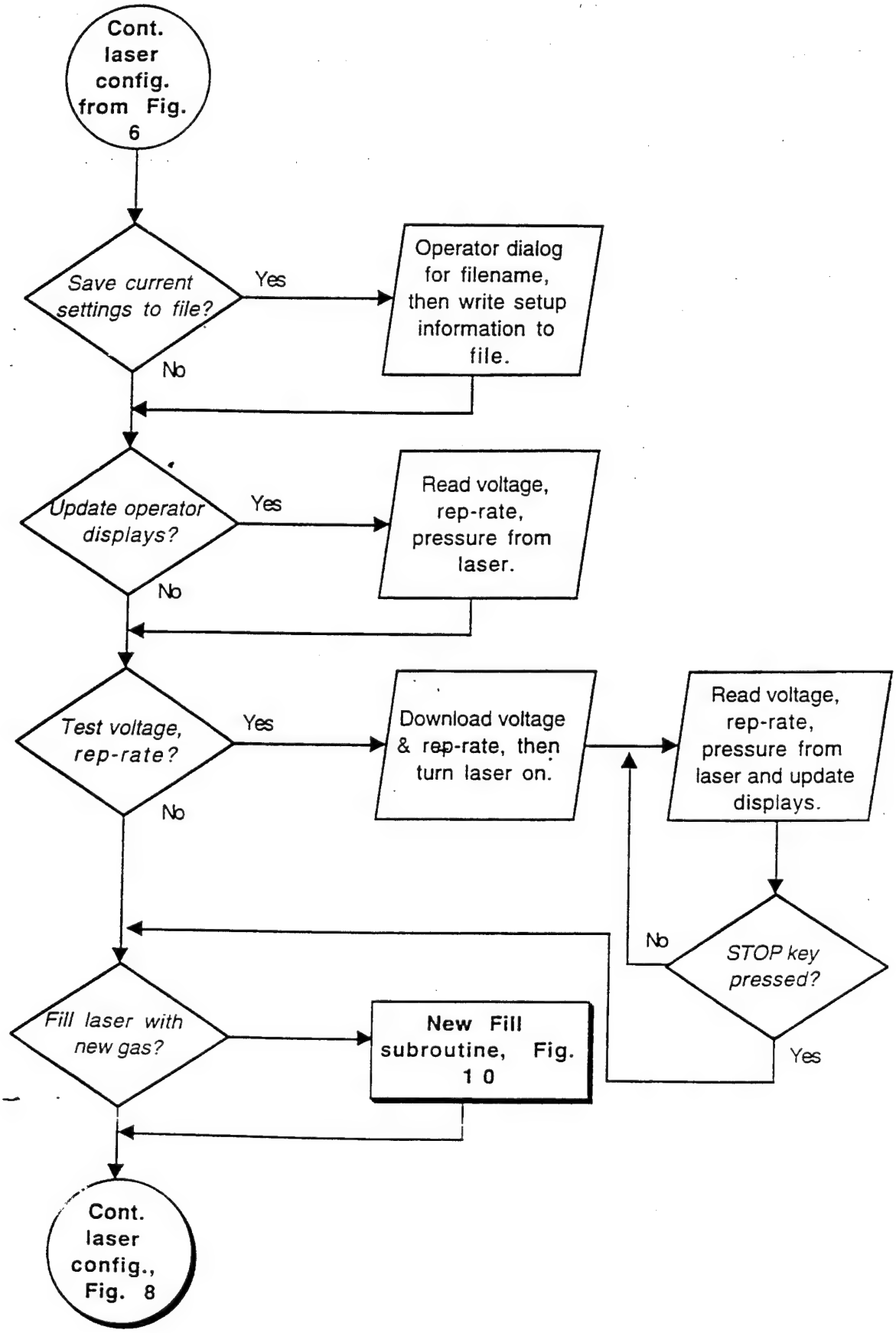

Cont. Laser Configuration subroutine, Fig. 8

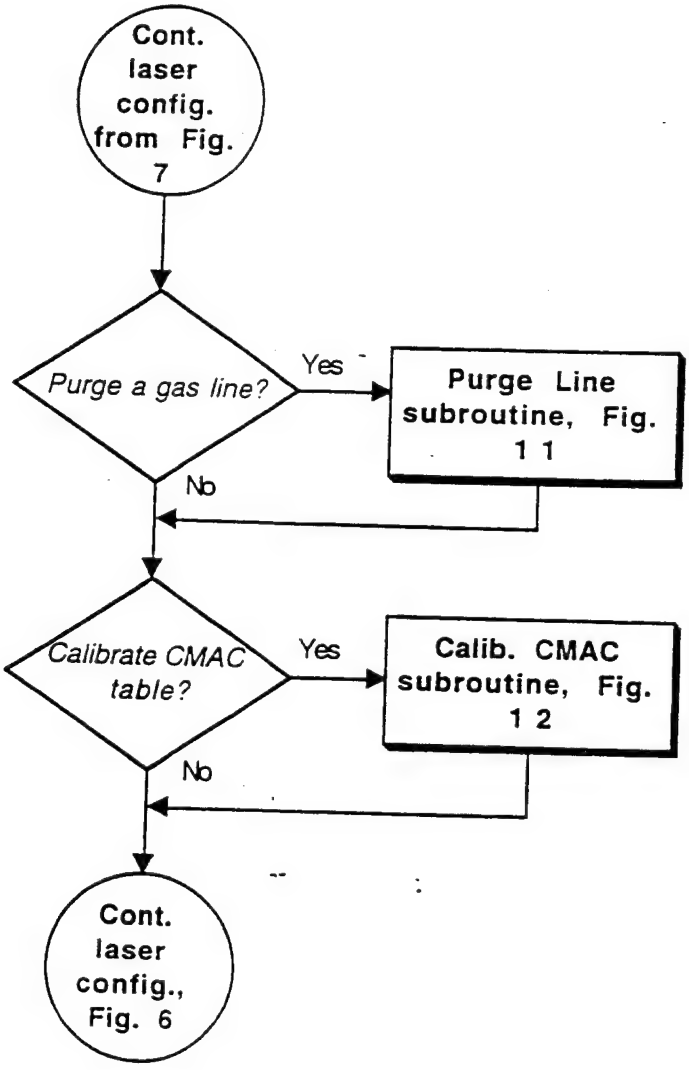

Energy Monitor Calibration subroutine, Fig. 9

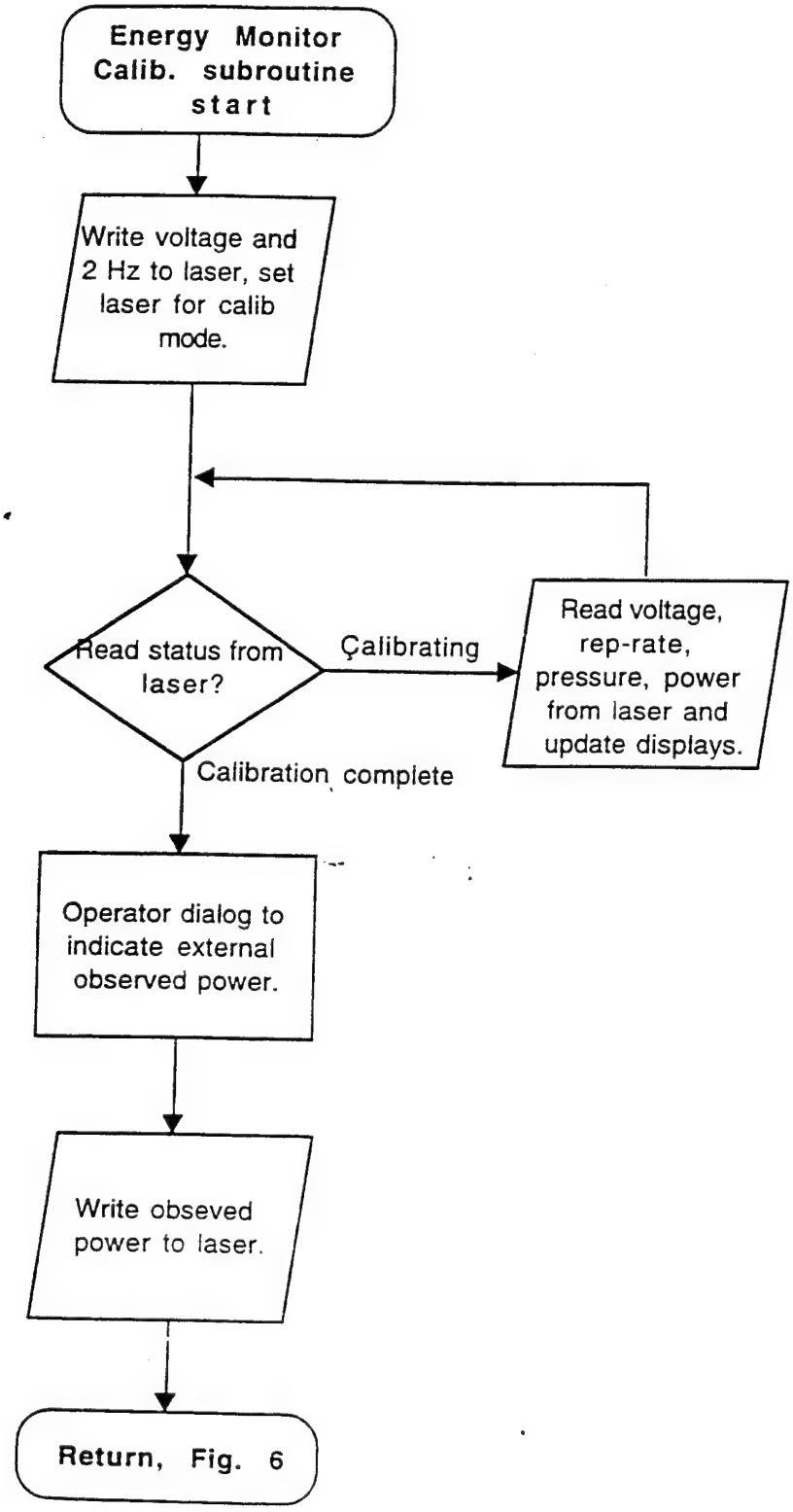

lew Fill Subroutine, Fig. 10

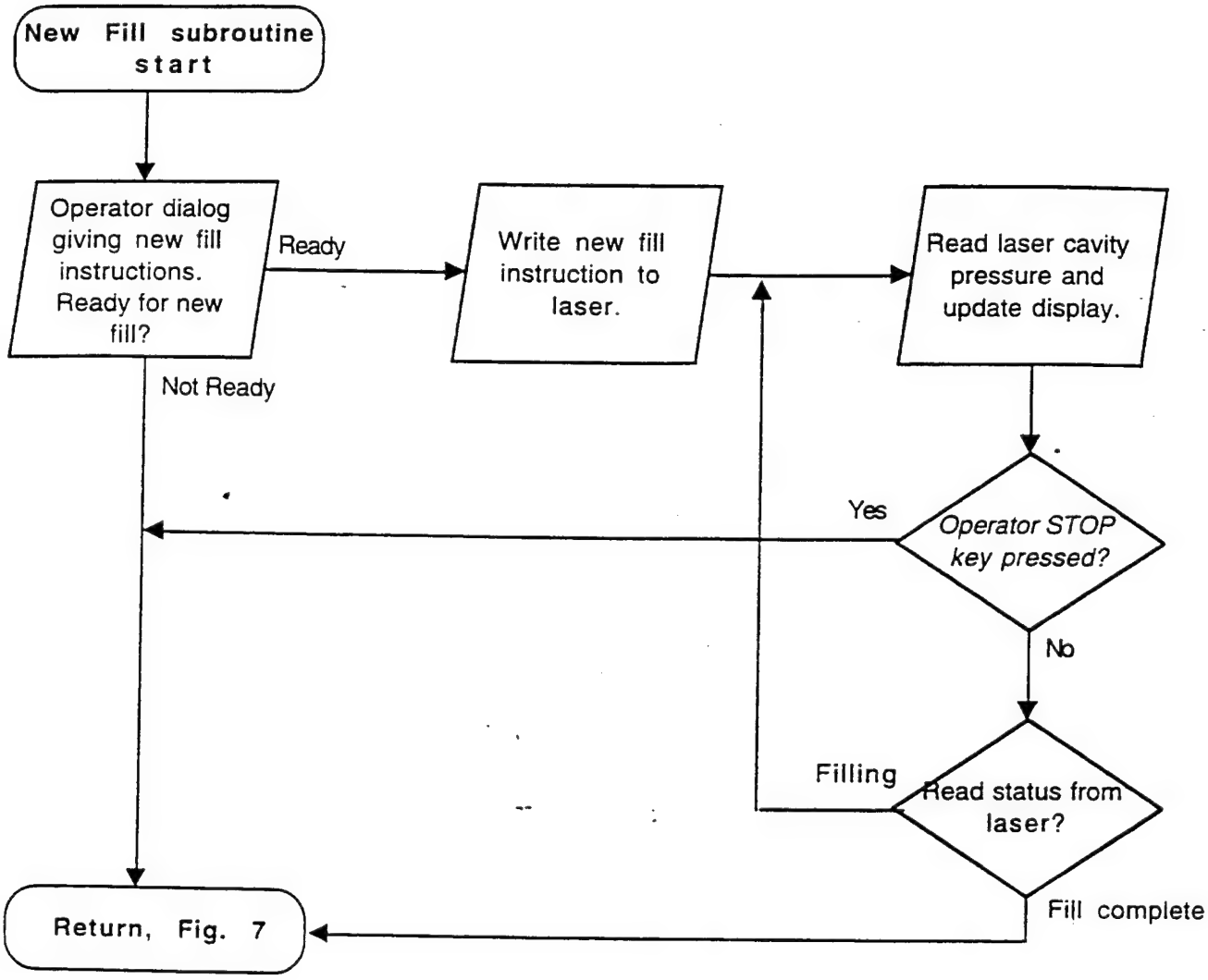

Purge Line subroutine, Fig. 11

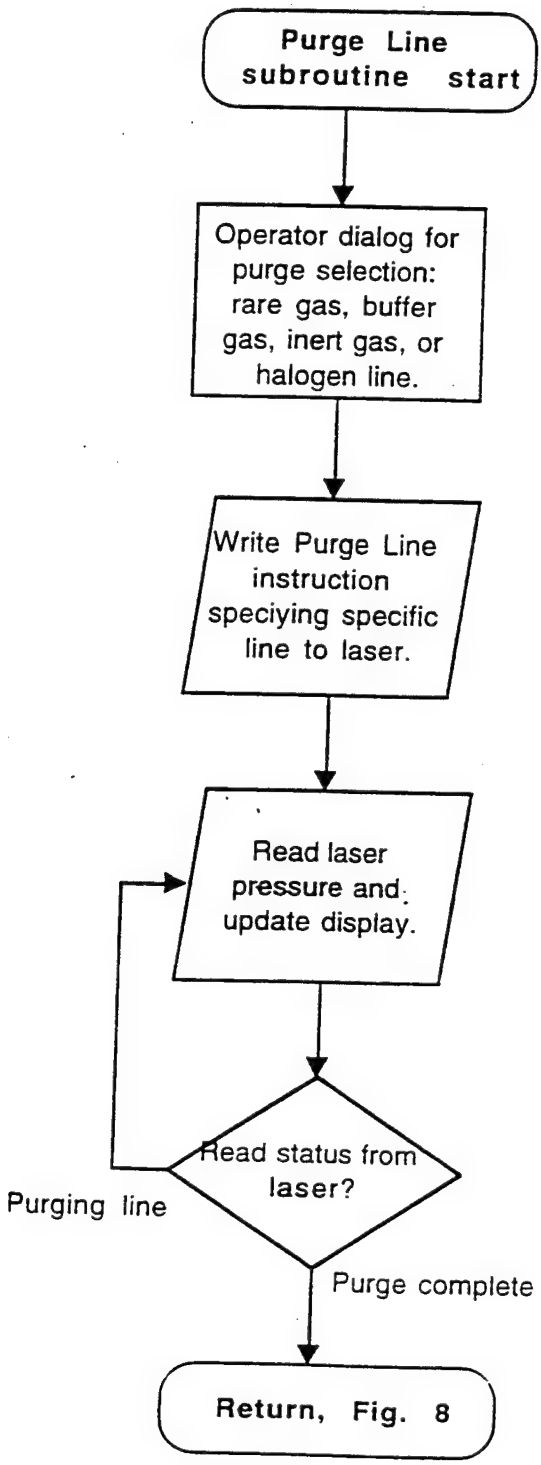

Calibrate CMAC subroutine, Fig. 12

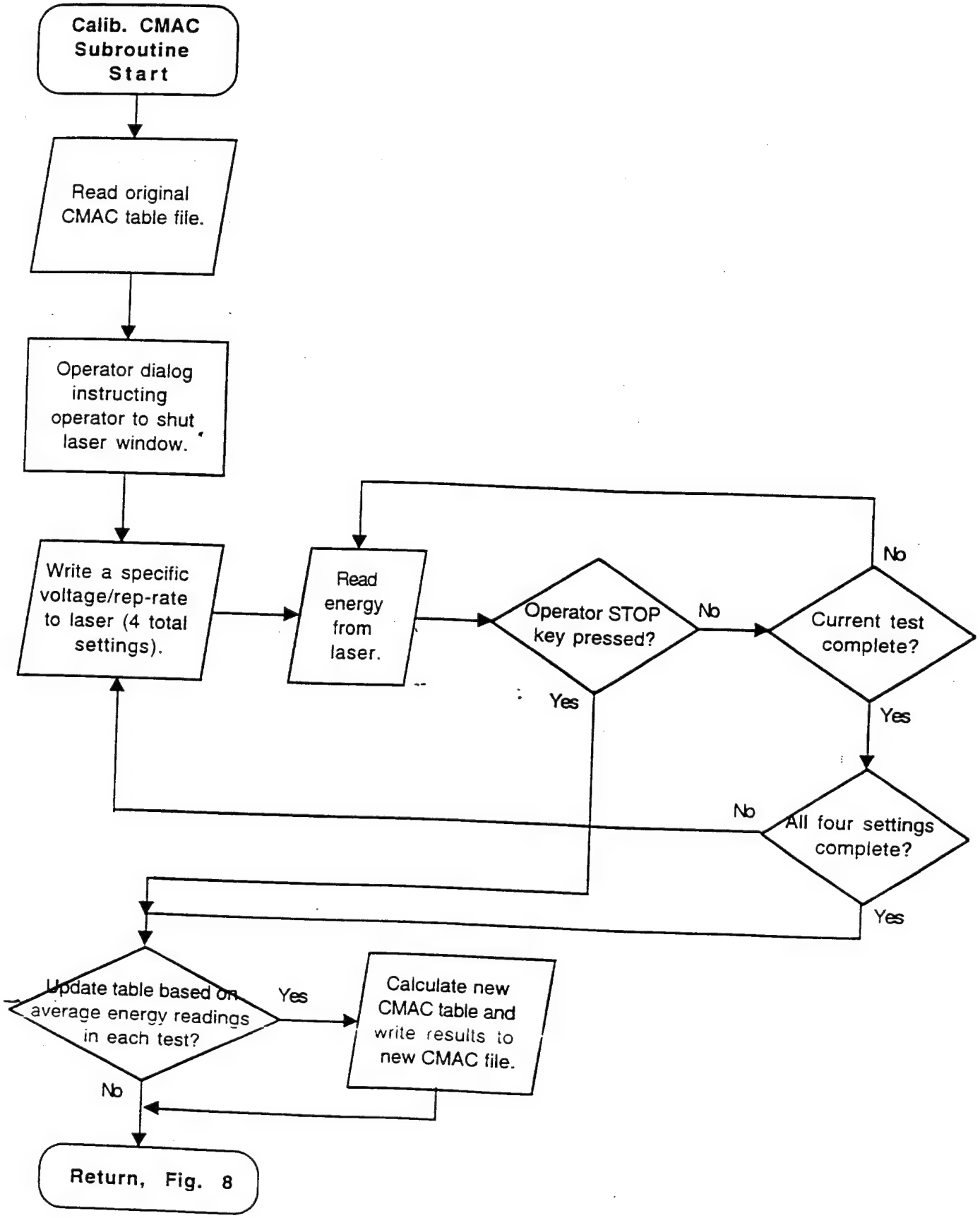

Mirror Setup Panel, Fig. 13

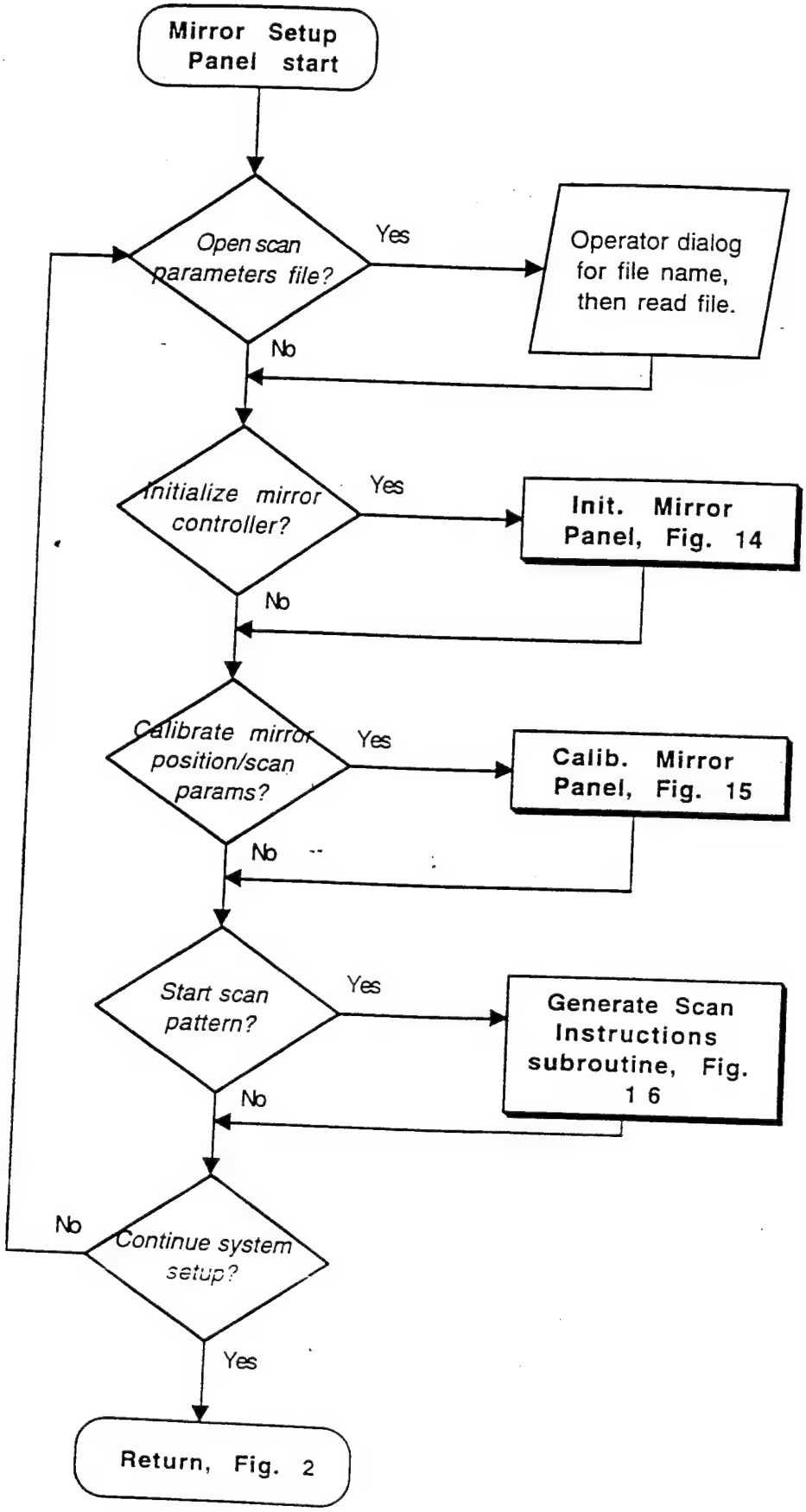

Initialize Mirror Panel, Fig. 14

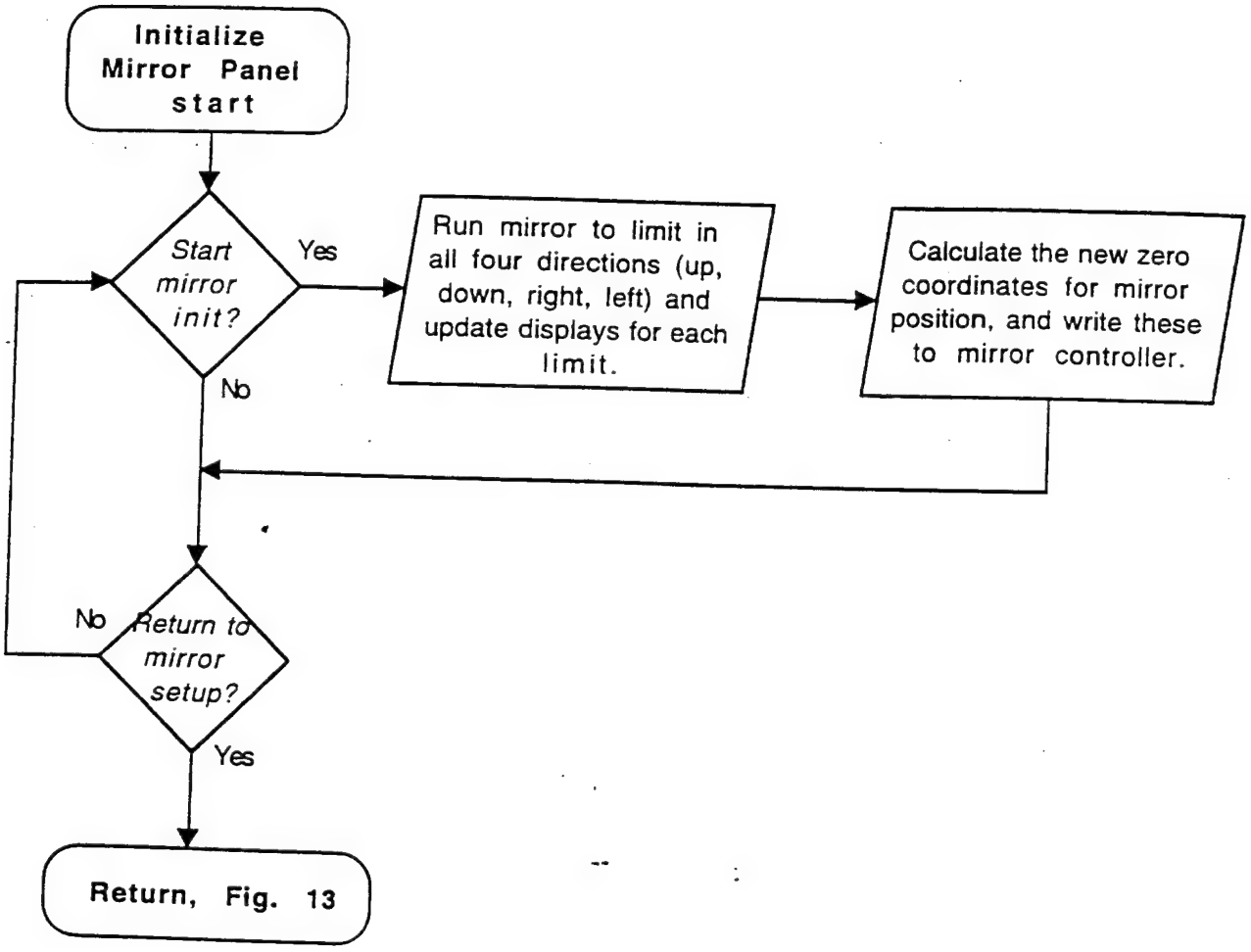

Calibrate Mirror Panel, Fig. 15

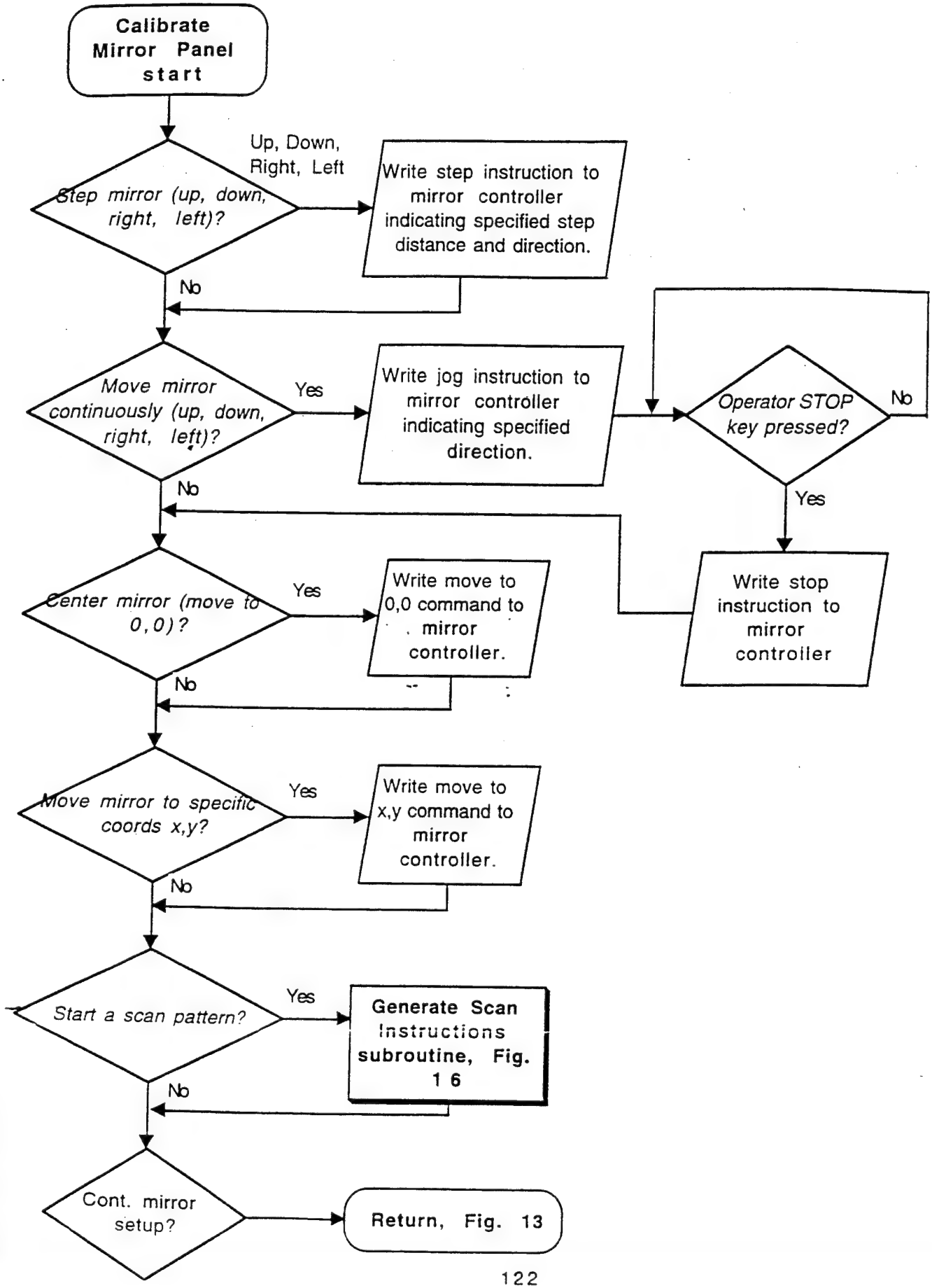

Generate Scan Instructions subroutine, Fig. 16

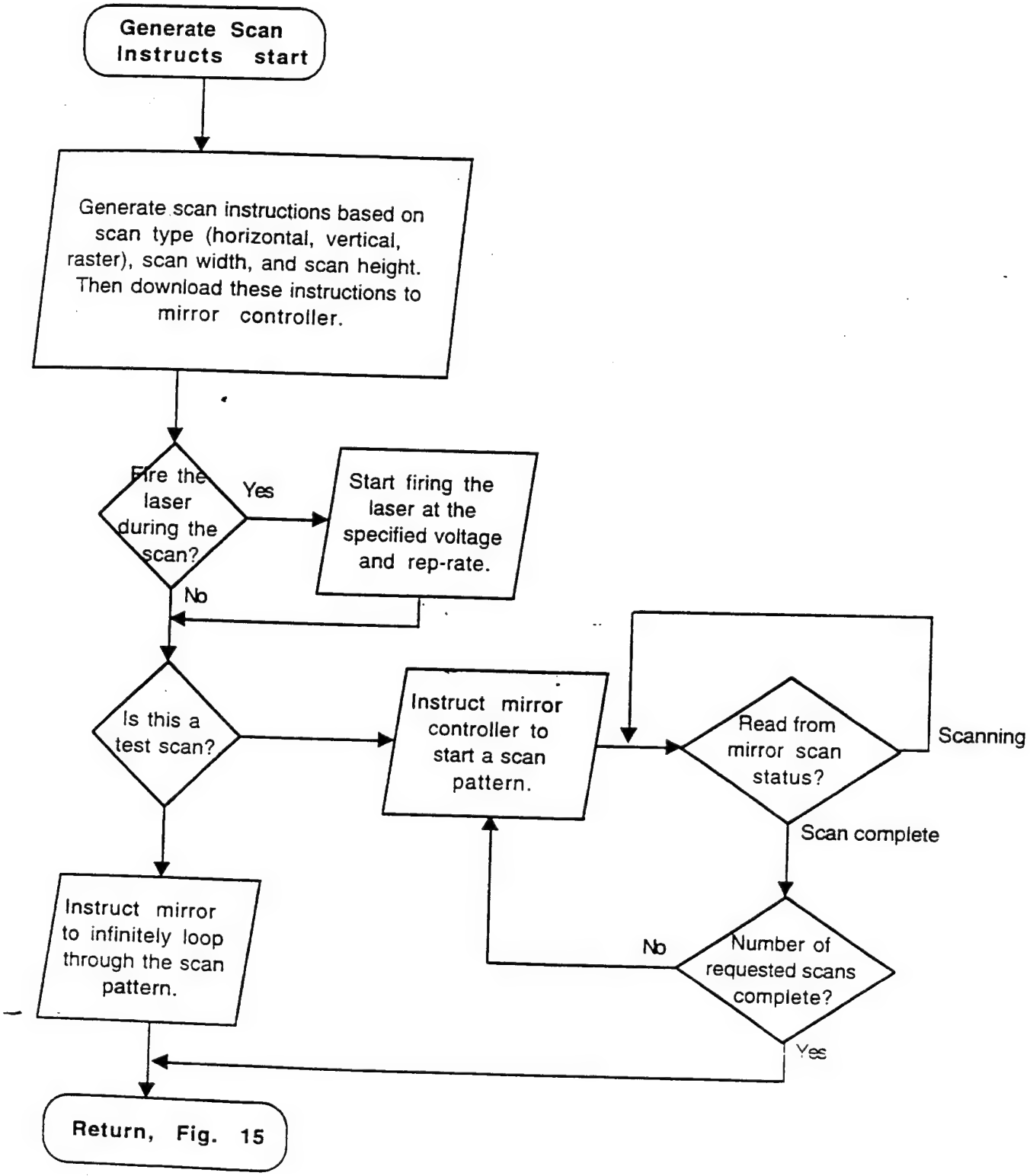

Chamber Pressure Gauge Setup Panel , Fig. 17

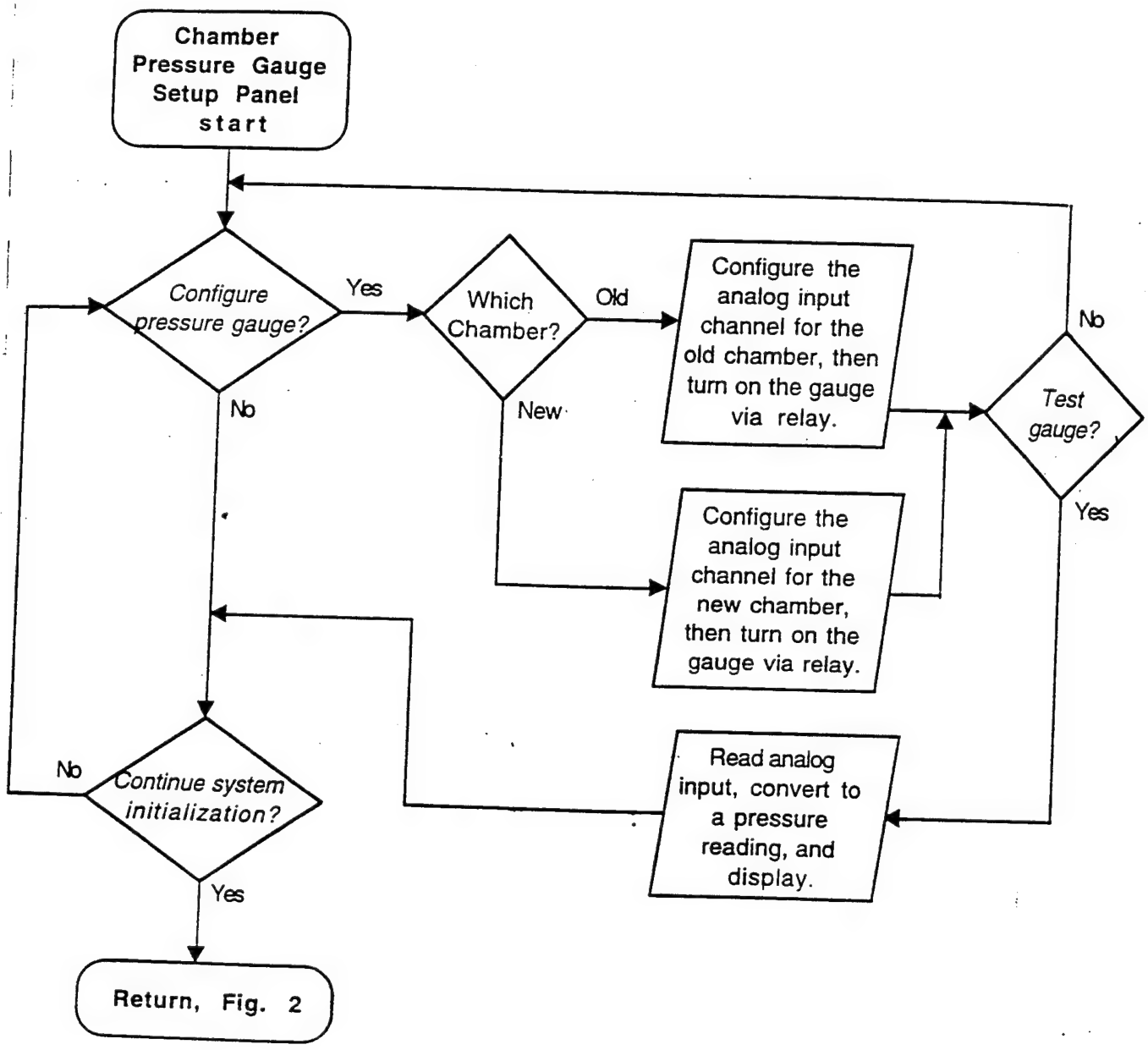

ID Control Setup Panel, Fig. 18

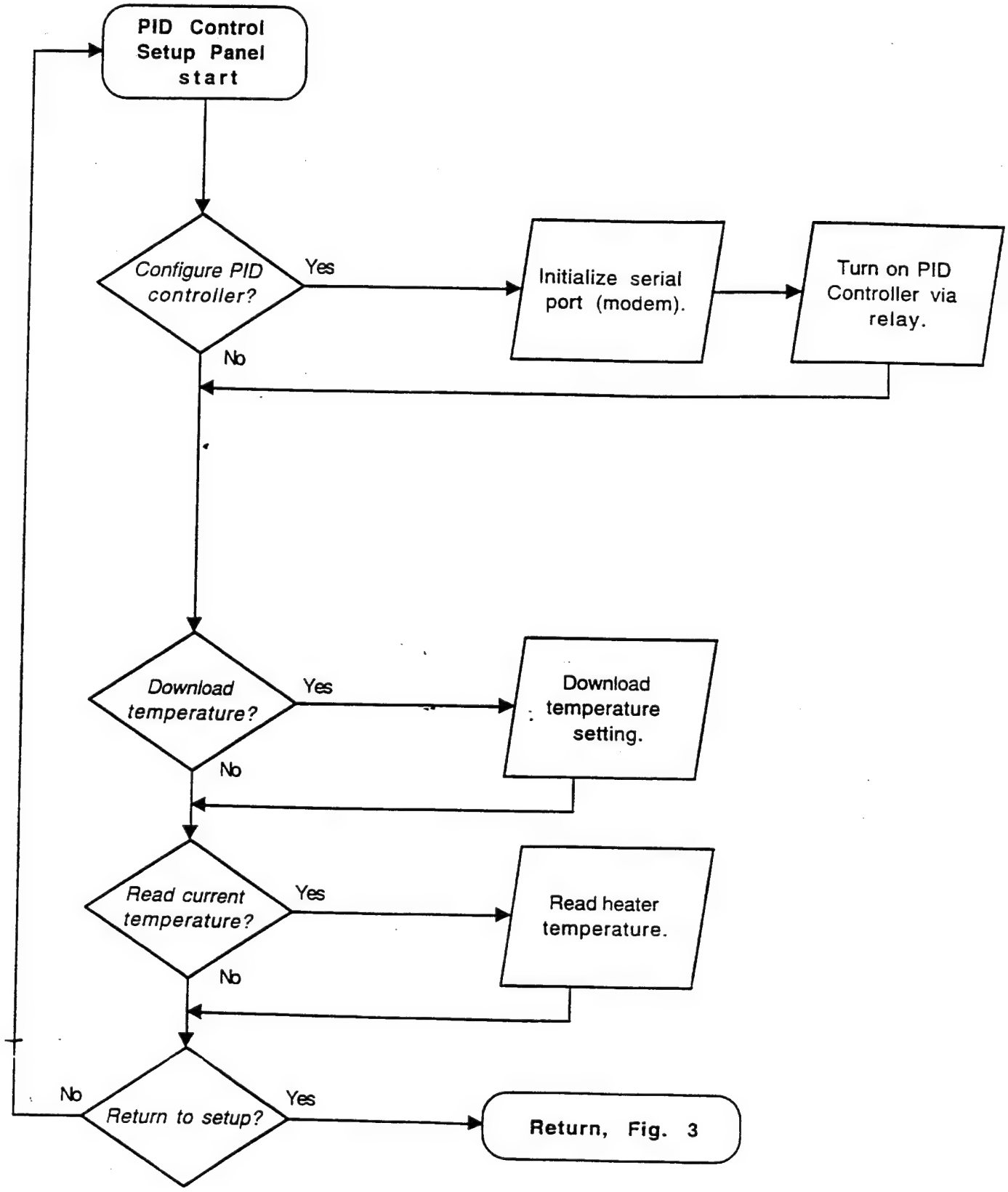

Deposition Panel, Fig. 19

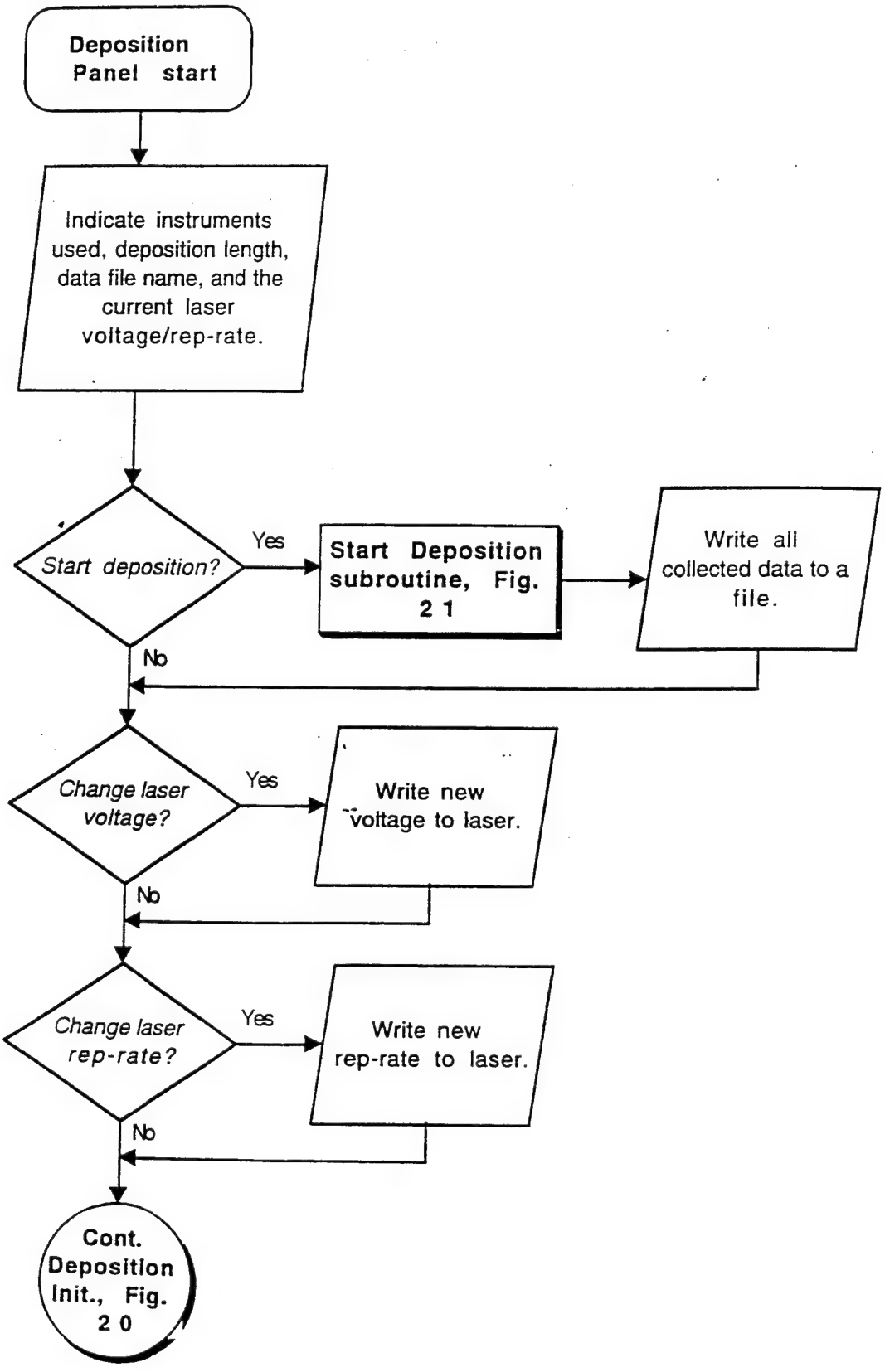

Continue Deposition Initialization, Fig. 20

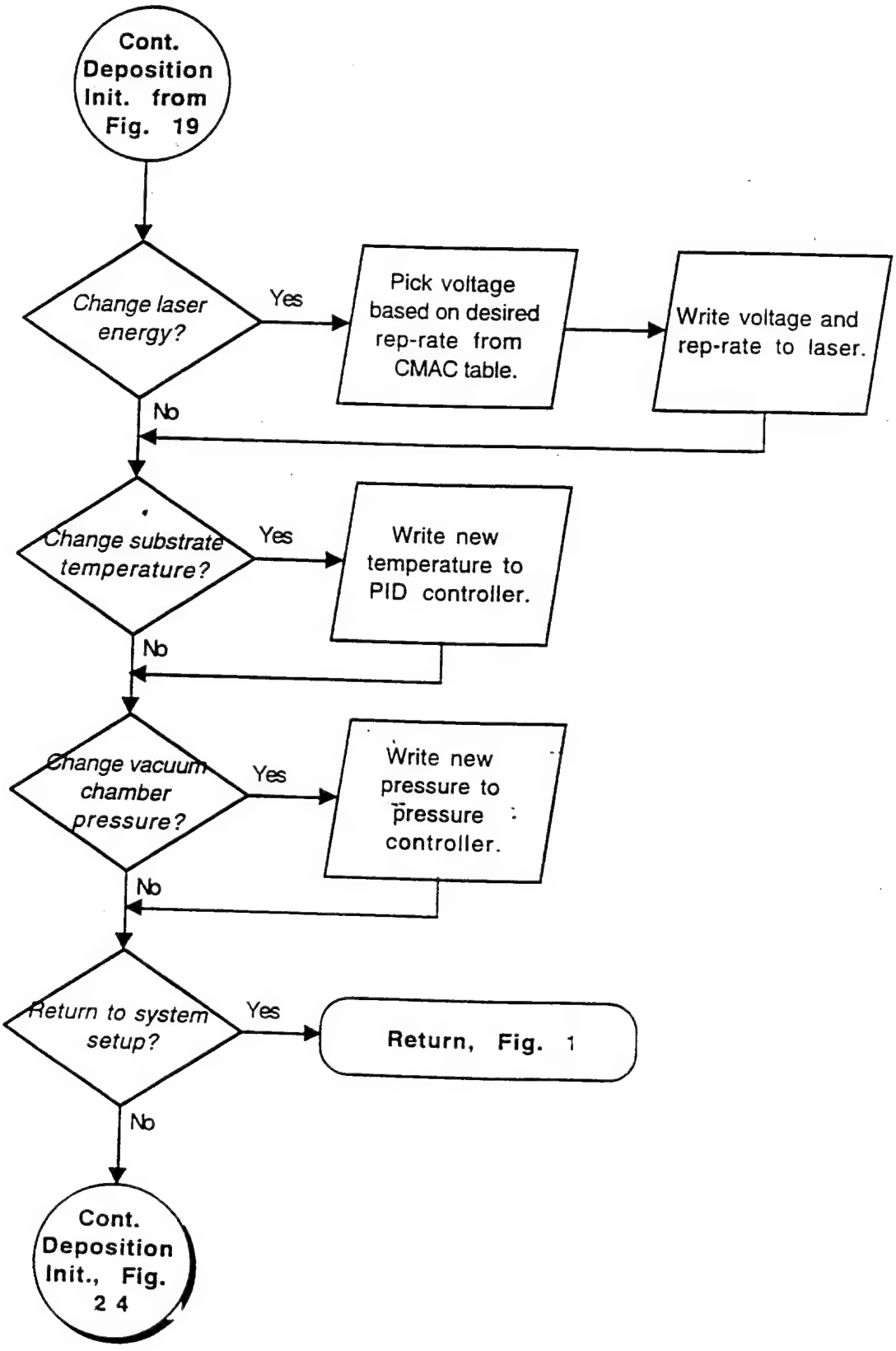

Start Deposition subroutine, Fig. 21

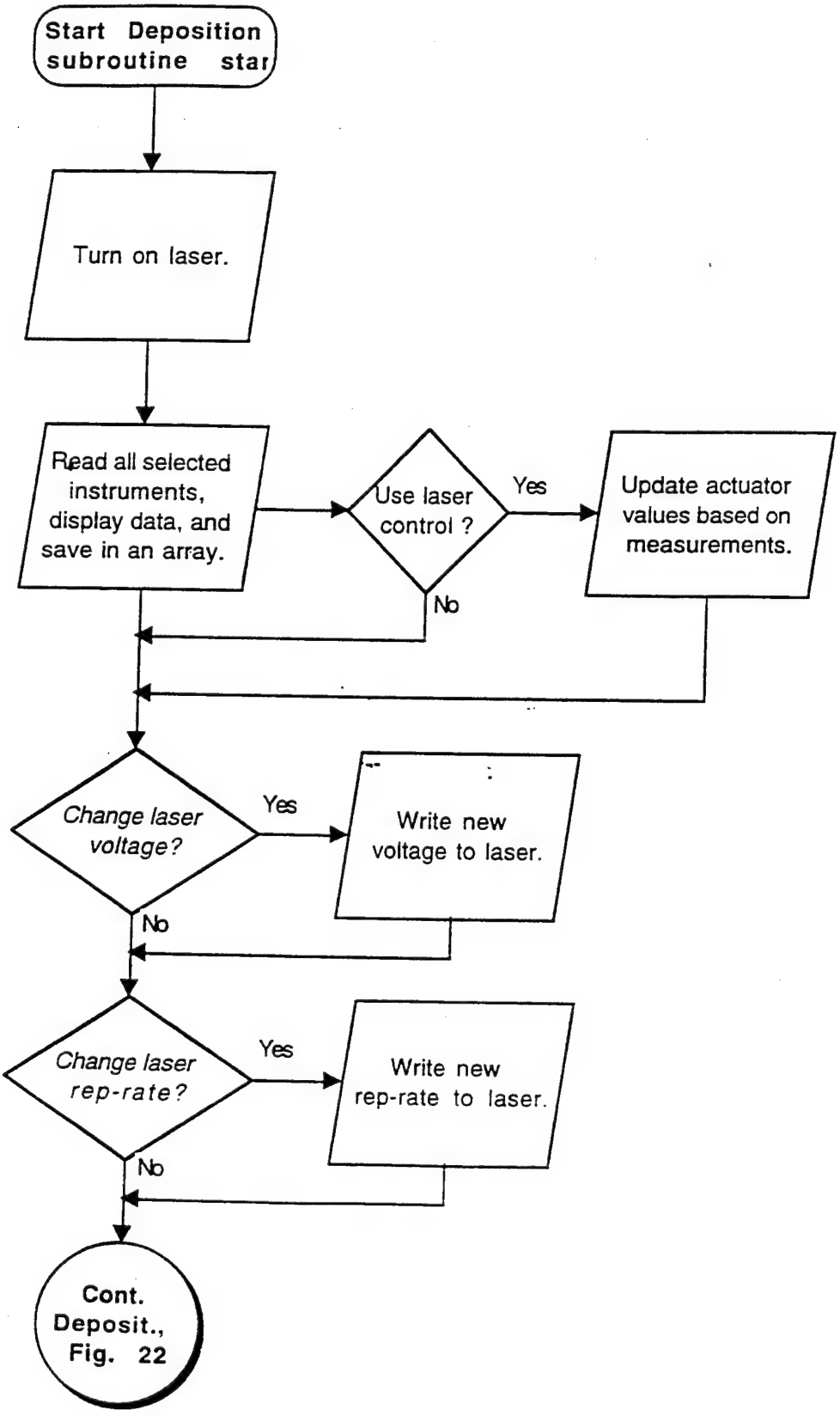

Cont. Start Deposition subroutine, Fig. 22

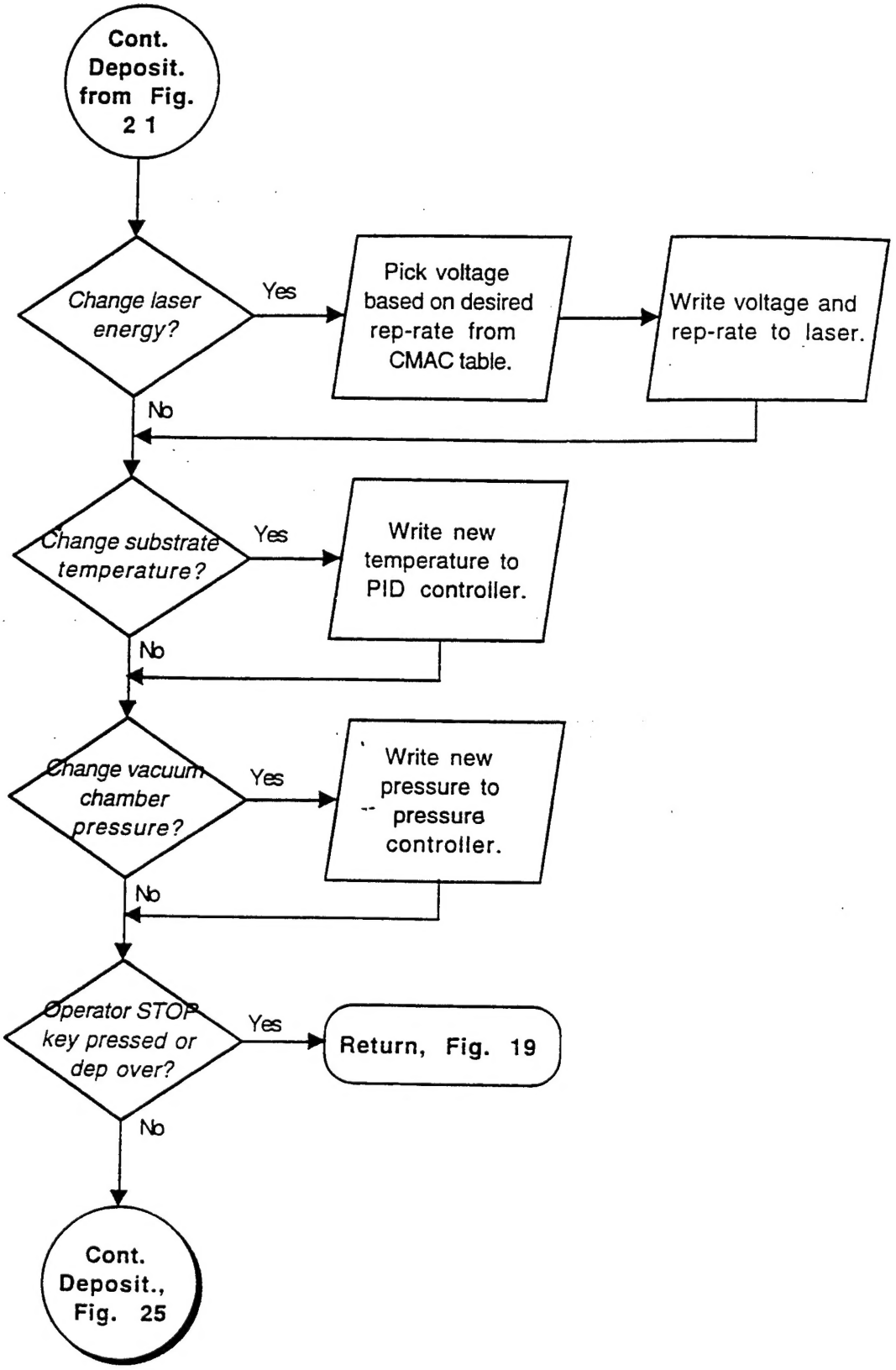

Pressure Control Subroutine, Fig. 23

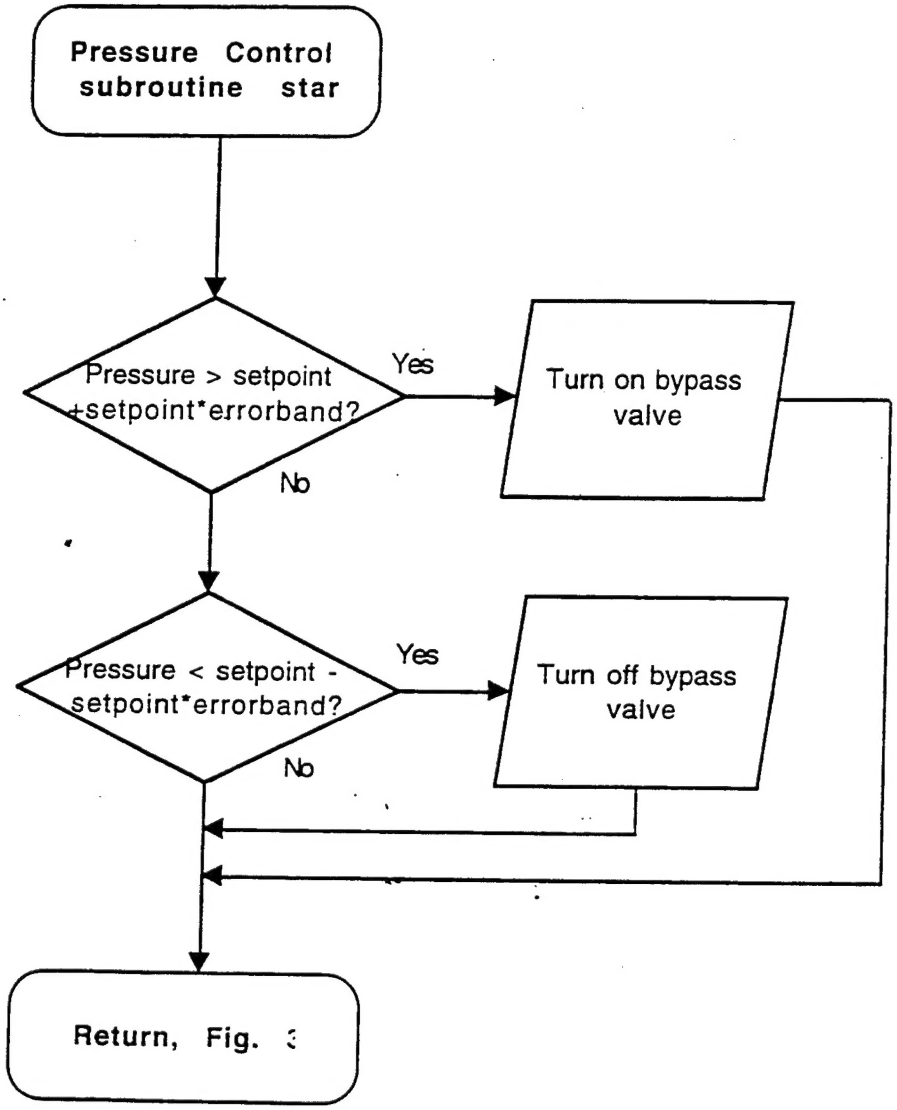

Continue Deposition Initialization, Fig. 24

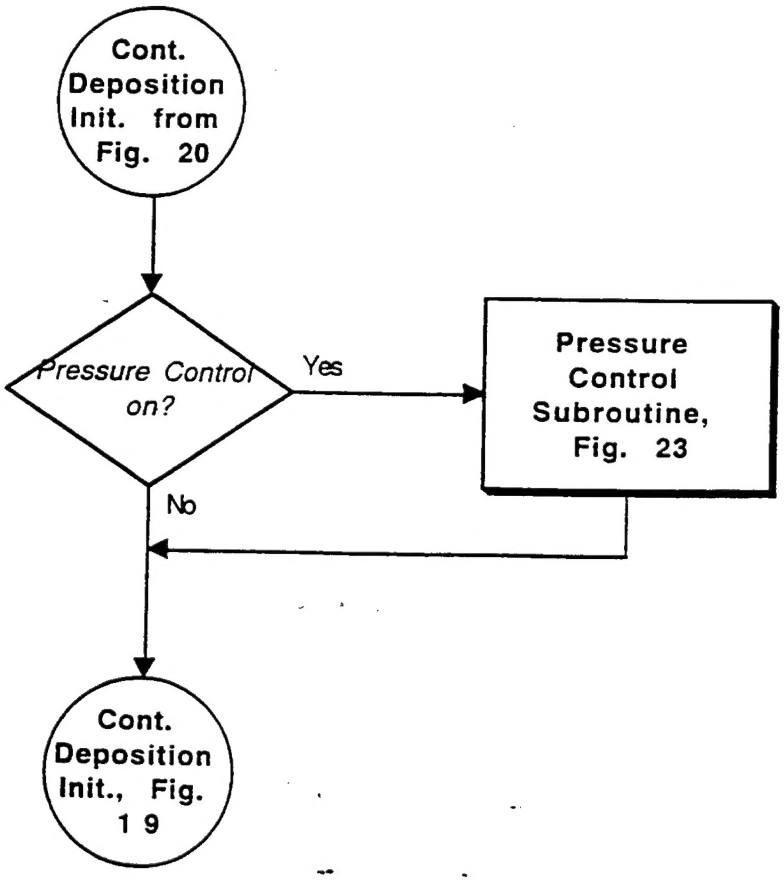

Cont. Start Deposition Subroutine, Fig. 25